DEVELOPMENT OF A LAPONITE PLURONIC COMPOSITE FOR FOAMING APPLICATIONS

James William Davis, M.S.

Dissertation Prepared for the Degree of

DOCTOR OF PHILIOSOPHY

UNIVERSITY OF NORTH TEXAS

December 2012

APPROVED:

Teresa D. Golden, Major Professor
Nandika A. D'Souza, Committee Member
Guido F. Verbeck, IV, Committee Member
Ruthanne D. Thomas, Committee Member
Joseph W. Boclair, Committee Member
William E. Acree, Chair of the Department of Chemistry
Mark Wardell, Dean of the Toulouse Graduate School

Davis, James William. *Development of a Laponite Pluronic Composite for Foaming Applications*. Doctor of Philosophy (Chemistry - Analytical Chemistry), December 2012, 171 pp., 11 tables, 80 illustrations, chapter references.

The focus of the following research was to provide an optimized particle stabilized foam of Laponite and Pluronic L62 in water by understanding (1) the Laponite-Pluronic interactions and properties for improved performance in a particle stabilized foam and (2) the interfacial properties between air and the Laponite-Pluronic complex. These studies were conducted using both bulk and interfacial rheology, XRD, sessile droplet, TGA and UV-vis. Two novel and simple techniques, lamella break point and capillary breakup extensional rheometry, were used to both understand the Laponite Pluronic L62 interaction and determine a different mechanism for foaming properties.

Bulk rheological properties identified an optimal Laponite concentration of 2% with Pluronic L62 ranging from 2.5% and 6.5%, due to the ease of flow for the dispersion. The Pluronic L62 was observed to enhance the Laponite bulk rheological properties in solution. Additionally TGA showed a similar trend in thermal resistance to water with both addition of Laponite and Pluronic L62. XRD demonstrated that 0.25% Pluronic intercalated into Laponite from dried 2% Laponite films. XRD demonstrated that the Laponite matrix was saturated at 1% Pluronic L62. UV-vis demonstrated that a monolayer of Pluronic L62 is observed up to 0.65% Pluronic L62 onto Laponite.

Interfacial rheology showed that Laponite enhances Pluronic L62 at the air-liquid interface by improving the storage modulus as low at 0.65% Pluronic L62 with 2% Laponite. The lamella breakpoint of Laponite with Pluronic films indicate strong film interaction due to higher increases in mass. Extensional rheology indicates that 2.5% to 6.5% Pluronic with 2% Laponite show the most filament resistance to stretching.

ACKNOWLEDGEMENTS

I would like to convey my gratitude to Dr. Teresa D. Golden for her willingness to take on a part-time graduate student, support and understanding. I would like to extend my gratitude to my committee members Dr.'s Nandika A. D'Souza, Guido F. Verbeck, IV, Ruthanne D. Thomas and Joseph W. Boclair.

I appreciate Alcon for allowing me to work nights and weekends on my research interests, specifically Dr.'s David Meadows, Howard Ketelson, Nissanke Dassanayake and Michael Marks.

Thank you, God for my wife, Katie, children, Tommy and Meagan, and the rest of the family.

Above all, I would like to thank Katie for her love and support. Not enough can be said about Katie except, Amen.

TABLE OF CONTENTS

Page

LIST OF TABLES

Page

LIST OF ILLUSTRATIONS

Page

CHAPTER 1

INTRODUCTION

There is a need for a more efficient, cost effective and eco-friendly foam technology in firefighting applications. Currently there is over 13,000 tons of foam production used per year for fire-fighting applications.[1] Of that, the majority contains fluorinated compounds which are not eco-friendly.[2] Fluorocarbon foam technology has numerous advantages but it is not the “be all end all” in fire fighting technology. One approach would be through particle stabilized foams.[3,4] This work focuses on novel characterization and development. One such system uses Laponite, a particle, and Pluronic L62, a foaming nonionic surfactant, suspension in water.

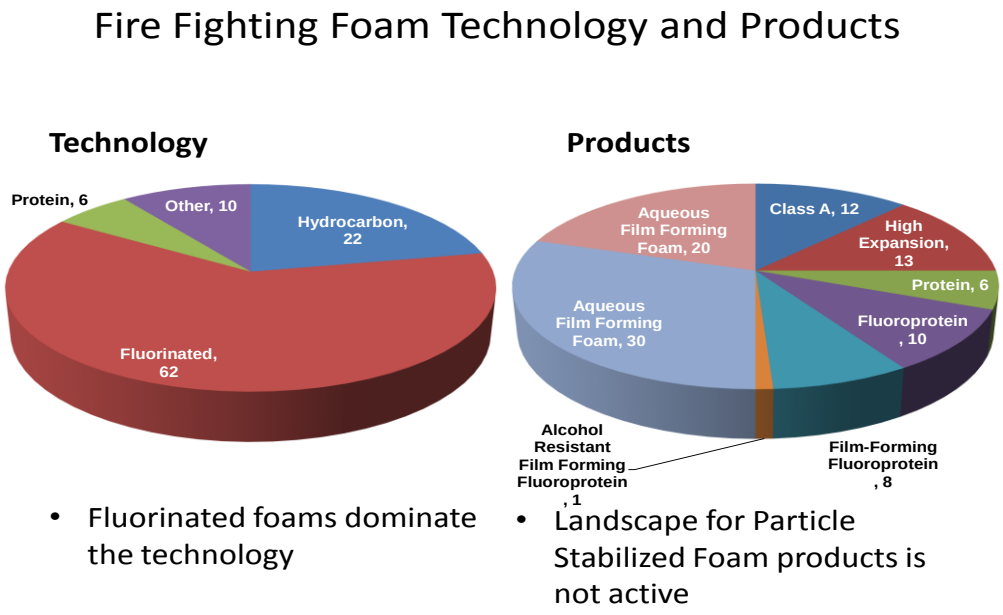

Figure 1. 1. Fire Fighting Foam Technology and Products. Pie charts representing percentage of types of technology as well as Product differentiation. (Data obtained from reference 1.)

Figure 1 gives the landscape of both fire fighting foam technology and product areas. On the technological side, 62% of the market is dominated with fluorinated foam technology. The foaming product areas show there is high potential for a foam technology that utilizes particle stabilized foams of Laponite and Pluronic systems. This summarizes the need and opportunity for firefighting applications with a particle stabilized foam system.

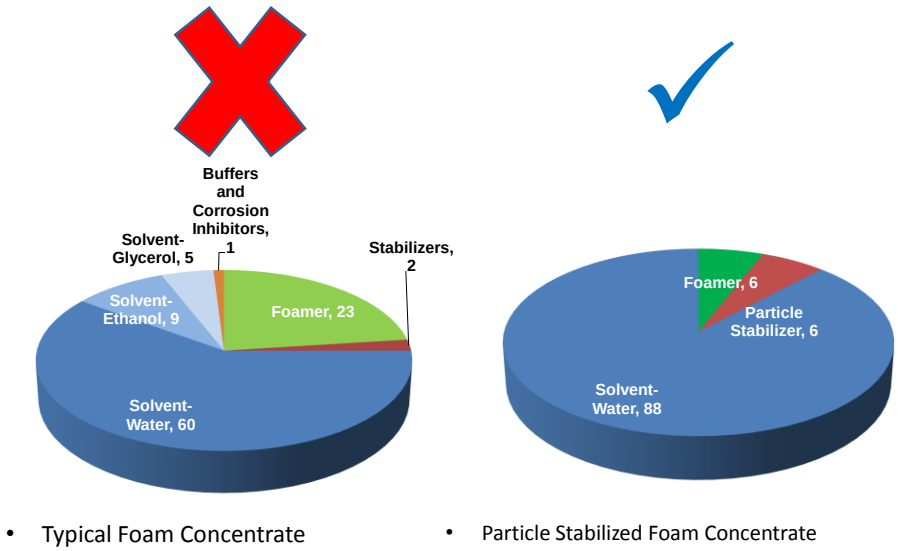

Figure 1. 2. Foam Concentrate Ratios of current technology compared to proposed particle stabilized technology. Reference 1.

Figure 2 shows the typical foam concentrate[5,6] ratios. Some disadvantages are evident one of which includes a multi component system to obtain desirable foaming. There is roughly 30% foamer in the concentrate. Many have cosolvents and other

excipients to provide better foam properties. In the particle stabilized foam concentrate, the ratio of foamer is reduced to below 10% with an incorporation of the particle of choice is a clay providing eco-friendly benefits. Potentially, this would reduce foam production currently at 13,000 tons down to 3,500 tons per year and eliminate the need for fluorinated foam technology.

The following work focuses on the clear need for alternate solutions in firefighting application by providing particle stabilized foams. The two goals of this work are to investigate the value of Laponite, a particle, with Pluronic, a nonionic surfactant polymer with good foaming properties, to provide an optimized particle stabilized foam by understanding:

I. Laponite-Pluronic interactions and properties for improved performance in a particle stabilized foam.
II. Interfacial properties between air and the Laponite-Pluronic complex

For a better understanding, the science behind foaming is discussed in this chapter emphasizing basic concepts, structure and classification, drainage and stability, theories of foam stability and thermodynamics of particle stabilized foams.

1.1 Foams

Foams[7] are a type of dispersed system that consists of air and liquid. Figure 3 shows three phases: air, interface and liquid.

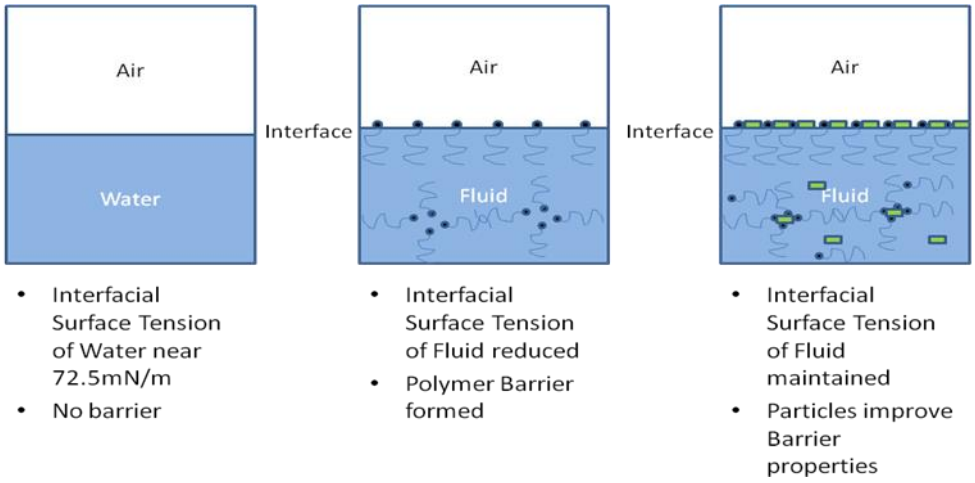

1.3.a. 1.3.b. 1.3.c.

Figure 1. 3. Three dispersed systems. 1.3.a. Water alone, 1.3.b. Surfactant added, 1.3.c. Particle and Surfactant added. Notes on advantages under each dispersed system.

Figure 1.3 is a representation of what happens at an air-water interface, giving a better understanding for what begins to happen in foams. In the Figure 1.3.a, there are two phases separated by an interface. In this scenario, the interfacial surface tension is high. Figure 1.3.b shows when a surfactant is introduced into the water phase, fluid interface reduces in interfacial surface tension. The adsorption of the surfactant to the interface is concentration dependent. Thus leading to a concentration saturation point at the interface where the surface tension is minimized and plateaus, i.e. critical micelle concentration. This surfactant also provides a barrier at the interface where deformation can be minimized. Figure 1.3.c shows the addition of a clay colloid to this fluid. Note that it enhances the structural component of the fluid. The polymer now has to adsorb on the

colloid and at the air water interface. The surfactant at a certain concentration can drive the colloid to the interface and provide enhanced structure.[8] The thermodynamics of this process will be explained in the following section. The characterization and optimization of bulk properties for Laponite with Pluronic L62 suspensions are the focus in Chapter 3.

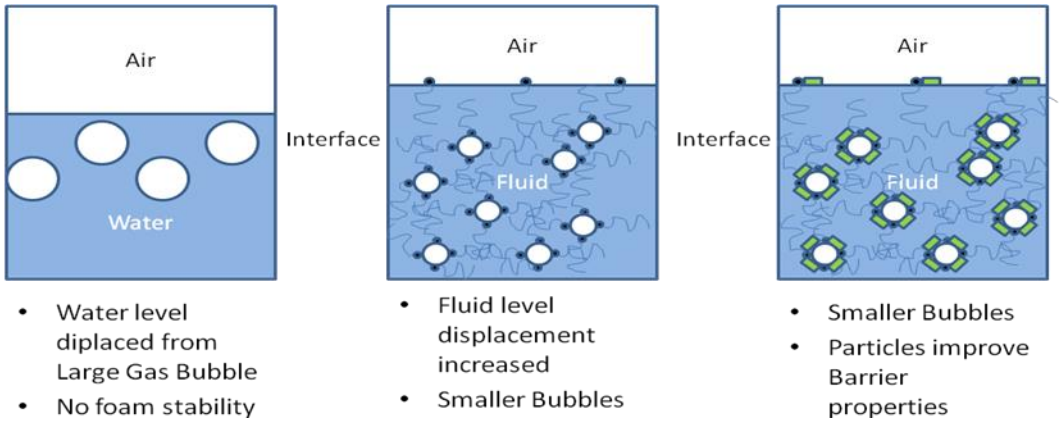

1.4.a. 1.4.b. 1.4.c.

Figure 1. 4. Three dispersed systems with gas bubbles. 1.4.a. Water alone, 1.4.b. Surfactant added, 1.4.c. Particle and Surfactant added. Notes on advantages under each dispersed system.

Figure 1.4 is a representation of bubbles in three different scenarios. This can be also thought of as air bubbles inside a pure liquid medium, i.e. water. In pure water, the bubbles quickly separate to the top. This is due to the high interfacial surface tension water has at the air interface and density gradient of air relative to water. Surfactants are added to many systems that can reduce the surface tension between two different phases. Additionally, surfactants can provide elasticity, or barrier, at the interface and

mechanically improve the structure by providing a film to the surface. In a foaming system, this reduction of tension is between the air and solution with the surfactant. The structure provided from the surfactant and reduced tension stabilizes the air bubble in the liquid. The structuring that stabilizes the foam prevents thinning of the liquid and collapsing of the air bubbles. This process of surfactant stabilizing the interface and surfactant diffusing to the interface to prevent collapse is better known as the Gibbs-Marangoni effect.[9] In summary, if something can accumulate at the air- water interface, then it has foaming potential. In many cases, it includes ionic and nonionic surfactants, particles and ions. The following work will focus on the synergies observed with Laponite and Pluronic L62.

1.2 Foam Structure and Surfactant Classification

Foams are a dynamic system leading to different structures that are unstable. The following work focuses on the foam stability provided from Laponite to the Pluronic L62 foaming surfactant. There are two types of foam structures which are driven by different mechanisms. Both are further discussed in the theories section. Figure 1.5 shows a pictorial of foam structures that may form. Starting from the bottom and moving upwards, bubbles are completely symmetrical and spherical in the dominate bulk liquid phase. The bubble is thermodynamically driven to the surface and the liquid phase begins to thin due to density and surface tension. Bubbles begin to pack closer together at this point. This type of bubble is referred to as kugelschaum.[10]

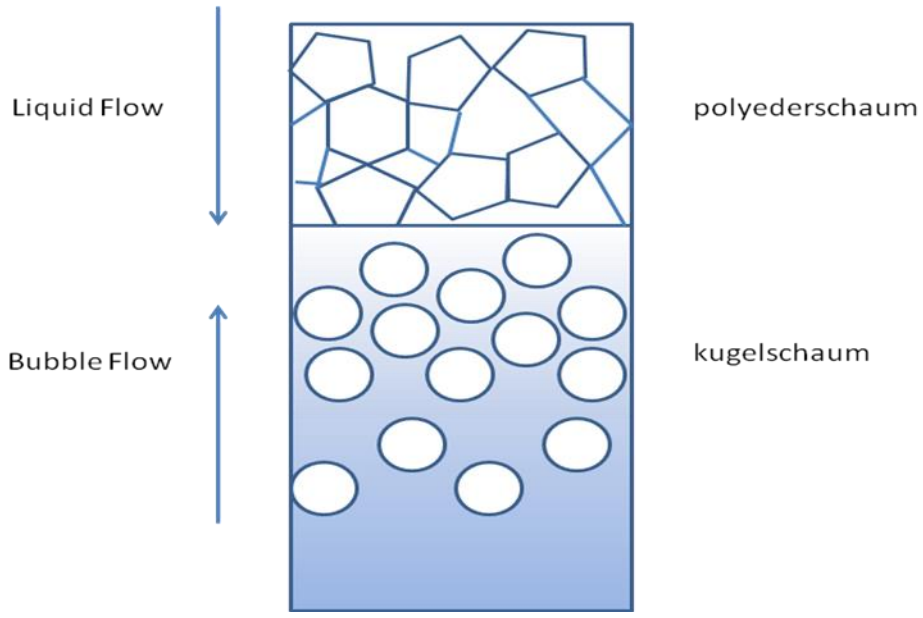

Figure 1. 5. Bubble Classification and flow direction for bubble and liquid.

The second type of foam is the polyderschaum, in which gas is the dominant phase divided by thin films and lamellaes. The films and lamellae meet at an intersection known as the plateau border.[11,12] This process facilitates film drainage and stability. Figure 1.6 shows the value of a surfactant with and without the colloid present in the plateau border.

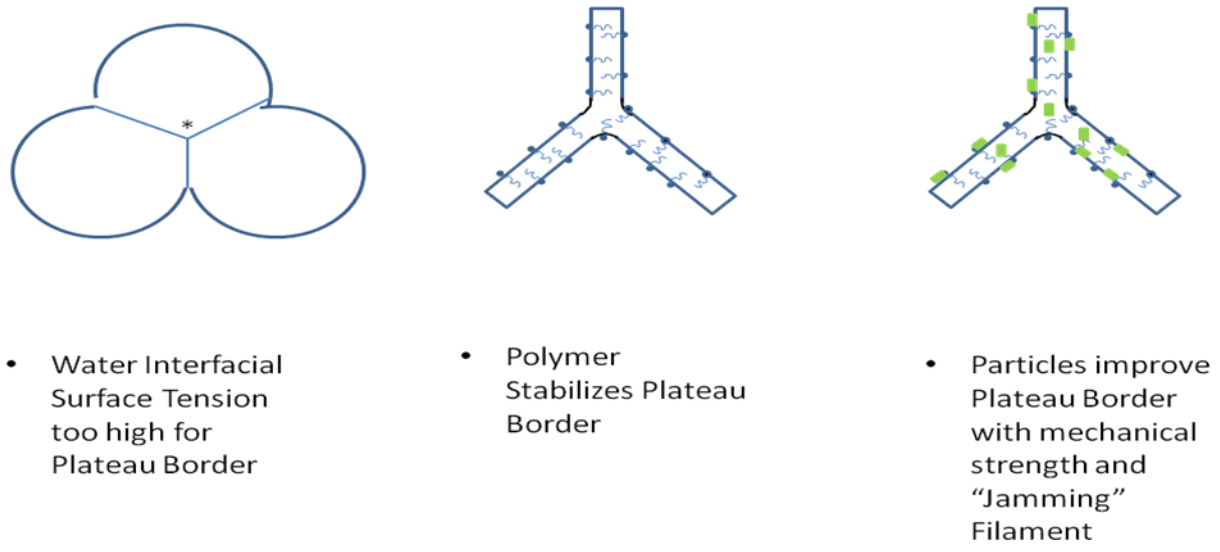

Figure 1. 6. Representation of Plateu Borders from three bubbles stabilized by polymer surfactant and particle-polymer.

From Figure 1.6, the ability of a particle-surfactant system to stabilize the film is a key contributor to foam drainage and stability[13]. The following work focuses on the added value of the Laponite-Pluronic interactions impacting foam stability and drainage.

1.3 Drainage and Stability

Drainage can be separated by films and foams. Film, also known as a lamella, thickness can decrease in one of two ways: 1.) height of the film from bulk interface or 2.) length of time. In both cases, a common feature with the film is the unique interference patterns leading to black films.[14,15] There are different experimental methods to determine and characterize thin films using surfactants that include horizontal and vertical films.[16 ,17]One aspect of a lamella is its adhesive properties as it "pulls" on a du Nuoy ring balance. Commonly, one can obtain a surface tension value.

But there is value in how lamellas behave as the ring is pulled back to a breakpoint. This may give insight to the adhesive and surface structure component of the lamella films. The following work focuses on how the lamella film behaves with Laponite and Pluronic L62 at the air-water interface and how it impacts foam stability.

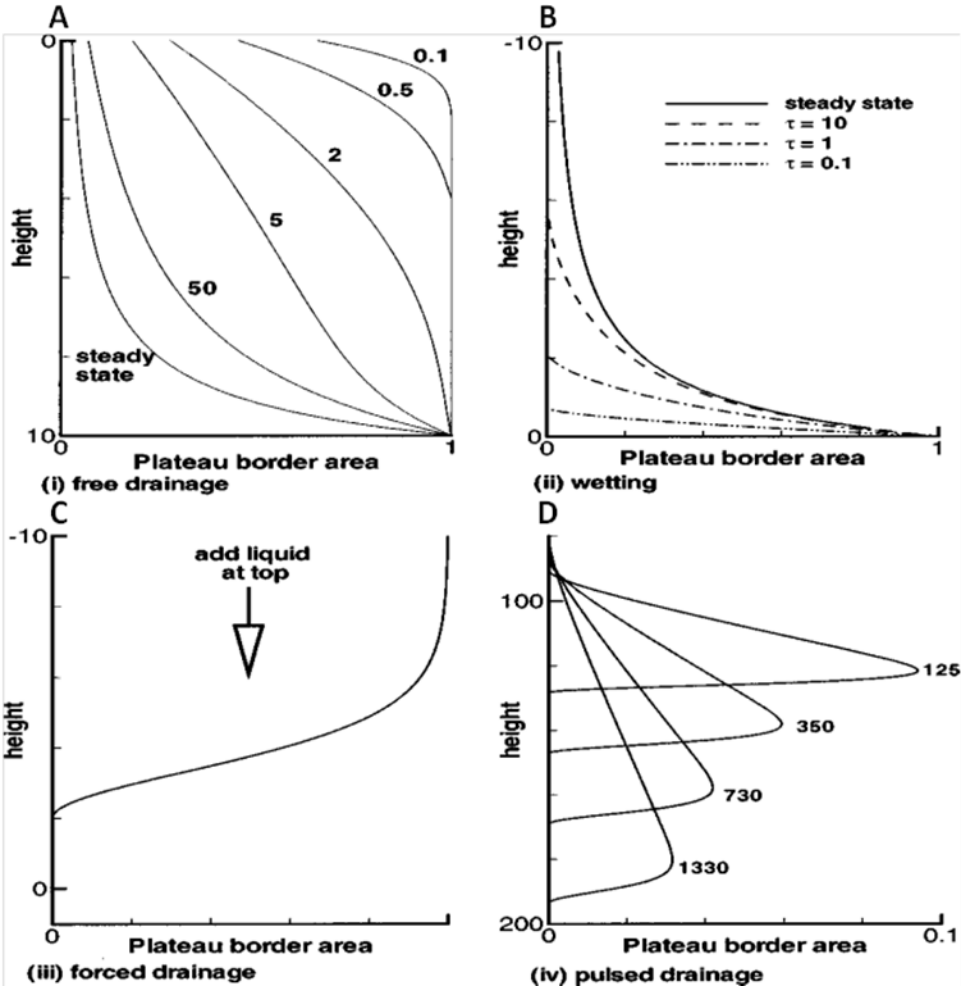

Figure 1. 7. Drainage profiles Height vs Plateau Border Area for A.) Free Drainage, B.) Wetting, C.) Forced Drainage and D.) Pulsed Drainage. Reference 18.

The second type of drainage deals with three-dimensional dynamic foam drainage. There are four common types of drainage experiments. Figure 1.7 is a

representation of how foam drainage height and plateau border area are related.[18] The plateau border leads to a filament that is formed. Flow is dependent upon the plateau border area. If plateau border area is large, then liquid flow increases resulting in faster drainage height increases. However, flow through the filament facilitates drainage. Flow drainage models have only looked at simple cases from a bulk viscosity and viscoelastic parameter.[19] The following work focuses on the free drainage process as it pertains to a Laponite Pluronic system.

Foam drainage models have been an active area of research for the past 30 years and are still being updated due to the complexities of foaming parameters that are discussed throughout this work. Foam drainage has its origins from Darcy's law.[20] Darcy's law describes the fluid flow through porous media as described below:

$$Q=\frac{K}{\eta}(\nabla p-\rho g) \quad (1)$$

where Q is the total discharge (volume flux in length per time, m^2/s), K is the porous mediums permeability (m^2, for this work gas), ρ is the density of the liquid, ∇p is the pressure gradient and *g* is gravitational acceleration. Research on foam drainage modeling has developed many different models depending on the experimental parameters.

The following work focuses on free drainage of foams because of the end use is firefighting technology. The most current free draining equation is modified from Darcy's law and takes into account the following:

$$\frac{\delta\varphi}{\delta\tau} + \frac{\delta}{\delta\xi}\left[\frac{\varphi^2}{1-\varphi} - \frac{\varphi^{1/2}}{(1-\varphi)^{3/2}}\frac{\delta\varphi}{\delta\xi}\right] = 0 \qquad 2$$

where φ is the liquid fraction, τ is time and ξ is the foam height all of which are non-dimensional units.[21] The following work uses this free drainage equation under the limits of foam production.

There has been a recent amount of work that can distinguish extensional flow of various fluid types using capillary thinning.[22] This work characterizes and proposes a new mechanism on extensional flow and how it provides improved foaming properties for particle stabilized foams. The following figure demonstrates similarity of foam filament to an extensional rheological experiment with a fluid filament formed. The figure shows that as the fluid is pulled back a filament is formed and "drains" over time. Different fluids provide different filament profiles. The longer the filament takes time to snap off the more strength it may provide against foam drainage. This is dependent on the viscoelastic and surface tension properties of the fluid.[23] This is a novel concept that was pursued in this work.

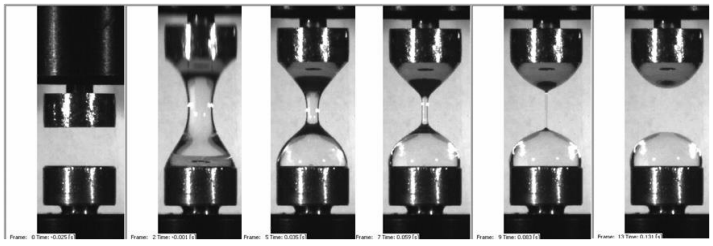

Figure 1. 8. Image snapshots from Extensional Filament stretch of a fluid time course.

1.4 Concepts on Foam Stability

Table 1. 1. Foam Stability Concepts, Mode of Action and Areas of Focus in the following research.

Concept	Mode of action	Focus
Surface Viscosity and Elasticity	Adsorbed film controls pure mechanical structure to impact drainage	✓
Gibbs-Marangoni Effect	Adsorbed film accounts for surfactant concentration=> maximum foam with intermediate concentration of surfactant that impacts rupture	✓
Surface Forces	Drainage of film to low thicknesses to characterize charge, van der Waals, steric effect	✓
Micellization	Drainage based on Stratification	-
Liquid Crystallinity	Some surfactants form larger structures above cmc that enhance viscosity of film	-
Mixed Surfactants	Mixed surfactants have improved bulk and interfacial structure	-

For the surface viscosity and elasticity concept in Table 1.1, differentiation has been characterized between interfacial shear and dilatational elasticity impact foam stability for systems of oppositely charged polyelectrolytes, CTAB and PSS.[24] In some instances, there was a direct link between foam drainage for interfacial shear than there was for dilational surface rheology.[25] Table 1.2 identifies that shearing probes the interaction of film network and molecules. Interfacial shear has been correlated to foam drainage. Recent work has looked at the dilatational characterization of the intra- and intermolecular interactions and adsorption/desorption dynamics of the film.[26] This may correlate more with film rupture.

Table 1. 2. Techniques used for film structure and Characterization with value and how it impacts Foam properties.[27]

Technique	Value	Impacts
Interfacial Shear Rheometry	Interactions of film network and molecules	Drainage
Dilatational	Intra- and intermolecular interactions; adsorption/desorption dynamics	Rupture

For the Gibbs-Marangoni effect concept in Table 1.1, one mode of action for foam stability is in the resistance to mechanical perturbation.[28] The Gibbs-Marangoni property is from Gibbs proposal that film elasticity contributes to foam stability:

$$E = 2\,\frac{d\gamma}{d\ln A} \qquad 3$$

where E is the elasticity of the film; γ is the interfacial tension at the air-liquid interface; A is the area of the film formed. If the film is put under mechanical stress, the elasticity is such that is does not rupture. Generally, as E increases so should foam stability. Gibbs elasticity does not take into account bulk diffusion of the surfactant. Figure 1.9 gives a better representation as to why rupture occurs upon deformation from the Gibbs Maragoni effect.

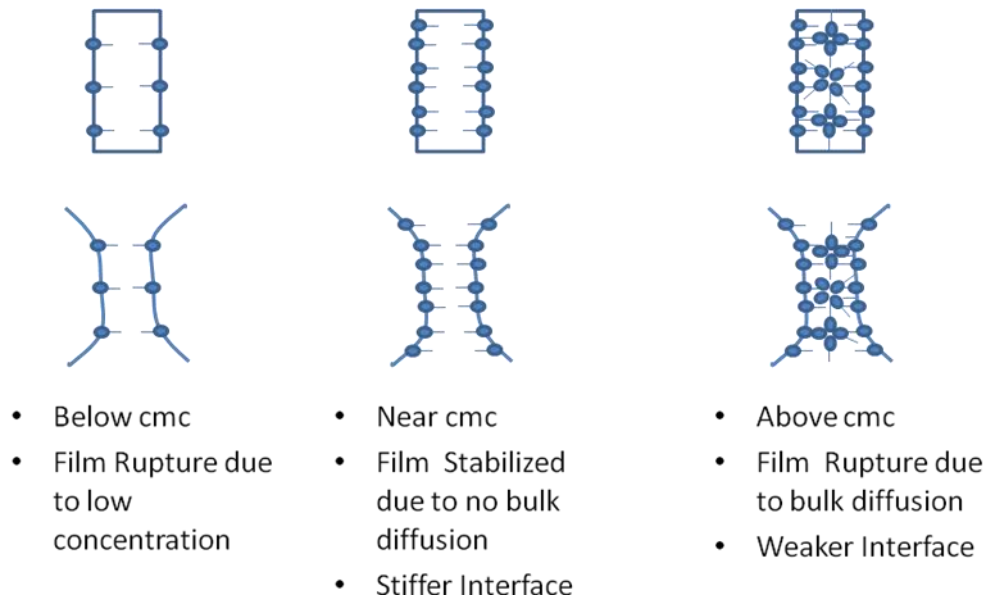

Figure 1. 9. Film properties as a function of concentration used to describe the Marangoni effect.

Surfactant concentration has a limit up to or near its critical micelle concentration without rupturing as well. To account for rupturing, particles have been added to foams in order to increase foam stability while maintaining reasonable surfactant levels and ultimately improving the foam stability.[29] Rupturing or drainage of the film is the main phenomena of foam instability.

For the surface forces concept in Table 1.1, foam stability is the desired property for the applications presented in Chapter 5. Film elasticity and drainage are the two factors that contribute to foam instability. As the interface of two gas bubbles approach each other, the particles begin to interact with one another. This interaction is related in terms of disjoining pressure, Π.

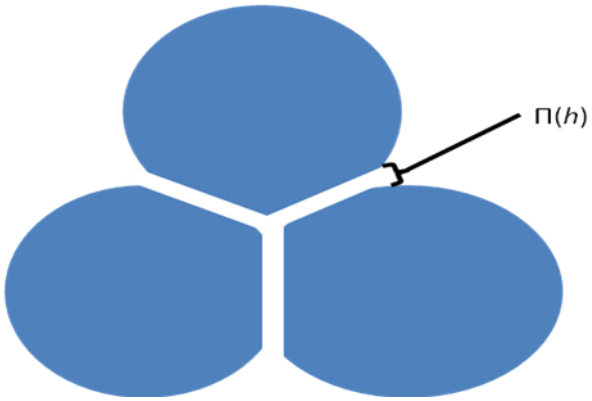

Figure 1. 10. Film of thickness, h, used to relate the disjoining pressure.

$$\Pi = -\frac{1}{A}\left(\frac{\partial G}{\partial x}\right)_{A,T} \quad 4$$

Disjoining Pressure is the free energy, G, of the film thickness, x per unit area, A, normal to the film thickness. As films approach thicknesses of 100 nm surface forces become a factor on the stability. The sum of the overall disjoining pressure is taken from current Derjaguin-Landau-Verwey-Overbeek (DLVO) theory of electrostatic, dispersive, polar and steric interactions.[30] This work looks at the dispersive and polar interactions of Laponite Pluronic L62 Films.

In summary, the surface viscosity, elasticity, Gibbs Maragoni effect and Surface forces contribute in various ways to foam properties. These concepts will be investigated in the following work for the Laponite Pluronic systems.

1.5 Thermodynamics of Particle Stabilized Foams

There is a clear need for particle stabilized foam for added value in firefighting foam technology as well as a need for novel characterization tools to differentiate between foam properties.

Some general particle properties have critical impact on foam stabilization. One factor includes foam production that includes some form of high energy impact from a gas or mechanical shearing. This work will utilize a high shear mixer, due to the end application of firefighting. The geometry of a particle has an impact on the foam stability, where a critical aspect ratio was optimal relative to a spherical particle all other properties being equal.[31,32] Additionally, a critical particle concentration optimizes foam stability. Particles can become trapped within the film and “jam” the film to slow down drainage[33].

Particle stabilized foams thermodynamically are in a quasi-equilibrium state with two main optimized contributions, i.e. contact angle and bubble coverage.[34] Figure 1.11 shows four scenarios of a three-phase solid/liquid/gas system.[35] The following conditions apply:

1. Particles are monodisperse hard spheres
2. The three phases do not dissolve into each other and influence the bulk Gibbs energy
3. All interfaces are stable positive interfacial energies
4. Contact between particles is negligible
5. Liquid has a contact angle of θ on the particles in the gas phase
6. Particles are small with no contribution from gravity
7. Bubbles have a much greater volume compared to the particle
8. No wall interaction with foam (θ at least 90°)
9. A_s and A_g are surface area of bubble and particle, respectively ($a \equiv A_s/A_g$). σ_{sg}, σ_{lg} and σ_{ls} are the interfacial surface tensions between the s-solid,l-liquid and g-gas phases. Θ is the contact angle of the liquid on the particle surface. Bubble coverage is defined as *f*.
10. The surface area on the top is negligible to A_s and A_g.

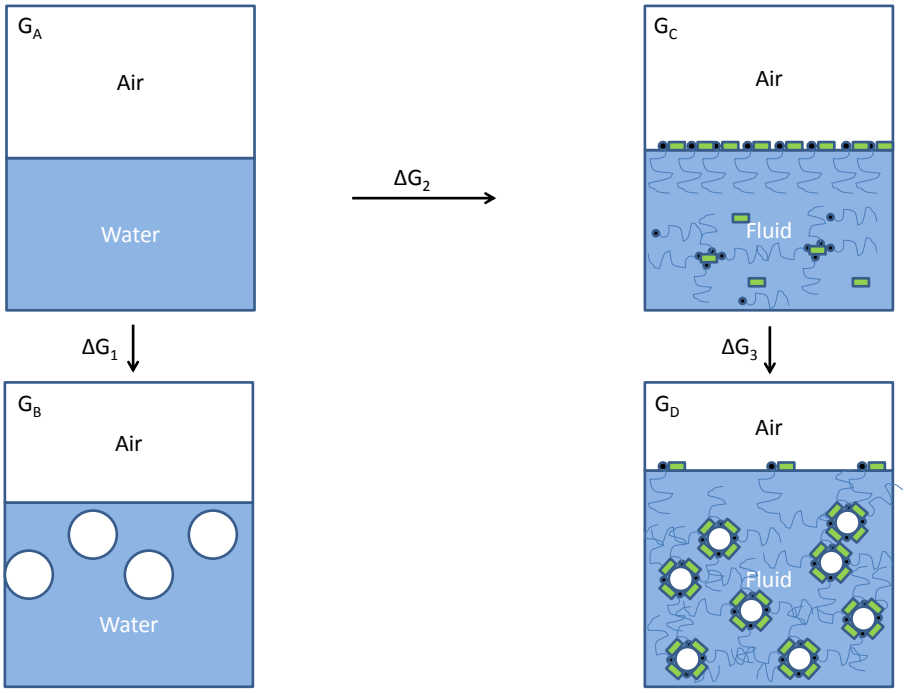

Figure 1. 11. Gibbs Energy State of four systems with three changes of states.

From Figure 1.11 there are four Gibbs energy states and three changes examined. The Gibbs energy states for three conditions are:

$$G_A = G^0 + A_s \cdot \sigma_{sg} \quad (5)$$

$$G_B = G^0 + A_s \cdot \sigma_{sg} + A_g \cdot \sigma_{lg} \quad (6)$$

$$G_C = G^0 + A_s \cdot \sigma_{sl} \quad (7)$$

G^0 is the bulk Gibbs energy of the system and σ at *sg*-solid/gas, *lg*-liquid/gas and *sl*-solid/liquid are the respective interfacial energies. To define the change in state for the first condition where the liquid has no particle and the change is to bubble formation, the relationship is as follows:

$$\Delta G_1 = \sigma_{lg} \quad (8)$$

where the change in Gibbs energy is directly proportional to the air liquid interfacial tension. The Gibbs value, even with a surfactant alone, is always positive allowing only temporary stability. In the case of adding particles to the liquid, the Gibbs energy change for a suspension is related by

$$\Delta G_2 = -a \cdot \sigma_{lg} \cdot cos\theta \quad (9)$$

Using the Young Laplace equation, $\cos\theta = (\sigma_{sg}-\sigma_{ls})/\sigma_{lg}$, ΔG_2 reduces to

$$\Delta G_2 = -a \cdot (\sigma_{sg} - \sigma_{ls}) \quad (10)$$

This alone shows that the suspension is more thermodynamically stable just by having a liquid that can wet the particle.

Some more relationships need to be addressed for the suspension to change into particle stabilized foam. Initially, the number of particles is related to the total surface are

$$N = \frac{A_s}{4 \cdot \pi \cdot r^2} \quad (11)$$

Particles can be in two positions, one in the gas phase the other in the liquid phase

$$N = N_g + N_l \quad (12)$$

The number of particles attached to the bubble can be expressed by

$$N_g = \frac{f \cdot A_g}{\pi \cdot r^2} \quad (13)$$

Substitution of equation 11 and equation 13 into equation 12 to determine the particles dispersed in the liquid phase is

$$N_l = \frac{A_g}{4\pi \cdot r^2} \cdot (a - 4 \cdot f) \quad (14)$$

The condition to keep particles in the liquid phase is satisfied when $a \geq 4*f$. The Gibbs energy for state D is

$$G_D = G^0 + N_l 4\pi r^2 \cdot \sigma_{sl} + N_g \cdot A_{sl} \cdot \sigma_{sl} + N_g \cdot (4\pi r^2 - A_{sl}) \cdot \sigma_{sg} + (A_g - N_g \cdot \Delta A_{lg}) \cdot \sigma_{lg} \quad (15)$$

where the surface area is defined by a single particle. When the particle is in equilibrium at the gas/liquid interface, its immersion depth is related to contact angle by the following

$$x = r \cdot (1 + cos\theta) \quad (16)$$

Substitution of equations lead to a Gibbs energy for state D as

$$G_D = G^0 + A_g \cdot a \cdot \sigma_{sl} + 2 \cdot f \cdot A_g \cdot (1 - cos\theta) \cdot \sigma_{lg} \cdot cos\theta + A_g [1 - f \cdot (1 - cos^2\theta)] \cdot \sigma_{lg} \quad (17)$$

Substituting equations for states A and D for ΔG_3 leads to:

$$\Delta G_3 = \sigma_{lg} \cdot [1 - a \cdot cos\theta - f \cdot (1 - cos\theta)^2] \quad (18)$$

where contact angle and bubble coverage can be optimized to have a quasi-equilibrium thermodynamic state better than a surfactant system alone.

To summarize, particle stabilized foams are more favorable compared to surfactant foams alone when:

1. Bubbles are covered by a higher ratio of particles
2. Surface tension of liquid is higher
3. Particle size is small
4. Optimal contact angle of particle to liquid obtained
5. Volume fraction ratio of particle is higher in bulk to bubble surface area
6. Particles have high aspect ratio

From just looking at the thermodynamics alone, particle stabilized foams impart a clear advantage even to just a surfactant type system. The following work will focus on how Laponite and Pluronic L62 impart enhanced foaming properties ideal for firefighting applications.

1.6 Chapter and Dissertation Summaries

This chapter deals with foam properties and the clear need for improved firefighting foam technology by utilizing particle stabilized foams. This chapter emphasizes basic understanding, structure and classification, drainage and stability, concepts of foam stability and thermodynamics of particle stabilized foams.

Chapter 2 looks at the most relevant techniques and tools used to characterize, understand and provide newer models for the development and optimization of a particle stabilized foam (i.e. bulk properties- rheological, TGA, adsorption isotherm, electrostatic and DLS; interfacial properties- sessile droplet, DWR (interfacial flow),

ODG (dilatational rheology), low angle XRD and adhesion; foaming- production, drainage and capillary break up rheology).

Chapter 3 focuses on bulk studies for Laponite Pluronic L62 dispersions and contribution of polymeric components to provide a mechanism of action.

Chapter 4 focuses on interfacial studies and novel characterization techniques for Laponite Pluronic L62 dispersions and contribution of polymeric components to provide a mechanism of action.

Chapter 5 focuses on foaming studies and novel characterization techniques for Laponite Pluronic L62 dispersions and contribution of polymeric components to provide a mechanism of action.

Chapter 6 summaries the novel Laponite Pluronic L62 foam system technology for potential application in firefighting technology from a bulk, interfacial and foaming mode of action. As well as summarize the novel techniques that may differentiate modes of actions for improved foaming technology. Finally, future work will be discussed pertaining to foaming technology and other industrial applications.

1.7 References

(1) Stevenson, P., Foam Engineering: Principles and Applications, John Wiley & Sons Publishing, New York, **2012**, 415-418.

(2) Hagenaars, A.; Meyer, I. J.; Herzke, D.; Pardo, B. G.; Martinez, P.; Pabon, M.; De Coen, W.; Knapen, D., The search for alternative aqueous film forming foams

(AFFF) with a low environmental impact: Physiological and transcriptomic effects of two Forafac fluorosurfactants in turbot, *Aquatic Toxicology*, **2011**, *104 (3-4)*, 168-17

(3) Hunter, T.N.; Wanless, E.J.; Jameson, G.J., Effect of esterically bonded agents on the monolayer structure and foamability of nano-silica, *Colloid Surfaces A*, **2009**, *334*, 181–190.

(4) Tran, D.N.H.; Whitby, C.P.; Fornasiero, D.; Ralston, J., Foamibility of aqueous suspensions of fine graphite and quartz particles with a triblock copolymer, *Journal of Colloid & Interface Science*, **2010**, 348, 460–468.

(5) Clark, K.P.; Jacobson, M.; Jho, C.H., Compositions for polar solvent fire fighting containing perfluoroalkyl terminated co-oligomer concentrates and polysaccharides, US patent 5,218,021, June 8, **1993**.

(6) DiMaio, L.R.; Chiesa, P.J., Foam concentrate, US patent 5,225,095, July 6, **1993**.

(7) Prud'homme, R.K.; Khan, S.A., *Foams: Theory, Measurements, and Applications*, Surfactant Science Series 57, **1996**, Marcel Dekker, New York.

(8) Rouimi, S.; Schorsch, C.; Valentini, C.; Vaslin, S., Foam stability and interfacial properties of milk protein–surfactant systems, *Food Hydrocolloids*, **2005**, *19*, 467–478.

(9) Pugh, R.J., Foaming, Foam Films, Antifoaming and Defoaming, *Advances in Colloid & Interface Science*, **1996**, *64*, 67–142.

(10) Tadros, T.F., Applied Surfactants: Principles and Applications, Wiley VCH, **2005**, Germany, 271-273.

(11) Plateau, J.; *Mem. Acad. Roy. Soc.Belg.,* **1861**, *33*, 6th series and preceding papers.

(12) Gibbs, J.W.; Collected Works,*Vol. 1,* Longmans Green, New York, **1931**, 287- 307.

(13) Fujii, S.; Iddon, P.D.; Ryan, A.J.; Armes, S.P., Aqueous Particulate Foams Stabilized solely with Polymer Latex Particles, *Langmuir*, **2006**, *22*, 7512-7520.

(14) Platikanov, D.; Graf, H.A.; Weiss, A.; Clemens, D., X-Ray Scattering by Black Foam Films: New Data Analysis, *Colloid Polymer Science*, **1993**, *271*, 106-107.

(15) Rayleigh, J.W.S; *Scientific Papers*, **1964**, *Vol. 2*, Dover, New York.

(16) Tamura, T.; Takeuchi, Y.; Kaneko, Y., Influence of Surfactant Structure on the Drainage of Nonionic Surfactant Foam Films, *Journal of Colloid and Interface Science*, **1998**, *206*, 112-121.

(17) Sonin, A.A.; Bonfillon, A.; Langevin, D., Thinning of Soap Films: The Role of Surface Viscoelasticity, *Journal of Colloid and Interface Science*, **1994**, *162 (2)*, 323-330.

(18) Koehler, S.A.; Stone, H.A.; Brenner, M.P.; Eggers, J., Dynamics of Foam Drainage, *Physical Review E*, **1998**, *58 (2)*, 2097-2106.

(19) Safoune, M.; Saint-Jalmes, A.; Bergeron, V.; Langevin, D., Viscosity effects in Foam Drainage: Newtonian and Non-Newtonian Foaming Fluids, *The European Physical Journal E*, **2006**, *19*, 195-202.

(20) Koehler, S.A.; Hilgenfeldt, S.; Stone, H.A., A Generalized View of Foam Drainage: Experiment and Theory, *Langmuir*, **2000**, *16*, 6327-6341.

(21) Magrabi, S.A.; Dlugogorski, B.Z.; Jameson, G.J., Free Drainage in Aqueous Foams: Model and Experimental Studies, *American Institute of Chemical Engineers Journal*, **2001**, *47 (2)*, 314-327.

(22) Rodd, L.E.; Scott, T.P.; Cooper-White, J.J., McKinley, G.H., Capillary Break-up Rheometry of Low Viscosity Elastic Fluids, *Applied Rheology*, **2005**, *15(1)*, 12-27.

(23) Anna, S.L.; McKinley, G.H., Elasto-Capillary Thining and Breakup of Model Elastic Liquids, *Journal of Rheology*, **2001**, *45 (1)*, 115-138.

(24) Monteux, C.; Fuller, G.G.; Bergeron, V., Shear and Dilational Surface Rheology of Oppositely Charged Polyelectrolyte/Surfactant Microgels Adsorbed at the Air-Water Interface. Influence on Foam Stability, *Journal of Physical Chemistry B*, **2004**, *108 (42),* 16473-16482.

(25) Fruhner, H.; Wantke, K. D.; Lukenheimer, K., Relationship between surface dilational properties and foam stability, *Colloids Surfaces A,* **1999**, *162*,193-202.

(26) Koehler, S.; Hilgenfeldt, S.; Weeks, E. R.; Stone, H. A., Drainage of single Plateau borders: Direct observation of rigid and mobile interfaces, *Physical Re*view *E,* **2002**, *66*, 040601 1-4.

(27) Tadros, T.F., Applied Surfactants: Principles and Applications, Wiley VCH, **2005**, Germany, 267-274.

(28) Sonin, A. A.; Bonfillon, A.; Langevin, D. Role of surface elasticity in the drainage of foam films, *Physical Review Letters,* **1993**, *71 (14)*, 2342-2345.

(29) Zhang, S.; Lan, Q.; Liu, Q.; Xu, J.; Sun, D.; Aqueous Foams Stabilized by Laponite and CTAB, *Colloids and Surfaces A: Physicochemical Engineering Aspects*, **2008**, *317*, 406-413.

(30) Van Oss, C.J.; Giese, R.F.; Costanzo, P.M., DLVO and Non-DLVO Interactions in Hectorite, *Clay Minerals*, **1990**, *38 (2)*, 151-159.

(31) Binks, B., Particles as Surfactants-Similarities and Differences, *Current Opinion in Colloid and Interface Science*, **2002**, *7*, 21-41.

(32) Karakashev, S.I.; Ozdemir, O.; Hamptom, M.A.; Nguyen, A.V., Formation and Stability of Foams Stabilized by Fine Particleswith Similar Size, Contact Angle and Different Shape, *Colloids and Surfaces A: Physicochemical Engineering Aspects*, **2011**, *382*, 132-138.

(33) Hunter, T.N.; Pugh, R.J.; Franks, G.V.; Jameson, G.J., The Role of Particles in Stabilising Foams and Emulsions, *Advances in Colloid & Interface Science*, **2008**, *137*, 57–81.

(34) Hunter, T.N.; Jameson, G.J.; Wanless, E.J.; Dupin, D.; Armes, S.P., Adsorption of Submicrometer- Sized Cationic Sterically Stabilized Polystyrene Latex at the Air–Water Interface: Contact Angle Determination by Ellipsometry, *Langmuir*, **2009**, *25*, 3440–3449.

(35) Stevenson, P., Foam Engineering: Principles and Applications, John Wiley & Sons Publishing, New York, **2012**, *125-130*.

CHAPTER 2

FOAM PREPARATION, PRODUCTION AND CHARACTERIZATION TECHNIQUES

2.1 Foam Preparation

2.1.1 Particle Selection- Laponite

Clays are widely applied in many fields such as polymer nanocomposites as adsorbents for heavy metal ions[1], catalysts[2], forensic application[3], sensors[4], due to their high specific surface area, chemical and mechanical stabilities, and a variety of surface and structural properties.[5]

From Figure 2.1, all corners of silica tetrahedra are connected to adjacent blocks, but some of the corners in the outer blocks contain Si atoms bound to hydroxyls (Si–OH). The silanol groups at the external surface of the silicate, are usually accessible to organic species, and act as neutral adsorption sites. In addition, some isomorphic substitutions occur in the tetrahedral sheet of the lattice of the mineral leading to negatively charged adsorption sites which are occupied by exchangeable cations or water soluble polymers.

Table 2.1 provides the surface area and cation exchange capacity for Laponite, both are relatively high. The advantages Laponite has over other purified clays include; purity, very low polydispersity and nanosize. Figure 2.1 gives pictorial of the laponite. It is disk-like with a negative charge on both faces with a partial positive charge around the diameter of the plate.

Table 2. 1. Laponite properties for this study: Empirical Formula, Surface Area of clay (m^2/g) and Cation Exchange Capacity (meq/100g).

Name	Empirical Formula	Surface Area (m^2/g)	CEC
Laponite	$Na_{0.7}[(Si_8Mg_{5.5}Li_{0.3})O_{20}(OH)_4]^{-0.7}$	300-450	50-75

Laponite in water is a colloid. Laponite is a phyllosilicate that provides a multitude of enhanced properties ranging from structural (mechanical)[6], and thermal[7] resistance. It is commonly used in commercial products ranging from everyday cleaning to commercially and industrially relevant products. One advantage of this is that it is a synthetic material with very specific physico-chemical properties. This material can leverage its physico-chemical properties of charge, large surface area and lipophilic nature in advanced and novel applications that will be discussed in this work.

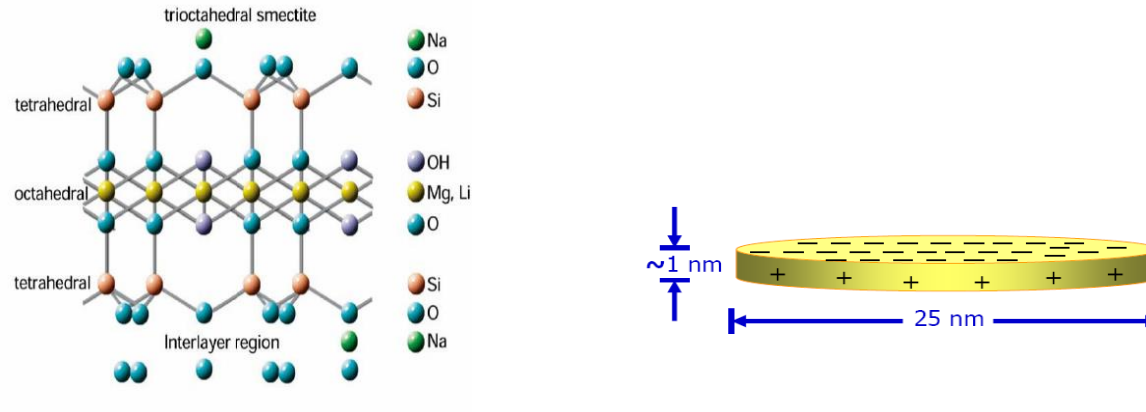

Figure 2. 1. The chemical structure and surface charge of Laponite. Reproduced for academic use from Rockwood Ltd.[8]

Laponite crystal structure is a trioctahedral smectite, with a sandwich motif of two tetrahedral silica-oxygen sheets on the outer layer and an octahedral magnesium(lithium)-oxygen-hydroxide layer in the middle. The charge is balanced with sodium ions on the exterior of the platelets. Silicates have some intrinsic hydrophobic character within the laponite matrix. This provides leverage by interacting with hydrophobic molecules. Figure 2.1 on the right shows a picture as to the charge around the platelet. The thickness of Laponite has been reported at 1nm with a diameter of 25 nm, leading to a high surface charge. The lattice parameters of laponite powder is d_{001}=13.4 Å with low crystallinity.[9]

The stoichiometry of synthetic laponite is the following:

$$Na^{+}_{0.7}[(Si_8Mg_{5.5}Li_{0.3})O_{20}(OH)_4]^{0.7-}.$$

This disc forms between 30,000 to 40,000 unit cells. Laponite's properties may provide enhancement when combined with polymers in modern applications of barrier properties, e.g. foaming[10] and thermal resistance[11].

2.1.2 Polymer Selection- Pluronic L62

There are a range of surfactants that are grouped as ionic or non-ionic. Both types of surfactants for ionic and non-ionic have different adsorption mechanisms to colloids. Nonionics have an inherent advantage in some applications where pH does not affect its properties and overall performance. There are two main groups of surfactants: ionic and nonionic surfactants. Both surfactants have advantages. Review of applications for ionic surfactants range in the following areas as medical, environmental, optical, etc.[12] Ionic surfactants major driving force with clays involves cation exchange.

Another factor is pH which has to be controlled with ionic surfactants in order to optimize sorption. This pH and ionic dependence limits its use in applications. This leads to some advantages nonionic surfactants have over ionic surfactants i.e. lack of pH and ionic contributions.

Moving into the nonionic realm, most nonionics are amphiphiles and are common derivatives of both ethyleneoxide and a hydrophobic moiety. Hydrophobic moieties cover a huge umbrella of sources. The most common include propylene oxides. The trade names of Pluronics which will be used to refer to the EOPOs come in ranges of molecular weights as well as varying hydrophilic-lipophilic balance (HLB). A brief description of HLB is the ratio of the hydrophilic, EO block length, to hydrophobic, PO block length in this case. High HLBs, 10-20, are used for foaming while low HLBs, are non-foamers.

The following are the chemical structures used in this work to understand the mechanism of enhanced foaming properties:

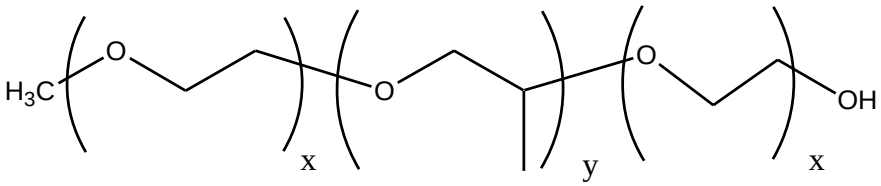

Figure 2. 2. General Chemical structure for a difunctional triblock (ABA) nonionic surfactant of Poly(ethyleneoxide)-Poly(propyleneoxide)-Poly(ethyleneoxide).

The outside x branches are the hydrophilic ethyleneoxide groups with a hydrophobic propyleneoxide in the middle denoted with a y. Most Pluronics on the market either include diblock, EOPO, or triblocks, EOPOEO or POEOPO. The limiting factor for Pluronics is in the hydrophobic, PO, block. Pluronics are biodegradable and nontoxic which makes this an attractive route for green chemistry.

Two types of Pluronics are used in this work. One is a foamer, Pluronic L62, and a defoamer, Pluronic 17R4. They are of similar molecular weight, the major difference is in HLB numbers. Pluronic L62 has an HLB ranging from 7-9 whereas Pluronic 17R4 has an HLB of 3-6. Additionally, a polyethyleneglycol monoether with a molecular weight similar to that of the two pluronics used (PEG Mw=2000g/mol) will also be studied. PEG2000 is a completely hydrophilic polymer with no PO block units. The PL17R4 and PEG2000 are used to differentiate how functionality and geometry impact the bulk, interfacial and foaming attributes of particle stabilized foams.

Poly(ethyleneglycol)-monoether

(PEG2000, hydrophilic)

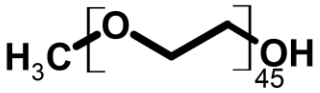

Poly(propyleneoxide)-Poly(ethyleneoxide)-Poly(propyleneoxide)

(Pluronic 17R4, defoamer)

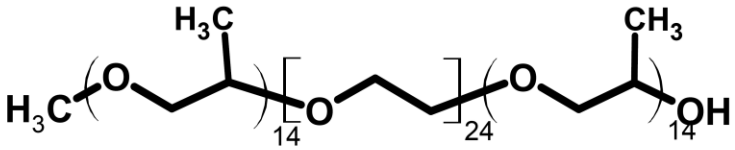

Poly(ethyleneoxide)-Poly(propyleneoxide)-Poly(ethyleneoxide)

(Pluronic L62, foamer)

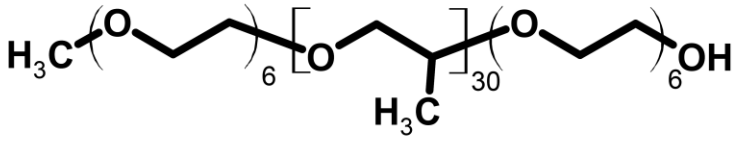

Figure 2. 3. Chemical structure for the three polymer systems used in this work to understand the mechanism with Laponite.

2.1.3 Dispersion Preparation

The method for preparation of all dispersions follows to ensure equilibrium of polymer adsorption to Laponite suspensions. A known amount of Laponite was meticulously added to deionized water with a low conductivity, 18 Ωcm. The Laponite was dispersed slowly to minimize agglomeration of particles and mixed at 10,000rpm for 30 minutes using a ULTRA-TURAX high shear mixer. Initially all laponite suspensions

are cloudy, eventually hydrating over time. The mixing using the ULTRA TURAX improves the dispersability and hydration due to it high shearing. The ULTRA-TURAX was turned off and removed after 30 minutes, then a magnetic stir bar was placed inside the beaker and the suspension mixed overnight for complete hydration. The Laponite concentration ranged from 0.5% to 10%. In most cases due to end use as a dilute suspension and repeatable processability, concentrations of Laponite were at or below 5%.

The appropriate polymer was added into this completely hydrated Laponite suspension with maximum mixing and minimal vortexing using a magnetic stir bar. This was allowed to equilibrate for 24 hours as well. Testing was initiated at least 24 hours after polymer addition. The polymer content was varied from 0.001% up to 10% for various Laponite concentrations.

2.2 Foam Production

Foam production using a high shear mixer is dependent on many factors, such as volume (including dimensions), mixing speed (rpm), depth of mixer in beaker, time and temperature. In all foam production experiments, volume was set at 50mL in a 250mL borosilicate glass beaker, depth was submerged at the same height at 10cm and temperature was maintained at 22 °C. Mixing speed and time were varied to obtain optimal processing conditions. It was found many had very similar foam production rates as well as overprocessing conditions. The high shear mixer was meticulously cleaned and air dried between each run with three mix rinse cycles for 1 minute at 10,000 rpm using a 500mL beaker with 400mL deionized water and air dried.

2.3 Characterization Techniques

The following is a list of techniques that define the property, tests, attributes and methods performed in this work. There are numerous firefighting foam tests for characterization. However, most techniques do not differentiate well between different foaming properties. The proposed techniques may fill this much needed gap.

Table 2. 2. Experimental Techniques for Particle Stabilized Foams

Property	Tests	Attributes	Methods
Bulk	Bulk Rheological Properties	Bulk Viscosity and Elasticity	Steady State Flow and Dynamic Oscillation
	Thermal Insulation Barrier	Thermal Resistance	TGA
	Electrostatic Properties	Dispersion Stability	Zeta Potential, Electrokinetic Mobility
	Aggregation	Adsorbed thickness layer	Dynamic Light Scattering
	Adsorption	Adsorption Layer type	Adsorption Isotherm
Interfacial	Surface Energy of films/Spreading Coefficients	DLVO components	Sessile Drop
	Interfacial Viscoelastic Properties	Mechanical Film strength to drainage	Steady State Flow and Dynamic Oscillation
	Dilatational Viscosity	Film Strength to rupture	Lamella Break Point
	Extensional Filament Strength	Extensional filament strength	Capillary Break Up Rheometer
Foam	Foam Stability	Duration of foam	Foam Production and Drainage

The following table summarizes the types of experiments for this work. It is divided into three main areas of bulk, interfacial and foaming. Each property has specific test attributes and methods used in this work for particle stabilized foams.

2.3.1Bulk Properties

Figure 2.4 shows the instrumentation used for the bulk rheological characterization. The dispersions in this work consist of low viscoelastic properties. The ideal geometry is a double concentric cylinder. A cross section shows that the geometry (in black) is submerged into the base (grey) filled with liquid (blue). The liquid covers both the inside and outside of the geometry once lowered into the base.

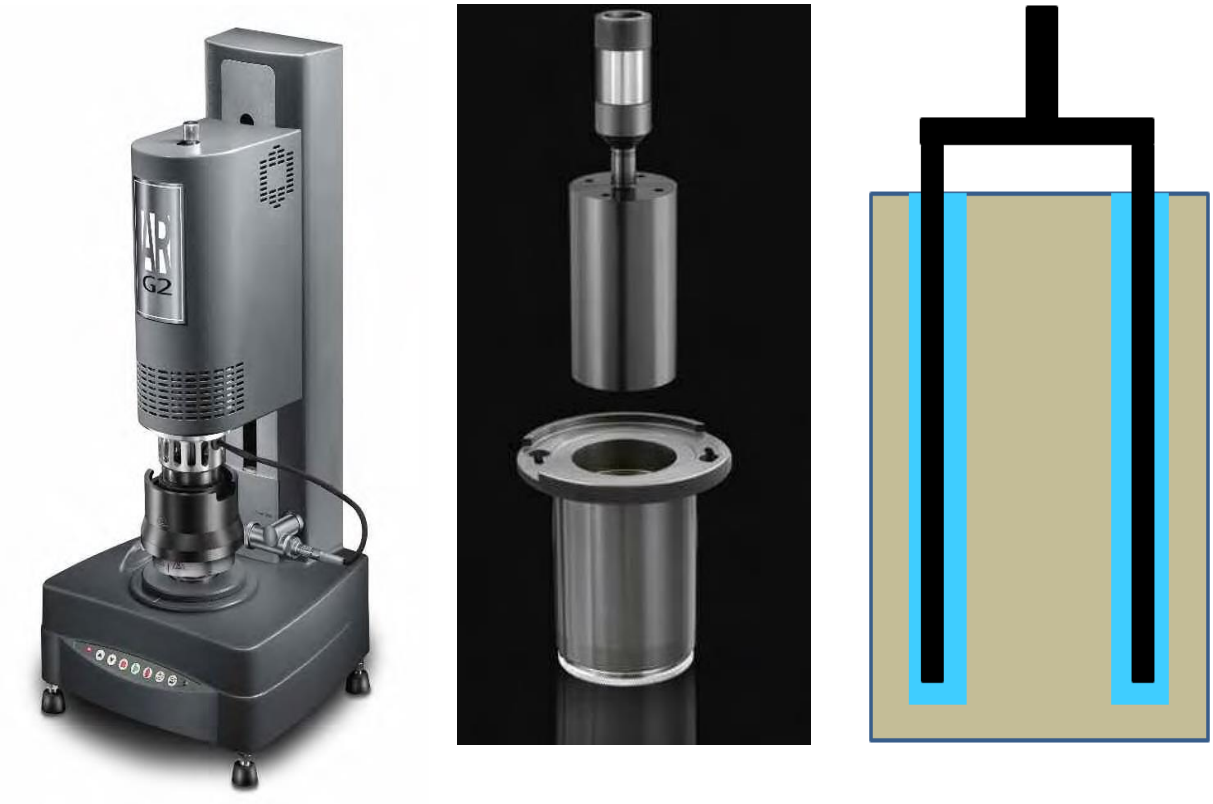

Figure 2. 4. TA2000ex Stress Rheometer (left), geometry (middle) and cross-section (right) of the double concentric cylinder used for bulk rheological characterization of aqueous Laponite with polymer dispersions.

2.3.1.1 Rheology

Rheology is the study of flow and deformation.[13] Rheology provides information on how a fluid behaves to a stress leading to structural information. For a pure solid the first simple relationship is Hooke's law, in that force is proportional to deformation:

$$\tau = G \cdot \gamma \qquad 1$$

where τ is the stress, γ is the strain or relative length change and G is the proportionality constant known as the elastic modulus. Elasticity is an intrinsic property of solids. For viscoelastic fluids, there is a time dependent response in stress and elastic moduli:

$$G(t) = \frac{\tau(t)}{\gamma} \quad (2)$$

The viscoelasticity of the laponite pluronic suspensions are measured by frequency sweeps to characterize suspension stability, polymeric repulsion and flocculation. All three of these phenomena show up directly in the frequency measurements.

For a pure liquid, Newton's viscosity law shows that stress is proportional to the strain rate, $\dot{\gamma} = \frac{d\gamma}{dt}$,

$$\tau = \eta \cdot \dot{\gamma} \quad (3)$$

where η, the Newtonian viscosity, is the constant of proportionality. In this work suspensions have both an elastic and viscous component that can be characterized.

In this work the Laponite and Pluronic system is considered a dilute suspension, or dispersion. Suspension rheology has general fluid and structural profiles. Suspensions are generally known to give a plastic yield during flow. In other words, there is minimal deformation up to a specific level of stress, the yield. Once this yield stress has been obtained the suspension flows readily. The Bingham model is as follows:

$$\tau = \tau_{yield} + \eta_{pl} \cdot \dot{\gamma} \quad (4)$$

In addition to flow and viscoelastic properties of dispersion, the adsorbed polymer changes the thickness of the particles, or volume, and ultimately changing the relative viscosity of the suspension through the following relationship:

$$\varphi_{eff} = \varphi_c \left(1 + \frac{\delta}{a}\right)^3 \quad 5$$

where φ_{eff} is the particle volume fraction with polymer, φ_c and *a* are the volume fraction and radius of the plain particle and δ is the adsorbed layer thickness. In dilute concentrations, the φ_{eff} can be determined from relative viscosity measurements by the following equation:

$$\frac{\eta_0}{\eta_s} = 1 + 2.5\ \varphi_{eff} = 1 + 2.5\ k\varphi_c \quad 6$$

where, η_0 and η_s are the suspension and filtrate viscosities, respectively.[14] A slope of the relative viscosity as a function of φ_{eff} gives a slope of k. This can be used to calculate the adsorbed layer thickness of the polymer on the particle. This work will focus on the bulk rheological properties of laponite pluronic suspensions to determine structural, flow and polymer layer thickness as it relates to foaming properties.

2.3.1.2 Thermal Gravimetric Analysis

Thermal Gravimetric Analysis[15] is a physical technique that measures the change in mass of a sample as a function of increasing temperature over time. A typical instrument consists of a 1. Sensitive analytical balance, 2. Furnace, 3. Inert purge gas, nitrogen in this work, 4. computer for control, data display and acquisition. A thermogram is generated and gives information of decomposition of samples. An additional feature to most TGA applications is the derivative of the thermogram that can

provide more information regarding a shift of a degradation product. TGA is a common technique that will provide a mechanism of degradation for thermal barrier improvements of Laponite Pluronic systems to identify foam film properties.

2.3.1.3 Dynamic Light Scattering

Dynamic Light Scattering[16] (DLS) is a useful technique that correlates how a monochromatic light beam passes through a liquid, scatters due to Doppler effect and decays over time to the size of the hydrodynamic radius of a spherical particle. DLS is useful for the determination of relative sizes of colloids and thickness of adsorbed polymer layers onto particles. DLS aids in understanding the interactions of the clay-polymer interactions. Polymer adsorption of polyethyleneoxides onto laponite has been studied to determine hydrodynamic polymer thickness.[17] It is well known that Laponite is an anisotropic clay platelet. DLS data is generated from an autocorrelation function (ACF). DLS is related to the relaxation time, τ, to that of the diffusion coefficient of a spherical particle, D:

$$g_2(Q,t) - 1 = e^{\left(-\left(\frac{2t}{\tau}\right)\right)} = e^{(-2DQ^2t)} \qquad 7$$

t is the correlator decay time; Q is the scattering vector (Intensity), Q= (4πn/λ) sin (θ/2). *n* is the refractive index of the solution, λ is the wavelength of the light and θ is the scattering angle. D is related to the hydrodynamic radius of the spherical particle, R_h, via the Stokes-Einstein equation $D = \{k_BT\} / \{6\pi\eta R_h\}$, where k_B is the Boltzmann constant, T is the absolute temperature and η is the solvent viscosity. In this work DLS will be used to characterize the particle size of Laponite, adsorbed layer thickness and

interactions it has with polymer systems of Polyethylene glycol (hydrophilic component of Pluronics, Mw=2000g/mol), Pluronic 17R4 (defoamer) and Pluronic L62 (foamer).

2.3.1.4 Zeta Potential

Electrophoretic mobility (EPM) is used to characterize surface charge of clays in solution by measuring the velocity of clay in an applied electric field which is detected by a phase angle shift in the monochromatic light shifted.[18,19,20] Surface charge aids in understanding the dispersion stability in relation to the charge of the clay. Surface charge of clays changes in the presence of polymers. For instance, addition of polyethyleneoxide polymers onto Laponite has been characterized for Laponite systems using electrophoretic mobility, small angle neutron scattering and rheology.[21,22] Very stable suspensions have strong electrostatic charges, whether positive or negative. This strong particle charge stabilizes the particle by resisting aggregation. As the particle approaches zero charge, instability of the particle occurs which leads to coagulation.

Commonly, Zeta Potential (ζ) is calculated from the electrophoretic mobility (μ) determined at a given temperature. In this study, kα>> 1(k- Debye-Huckel parameter and α is a calculated particle radius), the Smoluchowski relationship was used:

$$\zeta = \eta\mu/\varepsilon \qquad 8$$

where η is the viscosity of the medium, μ is the electrophoretic mobility (EPM) of the particle and ε is the dielectric constant of the medium. Laponite is known to have a very negative charge on its surface. In this study, EPM is used to give a more representative value, since these suspensions are not ideal.

2.3.1.5 Streaming Current Potential

Streaming Current Potential (SC) is a complementary technique to electrophoretic mobility. Figure 2.5 shows the experimental differences between EPM and SC. However, the setup for SC is through a piston creating a mechanical shearing effect giving an output voltage. Electrophoretic mobility is through an applied voltage. Classically, streaming potential is used to determine the end point of a colloid by titration of an oppositely charged electrolyte.[23] SC models are based solely on endpoints and not much emphasis is based on the shapes of the SC curves.[24] The following work characterizes the shape of the SC curves and relate to electrophoretic results of zeta potential for the laponite charge as a function of pluronic.

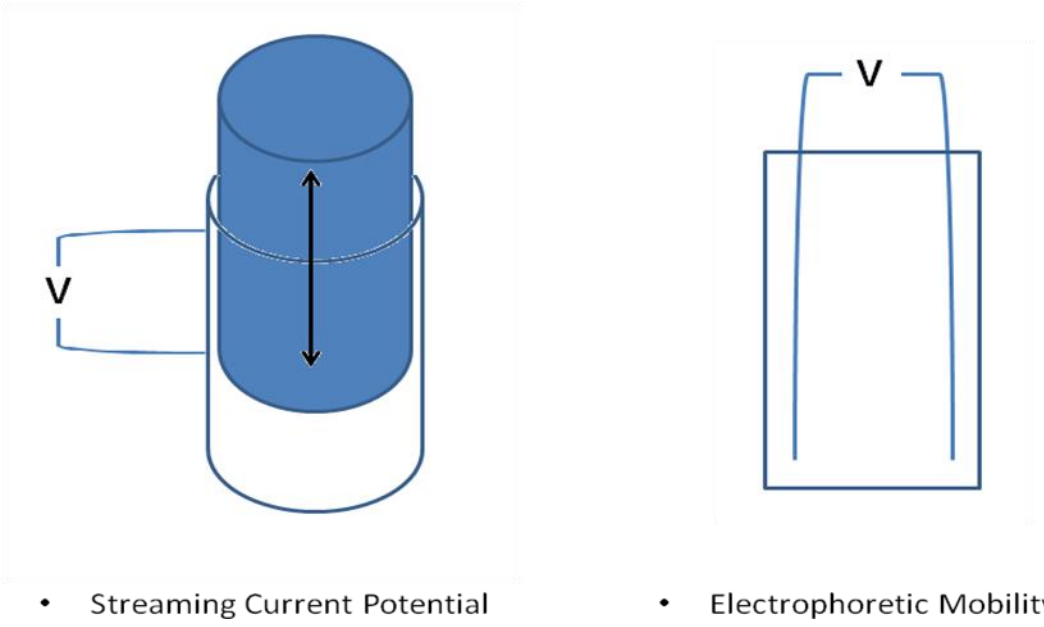

Figure 2. 5. Streaming Current Potential (left) and Electrophoretic Mobility (right) experimental cell designs.

Coverage of the polymer and changes in bulk viscosity has shown to improve the foam stability.[25,26] Ultimately this leads to a reduction in drainage. Challenges to overcome for foam stability would be to control hydrophobicity at the interface. Another challenge would be to use colloids to provide more elasticity, or structure, at the interface while maintaining a balance of surfactant and particle concentration.

2.3.1.6 Adsorption Affinity

Table 2. 3. General Adsorption Modes with relative Adsorption Energy, Time of Stay and Surface Concentration,

Adsorption Energy (Q, kcal/mol)	Time of Stay (τ, seconds)	Surface Concentration (Γ, mol/cm²)	Mode
Low	Fast	Low	No Adsorption
Moderate	Moderate	Moderate	Physisorption
High	Slow	High	Chemisorption

Adsorption can be divided into three main areas provided by Table 2.3. The most common mode for polymer adsorption onto laponite suspension is a physisorption. In this work, adsoprtion isotherms are used to determine the affinity of the polymers, adsorbate, to the laponite particle, adsorbent. There are many models that describe mechanisms of the adsorption process each with advantages and limitiations. These models include: Freundlich, Langmuir, Redlich-Peterson, Temkin and Dubinin-Radushkevich. The Langmuir equation is as follows:

$$\frac{c}{Y} = \frac{1}{kY_{max}} + \frac{c}{Y_{max}} \quad (9)$$

where c is the total concentration of solute, Y is the molar ratio of adsorbate per adsorbent, Y_{max} is the ratio at which the adsorbent is covered with a monomolecular layer of adsorbate and k is the binding constant. This work will focus on the Pluronic polymer affinity with Laponite to understand how this relates to foam properties.

2.3.2 Interfacial

2.3.2.1 Surface Energy of Films

Contact Angle of water has been used to characterize the hydrophobicity of particles in particle stabilized foams.[27] Optimal contact angles for particles fall between 70° and 90°.[28] Contact angle is a measurement of a liquid droplet on a surface. This droplet interacts with the gas and solid to give a measureable contact angle. This can give insight to the surface energy forces present in the solid, or film. The central theme to this measurement is the Young-Dupre equation:

$$\gamma_{LV} \cdot \cos\theta = \gamma_{SV} - \gamma_{SL} \quad (10)$$

where γ is the interfacial tension between two phases indicated by the subscripts (S: solid, L: liquid and V: vapor).

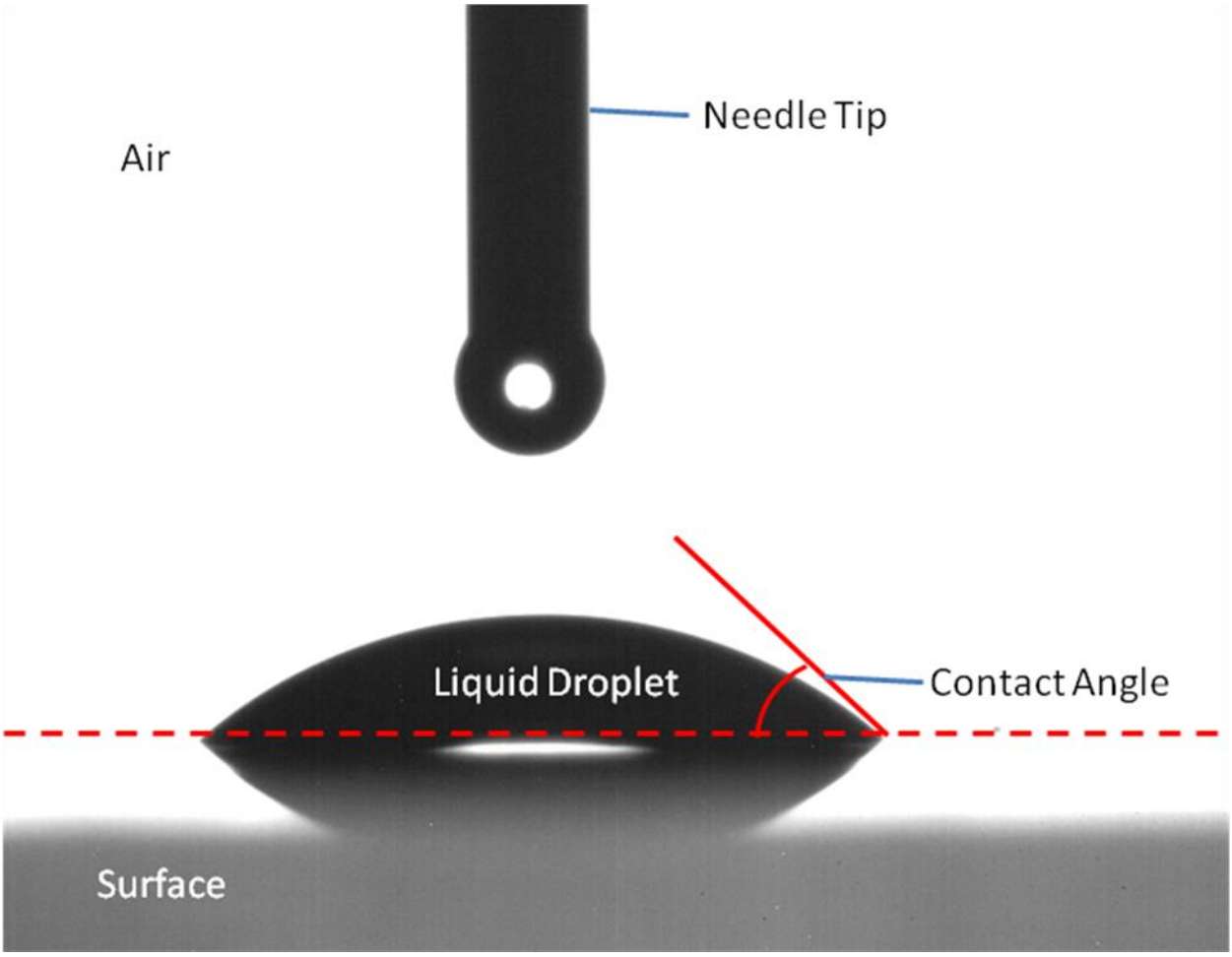

Figure 2. 6. Sessile Droplet Technique used to determine Surface Energy of Laponite with Polymer films.

Figure 2.6 is a 5 μL water droplet on a laponite film with Pluronic L62. Different liquids on the same surface will result in different contact angles. This is an important feature to firefighting applications due to Class B fires which are a result to volatile solvents not miscible with water. A solvent could drop on the Laponite film to determine the miscibility. Another way to look at this is will the liquid spread, “like the film”.

In general all three phases of matter have surface force components. Derjaguin-Landau-Verwey-Overbeek[29,30] (DLVO) interactions recognizes there is a balance of competing forces for colloid (suspension) stability in regards to potential net energy (Gibbs free energy) of the colloidal system.

$$V_T = V_A + V_R + V_B + V_S \quad (11)$$

The total potential energy of the colloid system depends on V_T. The nature of the dispersion gives way to four contributing forces to make up the total potential energy of the colloid system. The attractive interaction of the system is understood to be the van der Waals force, V_A. The repulsive electrostatic interaction of the colloid is known as the Electrical Double Layer of the colloid (V_R), looked at through zeta potential studies in this work. The polar component for the equation accounts for the Lewis Acid Base interactions (V_B). The energy from the solvent, V_S, is negligible in comparison to the other three forces.

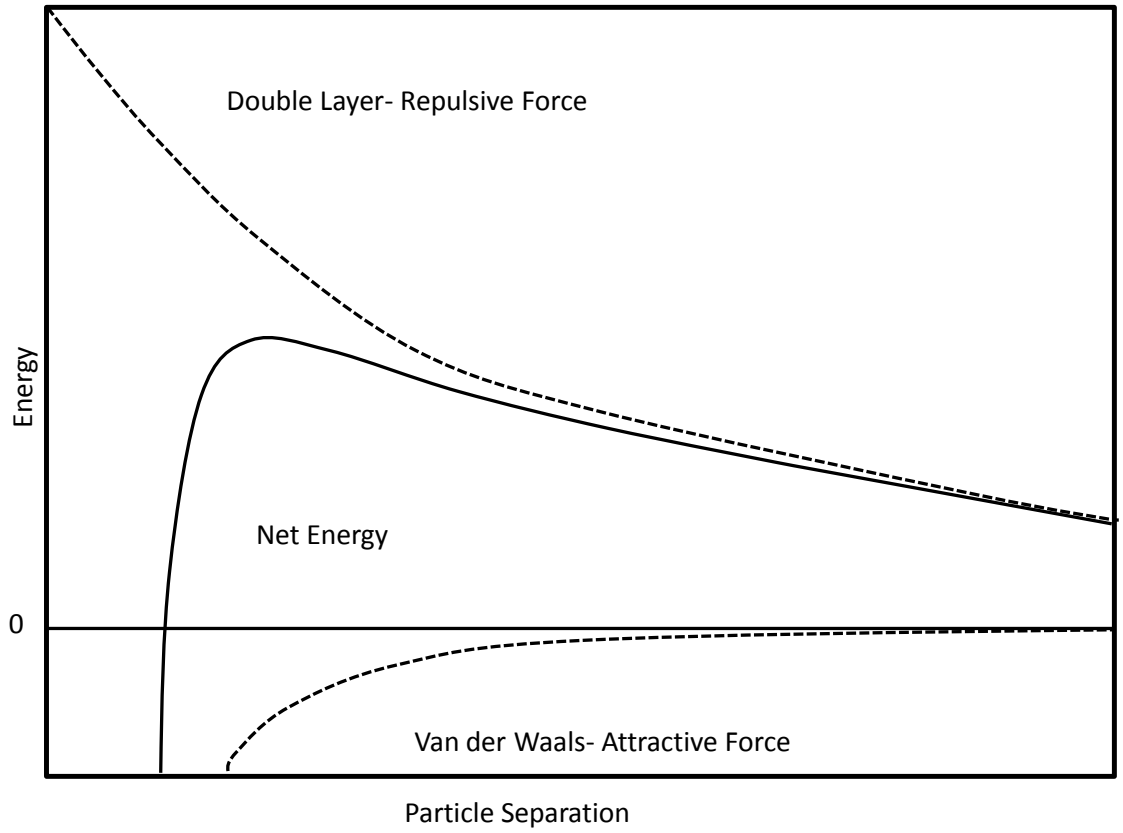

Figure 2. 7. Free Energy Diagram for Particle Forces based on DLVO theory.

From Figure 2.7, DLVO theory recognizes there is a balance of competing forces for colloid stability in regards to potential net energy (Gibbs free energy) of the colloidal system. The attractive interaction of the system is understood to be the van der Waals force, V_A.

$$V_A = -A/(12\pi D^2) \qquad 12$$

Hamaker assumption is denoted as A, which accounts for only two spherical particles ignoring the influence of the medium. As the distance increases from the particle surface, D, the van der Waals energy decays.

The repulsive electrostatic interaction of the colloid is known as the Electrical Double Layer of the colloid (V_R).

$$V_R = 2\,\pi\,\varepsilon\,\alpha\,\zeta^2\,exp^{-\kappa D} \quad (13)$$

Where α is the Stokes radii of the particle; ε is the dielectric constant of the medium, 80 for water; ζ is the zeta potential of the surface at the slipping plane, measured in electrostatic volts; κ is the inverse of the Debye length, which is the thickness of the double layer; D is this instance is the distance between the particles from the surface.

The polar component for the equation accounts for the Lewis Acid Base interactions (V_B):

$$V_B = -2\pi\,\alpha\,\lambda\,\gamma_B\,e^{(10-l)\gamma} \quad (14)$$

where λ is the decay length of the liquid molecule, i.e. water; γ is the interfacial surface energy from contact angle of the particle and medium, i.e. γ is derived from the Young-Dupré model.

Contact angle, θ, measurements can be used to determine DLVO interactions, specifically polar and van der Waals surface energy interactions from the following equations:

$$1 + cos\theta = 2\sqrt{\frac{\gamma_S^{LW}}{\gamma_L}} \quad (15)$$

where γ_S^{LW} is the nonpolar surface energy of the solid and γ_L is the surface energy of an apolar liquid of choice and θ is the contact angle from the apolar liquid on the solid surface. This equation is commonly refered to as the Young-Good-Girifalco-Fawlkes equation.

To account for polar forces, Lewis acid base interactions, of the colloid, the following applies:

$$(1 + cos\theta)\gamma_L = 2\left(\sqrt{\gamma_S{}^{LW}\gamma_L{}^{LW}} + \sqrt{\gamma_S{}^{+}\gamma_L{}^{-}} + \sqrt{\gamma_S{}^{-}\gamma_L{}^{+}}\right) \quad 16$$

The γ^+ and γ^- are the electron donor and electron acceptor surface energy components of the solid and liquid phases. This work focuses on finding all DLVO components for the Laponite and Pluronic L62 surfaces forces and how this contributes to the foaming and spreading properties.

2.3.2.2 Interfacial Shear

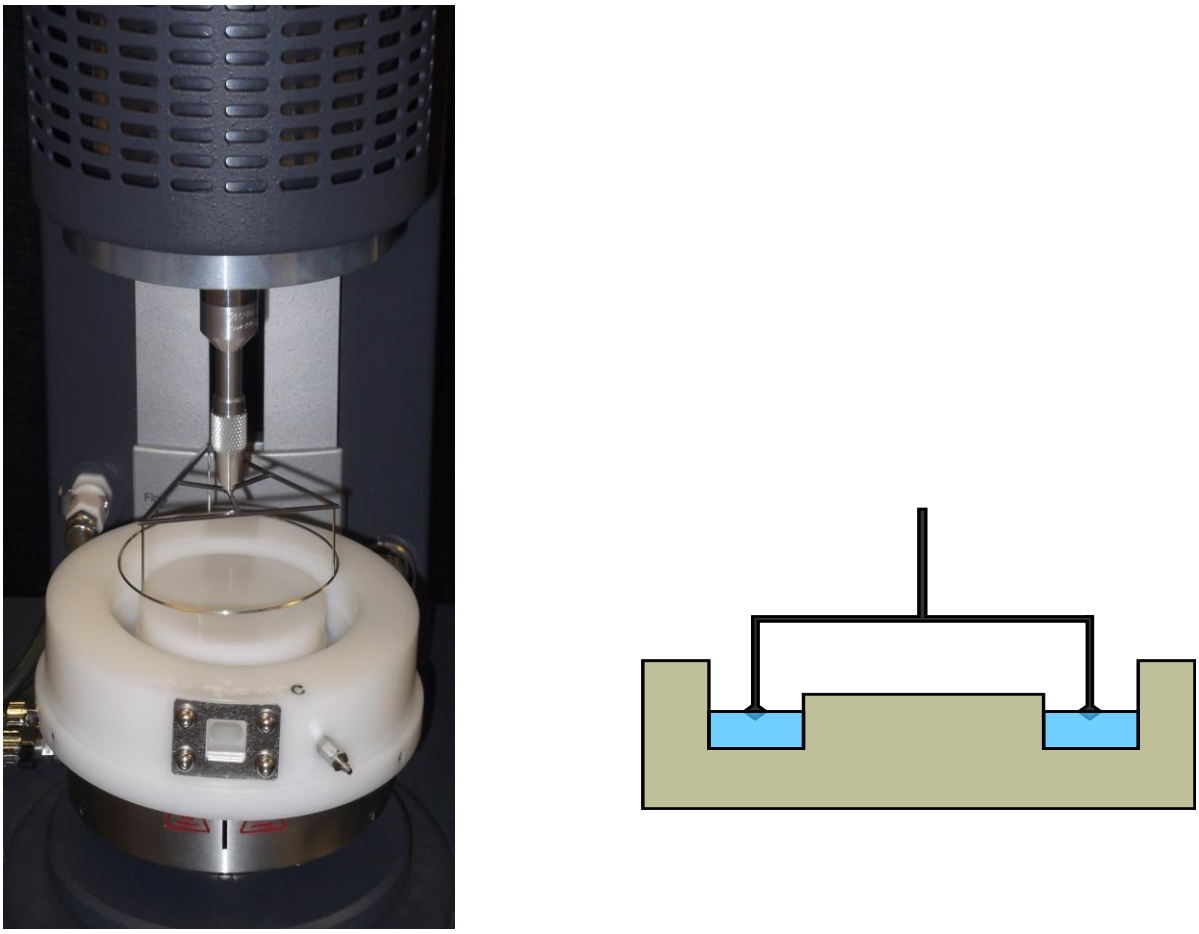

Figure 2. 8. ARG2 Stress Rheometer with geometry (left) and cross-section (right) of the Double Wall Ring to study the interfacial oscillation and flow of aqueous Laponite with polymers.

The same approach to elasticity and viscosity applies in the bulk as with the interfacial apparatus. From Figure 2.8, the geometry used is called the double wall ring (DWR) to investigate the interfacial flow and elasticity response. The DWR is made of Iridium/Platinum. The suspension is placed in a reservoir, the ring is lowered until it lies flat to the surface. One of the challenges of interfacial rheometers is the flow profile of

the interface and bulk phases.[31] This is related by a dimensionless number called the Boussinesq number that describes the surface and bulk drag for a defined shear flow:

$$B_0 = \frac{surface\ drag}{subphase\ drag} = \frac{\eta_S \cdot \frac{V}{L_I} \cdot P_I}{\eta \cdot \frac{V}{L_S} \cdot A_S} = \frac{\eta_S}{\eta \cdot G} \quad 17$$

where η_s is the magnitude of the surface shear viscosity in steady shear flow (Pa s m), η is the average bulk viscosity (Pa s), V is velocity (m/s), L_I and L_S are length scales which the viscosity decays at the interface and subphase, respectively (m), P_I is the contact perimeter between the surface probe and interface (m), A_S is the contact area between the geometry and surrounding subphase (m^2). The Boussinesq number depends on the ratio between surface and bulk viscosities and the length scale G, dependent upon geometry dimensions. The DWR maximizes the B_0 where interfacial stresses dominate and surface rheological properties can be calculated. At high frequencies, the effect of fluid inertia must be accounted captured by the Reynolds number. High frequencies will not be a concern in this work. This work focuses on the interfacial shear properties of Laponite Pluronic L62 aqueous films as it relates to foam drainage.

2.3.2.3 Dilatational Rheology

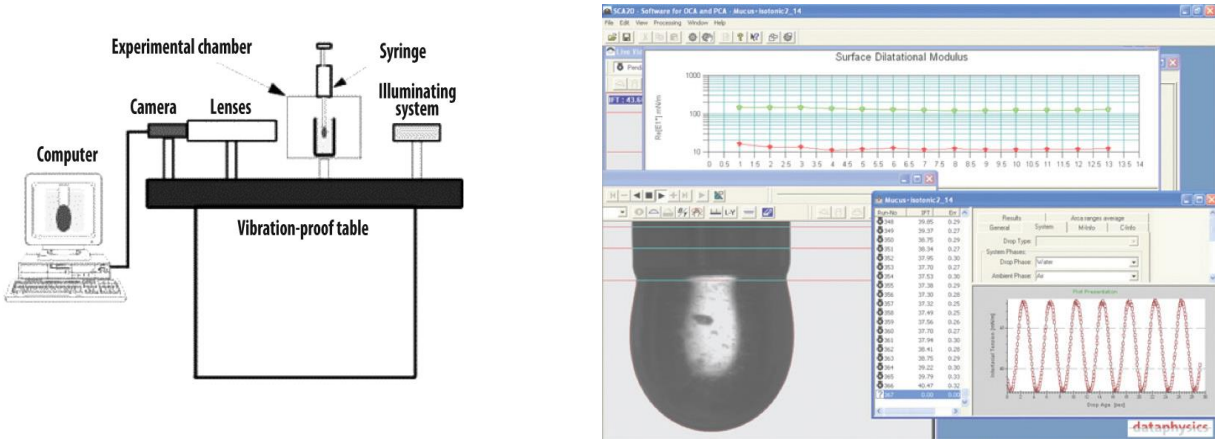

Figure 2. 9. Oscillating Drop Generator for dilational rheology

From Figure 2.9, the dilatational approach can be measured by oscillating a pendant drop of liquid that is attached to a piezo electric device which controls the oscillation and captured images using a high speed camera. The images are fitted to the Laplace equation providing surface tension and volume from the drop shape. The continuous variation can give us the surface dilatational surface moduli. The Gibbs interfacial dilatational modulus is given by a small change in surface tension, γ, relative to a change in surface area, A:

$$E = d\gamma / dA \qquad 18$$

The drop is oscillated back and forth, expanding and contracting the bubble, leading to two contributions: an elastic (structural/recoverable), E', and viscous (loss/relaxation), E", component. These are real and imaginary components to the Gibbs elasticity: ω=E'+*i*E". For sinusoidal oscillations the following applies:

$$E' = \Delta\gamma \frac{A_0}{\Delta A} \cos\varphi \quad (19)$$

$$E'' = \Delta\gamma \frac{A_0}{\Delta A} \sin\varphi \quad (20)$$

where Δγ is the amplitude in the periodic surface tension, A^0 is the surface area of the drop before oscillation, ΔA is the amplitude of the interfacial deformation and φ is the phase angle between area and surface tension curves. Determination of E' and E", surface area and tension are measured as a function of time from drop shape analysis. A least squares fitting method is used on γ(t) and A(t) using the following equations to obtain Δγ, A^0, ΔA and φ:

$$A(t) = A_0 + \Delta A \cos(\omega t + \varphi_1) \quad (21)$$

$$\gamma(t) = \gamma_0 + \Delta\gamma \cos(\omega t + \varphi_2) \quad (22)$$

where γ_0 is the average surface tension and $\Phi=\varphi_1-\varphi_2$.

2.3.2.4 Film Drainage- Lamella Break Point

Film drainage is retarded by the Marangoni effect as discussed earlier. When the lamella is stretched thinning occurs until a break point. Stretching the lamella, reduces the surface concentration of the particle while increasing the surface area of the film. The magnitude of the Maragoni effect is a function of the surface dilatational viscosity of the lamella by:

$$\eta_d = \frac{\Delta\gamma}{d\ln A/dt} \quad (23)$$

2.3.2.5 Extensional Filament Strength

This work provides a new concept to foam drainage by incorporating a novel Extensional flow device. It is based on step strain effect of the fluid placed between two parallel plates and one is rapidly pulled back to a set distance and the fluid is drains under gravitational forces, and is dependent upon two competing forces, fluid viscoelasticity and surface tension contributions. A thumb and finger stretch test is a common concept. Extensional rheology is a simple method that monitors the stretch of a fluid. Initial work using a capillary break up method was investigated using simple viscous and elastic solutions.[32] The experiment involves two basic parts:

- Initial stretch of fluid
- Capillary Break up of fluid diameter
    - Governed by surface tension, elasticity and polymers extensional viscosity

The most important result of this experiment is the fluid break up time. From this raw data an apparent extensional viscosity can be calculated. Extensional viscosity of a fluid is characterized by its midpoint diameter with respect to time:

$$\bar{\eta}_{app}(\dot{\varepsilon}) = \frac{[t_{ss} - t_{rr}]}{\dot{\varepsilon}(t)}; \quad \dot{\varepsilon} = -\frac{2}{D}\frac{dD_{mid}(t)}{dt} \qquad 24$$

Combining the equations gives:

$$\bar{\eta}_{app}(\dot{\varepsilon}) = \frac{k\sigma}{\frac{dD_{mid}(t)}{dt}}; \quad \varepsilon = \ln\left(\frac{D_0}{D_{mid}(t)}\right) \qquad 25$$

Extensional viscosity is proportional to the fluids surface tension and the change of the filament diameter with respect to time. The CaBER 1 ® (Capillary Breakup Extensional Rheometer) is shown in Figure 2.10.

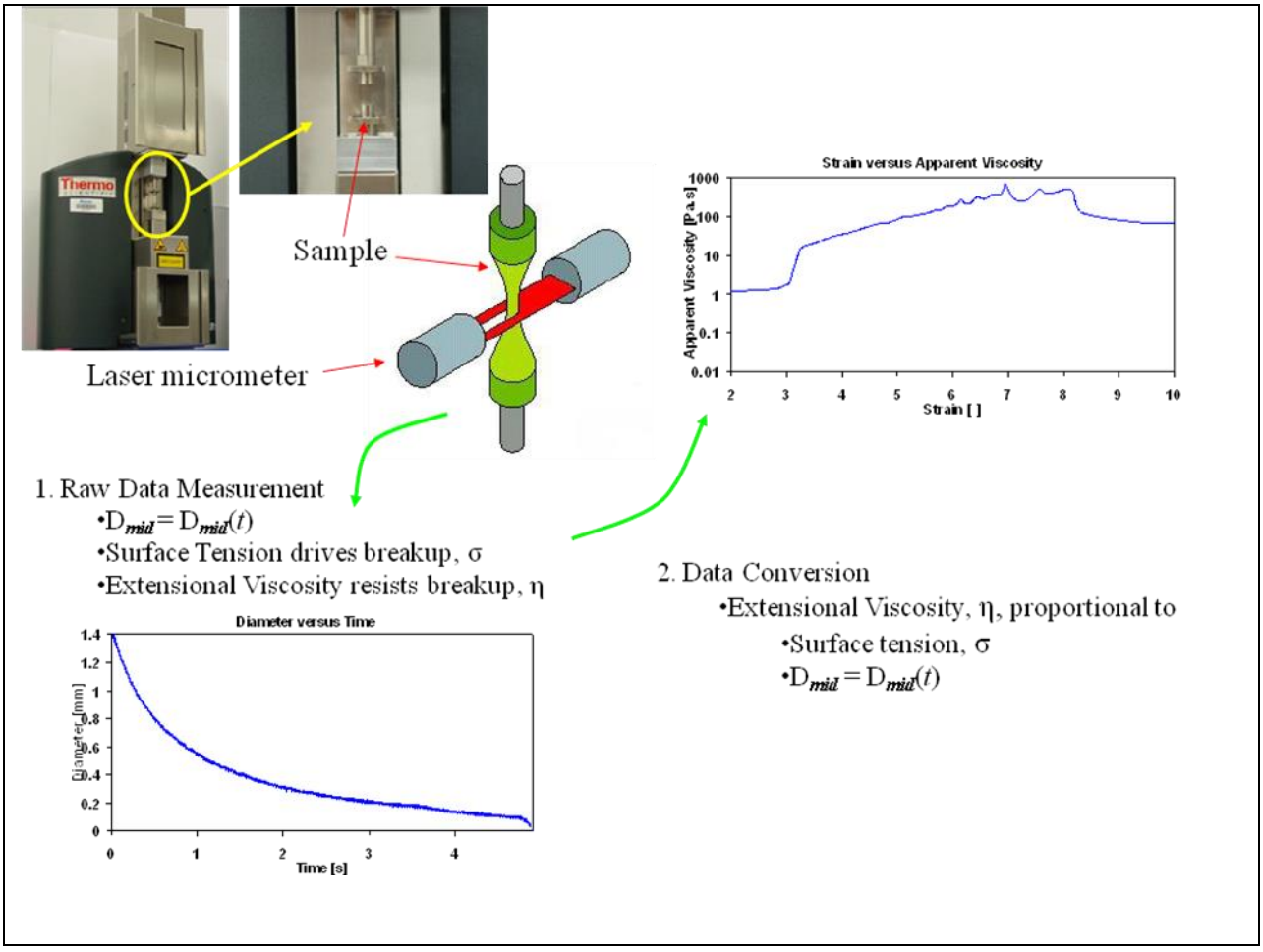

Figure 2. 10. CaBER instrument with a summary diagram of what raw data is generated and data conversion of what is obtained.

The following parameters were used in the experiments.

- Laser micrometer with a resolution of 5μm and response time of <1ms

- Drive system
    - Linear stretch of 50ms was optimal
- Plate Diameter: 6mm
- Initial Aspect Ratio: 1
- Final Aspect Ratio: 4.0
- Temperature: 25˚C

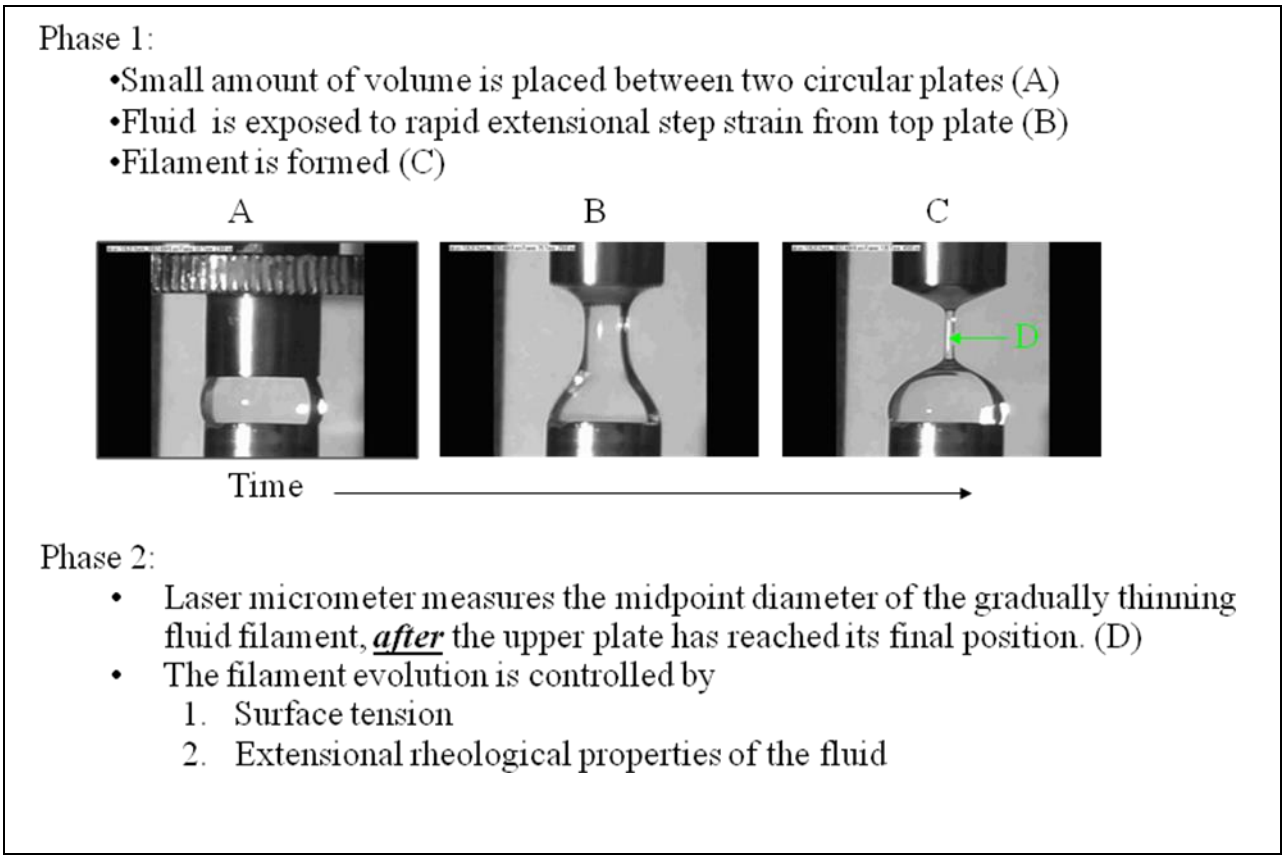

Figure 2. 11. How Capillary Breakup Extensional Rheometer works.

Figure 2.11 shows how the extensional rheology experiment works. A laser micrometer follows the diameter of the fluid until breakup. The fluid is pulled apart very quickly and then separates over time. The focus of this work is on the utility to

differentiate by a novel mechanism to foaming technology and characterize the Laponite Pluronic suspensions filament strength and correlate this to foam stability.

2.3.3 Foam Drainage

There are numerous types of foam drainage techniques that differ on how the foam is mainly generated. The focus of this study utilizes the high shear mixer due to the end use application in firefighting foam technology.

Foams are dispersions of gas in a continuous liquid phase, in a state of quasi-equilibrium.[33] After a foam is generated it irreversilbly flows under gravity due to the major difference in density of the air and liquid, water in this case. This has led to the development of foam drainage equations that have already been introduced. Foam drainage experiments were performed for a series of Laponite Pluronic systems and followed in 100mL and 250mL graduated cylinders made from polymethylpentene (PMP). PMP is a low surface energy material with contact angles using deionized water greater than 90°. This is important because many experimental setups use glass equipment. The liquid portion of the foam has an affinity with the glass leading to an unnecessary interaction with the column wall. PMP will not have this effect. Both the foam height and drainage levels were followed up to steady state.

2.4 Chapter Conclusions

This chapter discusses in detail the most relevant techniques and tools to characterize, understand and provide advanced models for the development and optimization of a particle stabilized foam (i.e. bulk properties- rheological, TGA, adsorption isotherm, electrostatic and DLS; interfacial properties- Sessile Droplet, DWR (interfacial flow),

ODG (dilatational rheology), Low Angle XRD and Adhesion; foaming- production, drainage and Capillary Break up Rheology. Practical applications of these techniques and methods will be further elaborated for bulk properties (Chapter 3), interfacial properties (Chapter 4), and foaming properties (Chapter 5), for the application in firefighting applications.

2.5 References

(1) Chen, L.F; Liang, H.W.; Lu, Y.; Cui, C.H.; Yu, S.H., Synthesis of an Attapulgite Clay@Carbon Nanocomposite Adsorbent by a Hydrothermal Carbonization Process and the Application in the Removal of Toxic Metal Ions from Water, *Langmuir*, **2011**, *27*, 8998-9004.

(2) Wallis, P.J.; Gates, W.P.; Patti, A.F.; Scott, J.L., Catalytic Activity of Choline Modified Fe(III) Montmorillonite, *Applied Clay Science*, **2011**, *53*, 336-340.

(3) Chen, Q; Kerk, W.T.; Soutar, A.M.; Zeng, X.T., Application of Dye Intercalated Bentonite for Developing Latent Fingerprints, *Applied Clay Science*, **2009**, *44 (1-2)*, 156-160.

(4) Patro, T.U.; Wagner, H.D., Layer-by-layer Assembled PVA/Laponite Multilayer Free-Standing Films and their Mechanical and Thermal Properties, *Nanotechnology*, **2011**, *22*, 455706 1-12.

(5) http://www.laponite.com.

(6) Li, P.; Kim, N.H.; Hui, D.; Rhee, K.Y.; Hee, J., Improved Mechanical and Swelling Behavior of the Composite Hydrogels prepared by Ionic Monomer and Acid-Activated Laponite, *Applied Clay Science*, **2009**, *46 (4)*, 414-417.

(7) Li, Y.C.; Schulz, J.; Grunlan, J.C., Polyelectrolyte/Nanosilicate Thin Film Assemblies: Influence of pH on Growth, Mechanical Behavior and Flammability, *Applied Materials & Interfaces*, **2009**, *1 (10)*, 2338-2347.

(8) http://www.laponite.com.

(9) Blanton, T.N.; Majumdar, D.; Melpolder, S.M., Microstructure of Clay-Polymer Composites, *Advances in X-Ray Analysis*, **2000**, *42*, 562-568.

(10) Zhang, S.; Lan, Q.; Liu, Q.; Xu, J.; Sun, D.; Aqueous Foams Stabilized by Laponite and CTAB, *Colloids and Surfaces A: Physicochemical Engineering Aspects*, **2008**, *317*, 406-413.

(11) Negrete-Herrera, N.; Puteaux, J.L.; David, L.; De Haas, F.; Bourget-Lami, E., Polymer/Laponite Composite Latexes: Particle Morphology, Film Microstructure and Properties, *Macromolecular Rapid Communication*, **2007**, *28 (15)*, 1567-1573.

(12) Tadros, T.F., Applied Surfactants: Principles and Applications, Wiley VCH, **2005**, Germany, 267-274.

(13) Macosko, C. W., Rheology: Principles, Measurements and Applications, Chapter 3. VCH, New York, **1994**.

(14) Weiss, A.; Dingenouts, N.; Ballauff, M., Comparison of the Effective Radius of Sterically Stabilized Latex Particles Determined by Small-Angle X-ray Scattering and by Zero Shear Viscosity, *Langmuir,* **1998**, *14*, 5083-5087.

(15) Skoog, D.A.; Leary, J.J., Principles of Instrumental Analysis, 4th ed., Ch 23, Harcourt Brace College Publishing, **1992**.

(16) Berne, B.J.; Pecora, R., Dynamic Light Scattering with Applications to Chemistry, Biology and Physics, Dover Publications, New York, **2000**.

(17) Nelson, A.; Cosgrove, T., Dynamic Light Scattering Studies of Poly(ethylene oxide) Adsorbed on Laponite: Layer Conformation and Its Effect on Particle Stability, *Langmuir*, **2004**, *20*, 10382-10388.

(18) Bergaya, F.; Theng, B.K.G.; Lagaly, G., Handbook of Clay Science Developments in Clay Science, Vol. 1, Elsevier Ltd, **2006**.

(19) Delgado, A.; Gonzalez-Caballero, F.; Bruque, J.M., On the zeta potential and surface charge density of montmorillonite in aqueous electrolyte solutions, *Journal of Colloid and Interface Science*, **1985**, *113 (1)*, 203-211.

(20) Barron, W.; Murray, B.S.; Scales, P.J.; Healy, T.W.; Dixon, D.R.; Pascoe, M., The streaming current detector: A comparison with conventional electrokinetictechniques, *Colloids and Surfaces A: Physicochemical and Engineering Aspects*, **1994**, *88 (2-3)*, 129-139.

(21) Morariu, S., Bercea, M., Effect of Addition of Polymer on the Rheology and Electrokinetic Features of Laponite RD Aqueous Dispersions, *Journal of Chemical Engineering Data*, **2009**, *54*, 54-59.

(22) Nelson, A.; Cosgrove, T., Small-Angle Neutron Scattering Study of Adsorbed Pluronic Tri-Block Copolymers on Laponite, *Langmuir*, **2005**, *21*, 9176-9182.

(23) Pelton, R.; Cabane, B.; Cui, Y.; Ketelson, H., Shapes of Polyelectrolyte Titration Curves. 1. Well-Behaved Strong Polyelectrolytes, *Analytical Chemistry*, **2007**, *79*, 8114-8117.

(24) Cui, Y.; Pelton, P.; Ketelson, H., Shapes of Polyelectrolytes. 2. The Deviant Behavior of Labile Polyelectrolytes, *Macromolecules*, **2008**, *41 (21)*, 8198-8203.

(25) Liu, Q.; Zhang, S.; Sun, D.; Xu, J., Aqueous Foams Stabilized by Hexylamine-Modified Laponite Particles, *Colloids and Surfaces A: Physicochemical Engineering Aspects*, **2009**, *338*, 40-46.

(26) Liu, Q; Zhang, S.; Sun, D.; Xu, J., Foams Stabilized by Laponite nanoparticles and alkylammonium bromides with different alkyl chain lengths, *Colloids and Surfaces A: Physicochemical Engineering Aspects*, **2010**, *355*, 151-157.

(27) Karakashev, S.I.; Ozdemir, O.; Hamptom, M.A.; Nguyen, A.V., Formation and Stability of Foams Stabilized by Fine Particleswith Similar Size, Contact Angle and Different Shape, *Colloids and Surfaces A: Physicochemical Engineering Aspects*, **2011**, *382*, 132-138.

(28) Stevenson, P., Foam Engineering: Principles and Applications, John Wiley & Sons Publishing, New York, **2012**, 125-130.

(29) Norris, J.; Giese, R.F.; Costanzo, P.M.; Van Oss, C.J., The Surface Energies of Cation Substituted Laponite, *Clay Minerals*, **1993**, *28*, 1-11.

(30) Van Oss, C.J.; Giese, R.F.; Costanzo, P.M., DLVO and Non-DLVO Interactions in Hectorite, *Clay Minerals*, **1990**, *38 (2)*, 151-159.

(31) Vandebril, S.; Franck, A.; Fuller, G.G.; Moldenaers, P.; Vermant, J., A Double Wall-Ring Geometry for Interfacial Shear Rheometry, *Rheologica Acta*, **2010**, *49*, 131-144.

(32) Rodd, E. L.; Scott, T. P.; Cooper-White, J. J.; McKinley, G. H., Capillary Breakup Rheometry of Low-Viscosity Elastic Fluids, *Applied Rheology*, **2005**, *15*, 12–27.

(33) Prud'homme, R.K.; Khan, S.A., Foams: Theory, Measurements, and Applications, Surfactant Science Series 57, **1996**, Marcel Dekker, New York.

CHAPTER 3

BULK PROPERTIES OF LAPONITE PLURONIC DISPERSIONS

3.1 Introduction

Suspensions of clays yield a wide variety of end-use applications ranging from wastewater treatment[1], cosmetic[2], novel nanocomposite materials[3] (firefighting use in this work), inks and paints[4]. These applications stem from the clays mechanical[5] or rheological[6,7], thermal[8], electrophoretic[9], streaming potential[10], aggregation[11] and adsorptive[12] properties.

Incorporation of electrolytes or polymers into clay suspensions have shown to modify the rheological and electrokinetic properties.[13] This is particularly important from a barrier perspective. In general, addition of electrolytes to clays induces aggregation therefore leading to enhanced rheological properties.[14] Addition of polymer provides an advantageous attribute for a clay suspension by providing a steric barrier from aggregation.[15] In firefighting applications electrolytes and polymers are both utilized but the components are not well understood.

Rheological and thermal properties of 17% Pluronic F127 with Laponite[16] have been investigated for medical applications. Rheological and small angle X-ray scattering was used to characterize the contribution of Laponite to 50% Pluronic P123 for soap and cleaning applications.[17] The adsorbed high molecular weight Polyethyleneoxide onto Laponite in dilute ranges and related to dispersion stability.[18] DSC discriminated between the functionality of Polyetethyleneglycols (PEG), Propyleneglycols(PPG) and Pluronic L64 interactions with Laponite RD when mixed in the molten state.[19]

Microcalorimetry work provided a fundamental mechanism of thermodynamic adsorption for PEG and PPG interactions with Laponite in very dilute concentrations.[20] These studies are important but not relevant nor advantageous for firefighting applications.

DLS, Small Angle Neutron Scattering (SANS) and adsorption studies of Laponite with PEO[21] and nonionic surfactants of $(Methyl)_x$-EO_y on hydrophilic colloidal silica, Ludox AS40,[22] have been characterized to understand the adsorption layer thickness and adsorption affinity properties, respectively. DLS and SANS provided the adsorbed layer thickness of high molecular weight PEO at very dilute regions for both Laponite and PEO but none have probed Pluronic surfactants, which have both a hydrophilic and hydrophobic component. SANS demonstrated that PEO at 100K g/mol can slow down and prevent gellation at Laponite concentrations higher than 2%.[23] SANS measurements for varying Pluronic systems (4K to 15K g/mol) on 0.05% Laponite concentrations increased layer thicknesses with increasing PEO block length of the Pluronic.[24] The adsorption isotherm of the diblock demonstrated an incomplete bilayer upon saturation plateau region. Adsorption isotherms of pluronics have been investigated with other clays demonstrating a Langmuir profile.[25]

This chapter discusses the bulk properties of Laponite aqueous dispersions with Pluronic L62, a wetting and foaming nonionic surfactant, Pluronic 17R4, a wetting and defoaming nonionic surfactant, and a Polyethyleneoxide, a hydrophilic homopolymer with no wetting or foaming properties. Investigating these three functional provides a mechanism of how Laponite and Pluronic L62 interact advantageously through bulk properties that can impact particle stabilized foams. In addition this chapter facilitates

how the different types of polymer structure and hydrophilicity impact particle stabilized foams.

3.2 Experimental

The rheology of suspensions was characterized with a AR2000ex Rheometer. The geometry used was an anondized aluminum double concentric cylinder. Two types of experiments were performed 1. oscillation, i.e. stress and frequency sweeps, and 2. steady state flow. In certain instances, a temperature ramp up was performed as well. The stress sweep parameters are as follows: equilibration of 10 minutes after the gap was set at the correct level, stress swept from 0.1 μNm to 1000 μNm with 5 steps each decade in logarithmic mode and the frequency was set at 10 Hz. Once the Linear Viscoelastic Region was determined, a frequency sweep was performed as follows: equilibration of 10 minutes after the gap was set, frequency sweep was from 0.1 Hz to 100 Hz at at stress of 100 μNm. In specific instances, Frequency and Stress sweep experiments outside of these parameters will be identified in the results and discussion. The temperature ramps were held at a constant stress of 10 μNm and a constant frequency of 10 Hz with a temperature ramp from 25 °C to 60 °C at a rate of 1 °C/min. In the steady state flow experiments, there was a ramp up and ramp down in torque. The ramp up (ramp down was in opposite order) torque was from 0.1 μNm to 10000 μNm with 5 steps per decade in logarithmic mode. Each step was allowed 5 minutes to equilibrate 3 shear values within 5% of the previous shear value for 30 seconds each.

TGA (Q50, TA Instruments) was performed on the suspensions under the following conditions: a platinum plate was used with a sample mass of 10-30 mg, Nitrogen gas

flow rate was 20mL/min, with a temperature rate of 5 °C/min ranging from 25 °C to 700 °C. Between each run, the platinum sample tray was meticulously cleaned with deionized water and a lint free absorbent tip then flame torched to a dull red heat and allowed to cool for the next use.

DLS (ZetaPALS, Brookhaven Istruments) was performed on the samples to determine the particle size and polymer thickness. The angle, temperature, viscosity of liquid, dielectric constant of water and refractive index of water and Laponite XLG used were 90° at a wavelength of 600nm, 298K, the viscosity of the liquid was predetermined from the rheometer and entered as η, ε=78.54 and n_w=1.33, n_L=1.44, respectively, for both DLS and EPM. Sample count rate was adjusted and maintained between 100-1000 kcps for DLS and EPM. For kα>> 1(k- Debye-Huckel parameter and α is a calculated particle radius), the Smoluchowski relationship was used. For zeta potential, a wavelength of 660nm was used to determine surface charge of the Laponite and characterize the polymer interactions.

Streaming Potential used a perfluorocarbon chamber with a stainless steel ring on the piston and external chamber ring with an applied voltage measured from the charge of the dispersion, in most cases -300 mV. This was titrated with the polymer to determine the electrokinetic surface charge effects and compare to the electrophoretic measurements from zeta-potential.

Adsorption isotherms were generated for polymer affinity to Laponite to provide a viscometric analysis of the adsorbed layer thickness and adsorption affinity profile. The Laponite suspensions equilibrated for 24 hours to ensure complete hydration. Addition

of polymer was next and equilibrated for 24 hours. The steady state flow curve of the sample before and after centrifugation was measured for the suspensions for viscometric analysis. To ensure complete separation of adsorbed particle to free polymer, the suspensions were centrifuge in a Beckman Coultier Ultracentrifuge for 2 hours at 35,000rpm (70,000g based on graph chart). A modified Scott's test was developed to determine adsorption affinity profile from excess polymer in supernatant. The Scott's test uses a cobalt thiocyante reagent to complex with the ethylene oxide block of the polymer.[26]

3.3 Results and Discussion

3.3.1 Rheological effects

Laponite Concentration

Figure 3.1 illustrates the effect of the oscillation frequency sweeps and steady state flow curve as a function of Laponite concentration. From this figure there is a general trend for the increase in both the elastic and loss modulus in the Laponite suspensions. A sol gel transition occurs at 2%Laponite where the frequency sweep shows an elastic dominant suspension, similar to previous literature findings.[27] For low Laponite concentrations of 1% and 2%, the elastic modulus is not observable and is a viscous dominant material. The slope of the viscous component increases with frequency, displaying Maxwellian behavior. Laponite Concentrations above 3% show an elastic dominant system, a plateau elastic modulus is observed. The plateau modulus indicates increased electrostatic repulsion of the more concentrated Laponite suspensions.

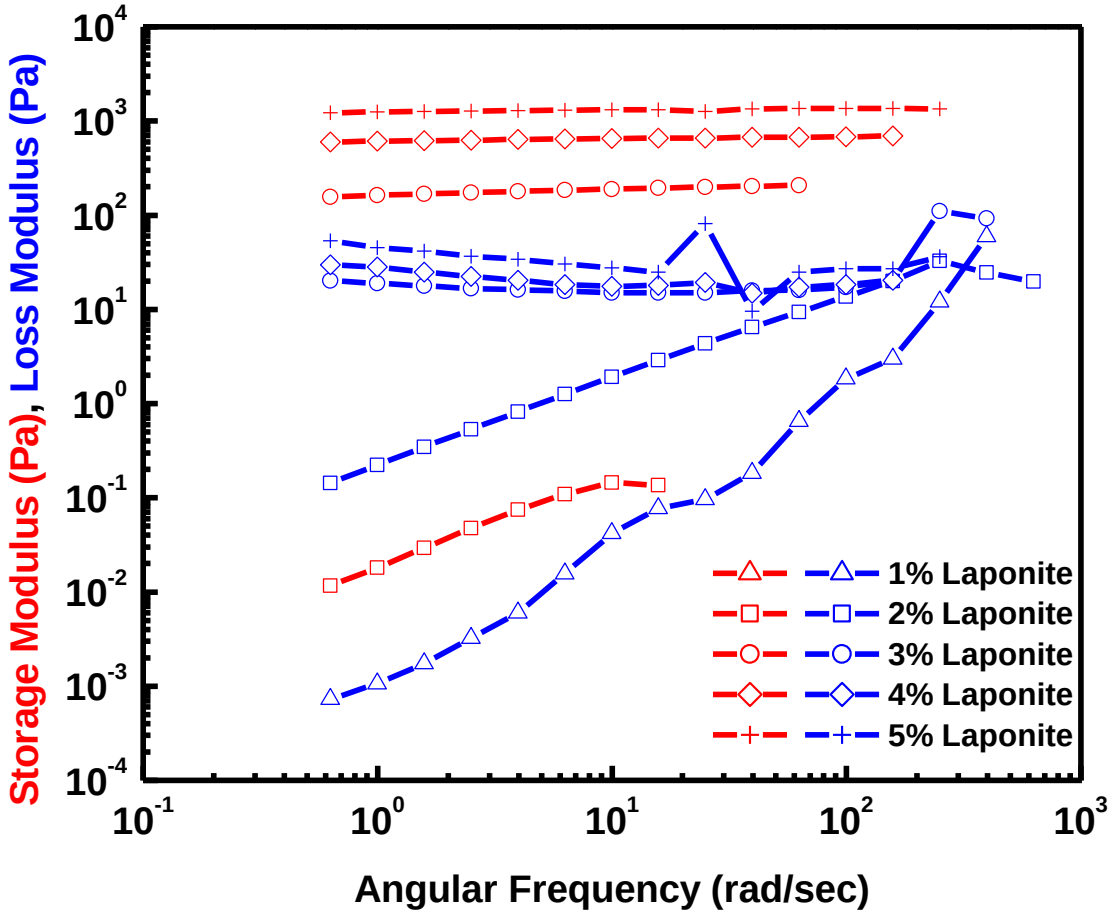

Figure 3. 1. Modulus versus Angular Frequency for 1%(△), 2% (□), 3%(○), 4%(◇) and 5%(＋) Laponite suspensions. Red- Storage Modulus (Pa) and Blue- Loss Modulus (Pa). Frequency Sweep is within the Linear Viscoelastic Region.

Figure 3.2 shows a similar trend of increasing viscosity relative to shear stress and rates is observed with the flow curves with increasing Laponite concentrations, also in agreement with the literature. Low concentrations of Laponite up to 2% display Power

Law behavior, shear stress is proportional to shear rate. Concentrations at 3% Laponite and higher concentrations show a pseudo-plastic yield stress. A yield occurs when shear rate is minimally changed as shear stress increases then reaches a point at which flow occurs. This indicates that low Laponite suspensions will be most desireable concentrations for end use as a firefighting application. This also suggests that minimal loss of water dramatically increases the bulk mechanical properties of the Laponite suspensions due to electrostatic effects. Another way to approach this is as the particle stabilized foam forms, the foam gels upon a 2% water loss. The following work focuses then on low Laponite concentrations.

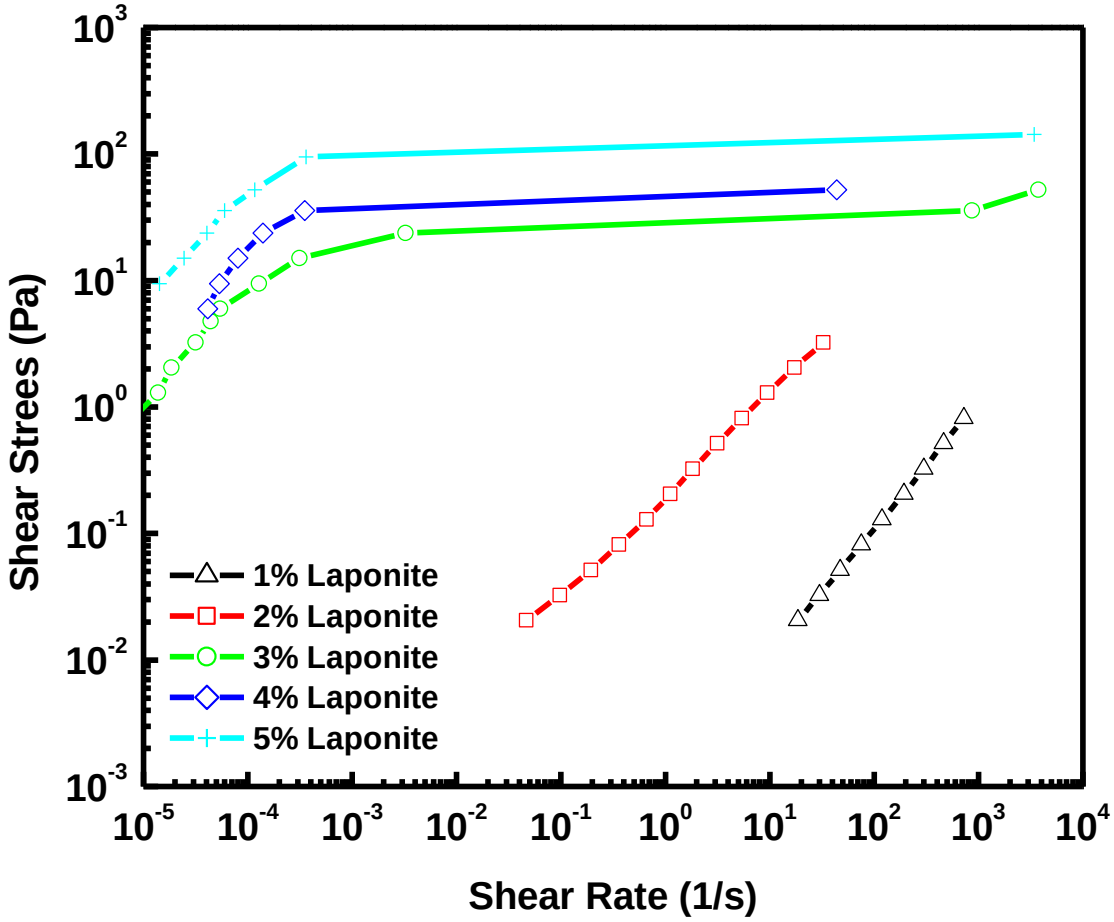

Figure 3. 2. Shear Stress versus Shear Rate for 1%(△), 2% (□), 3%(○), 4%(◇) and 5%(＋) Laponite suspensions.

Polymer Contributions

Figure 3.3 illustrates the frequency sweep for 2.0% Laponite with Polyethyleneglycol (PEG2000). Figure 3.4 shows the frequency sweep for 2.0% Laponite with Pluronic 17R4. Fiugre 3.5 shows the frequency sweep for 2.0% Laponite with Pluronic L62. Each polymer addition follows the same trend of increased viscoelasticity up to 1.0% polymer content. For the concentrations higher than 1.0% of

PEG2000, Figure 3.3, and Pluronic 17R4, Figure 3.4, the viscoelastic moduli values drop significantly. In all instances the polymers are layering onto the laponite. Figure 3.5 shows the elastic modulus values increase and approach a plateau for concentrations higher than 1.0% Pluronic L62. The increase in elastic and viscous modulus indicate polymeric repulsion. At 1.0% polymer, laponite approaches maximum adsorption. The role of hydrophobic functionality and geometry of the polymer play an important role for reduced viscoelastic properties.

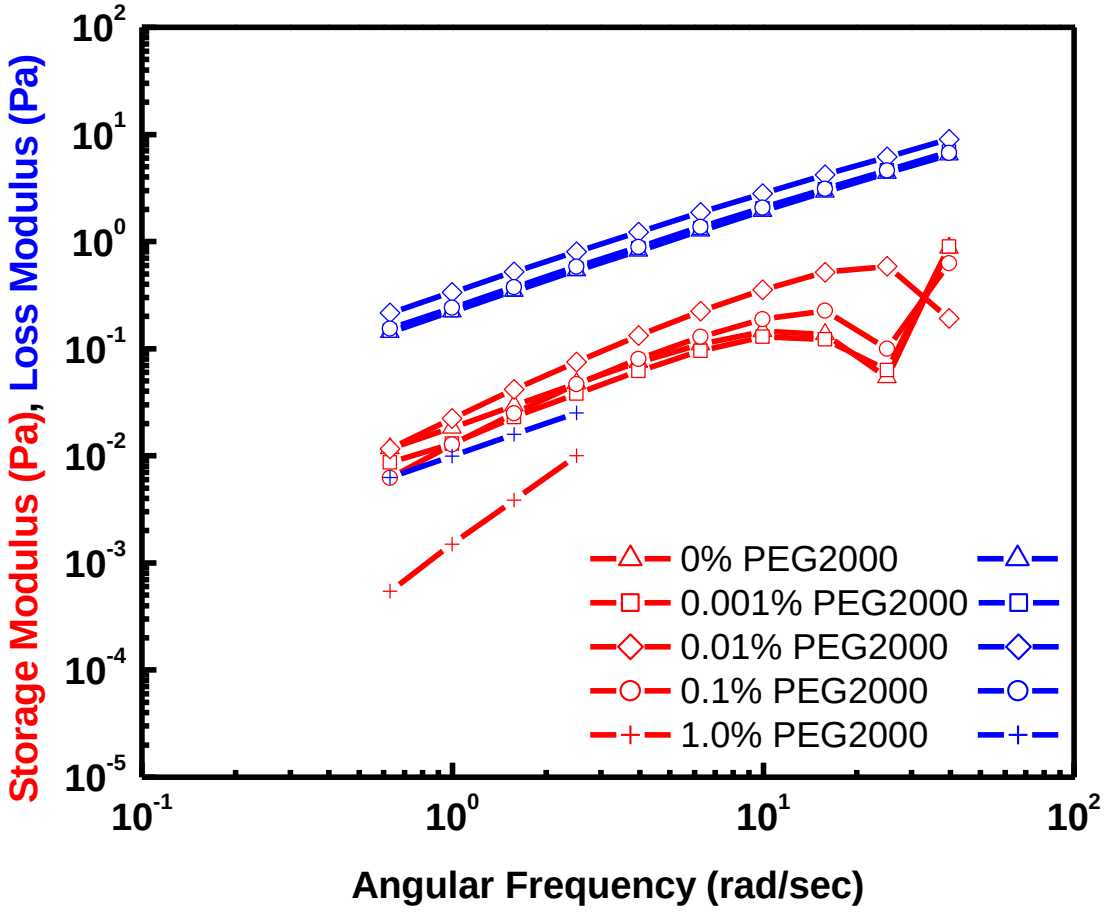

Figure 3. 3. Modulus versus Angular Frequency for 0% PEG2000(△), 0.001% PEG2000 (□),0.01% PEG2000(○), 0.1% PEG2000(◇) and 1.0% PEG2000(+) at 2.0% Laponite suspensions. Red- Storage Modulus (Pa) and Blue- Loss Modulus (Pa). Frequency Sweep is within the Linear Viscoelastic Region.

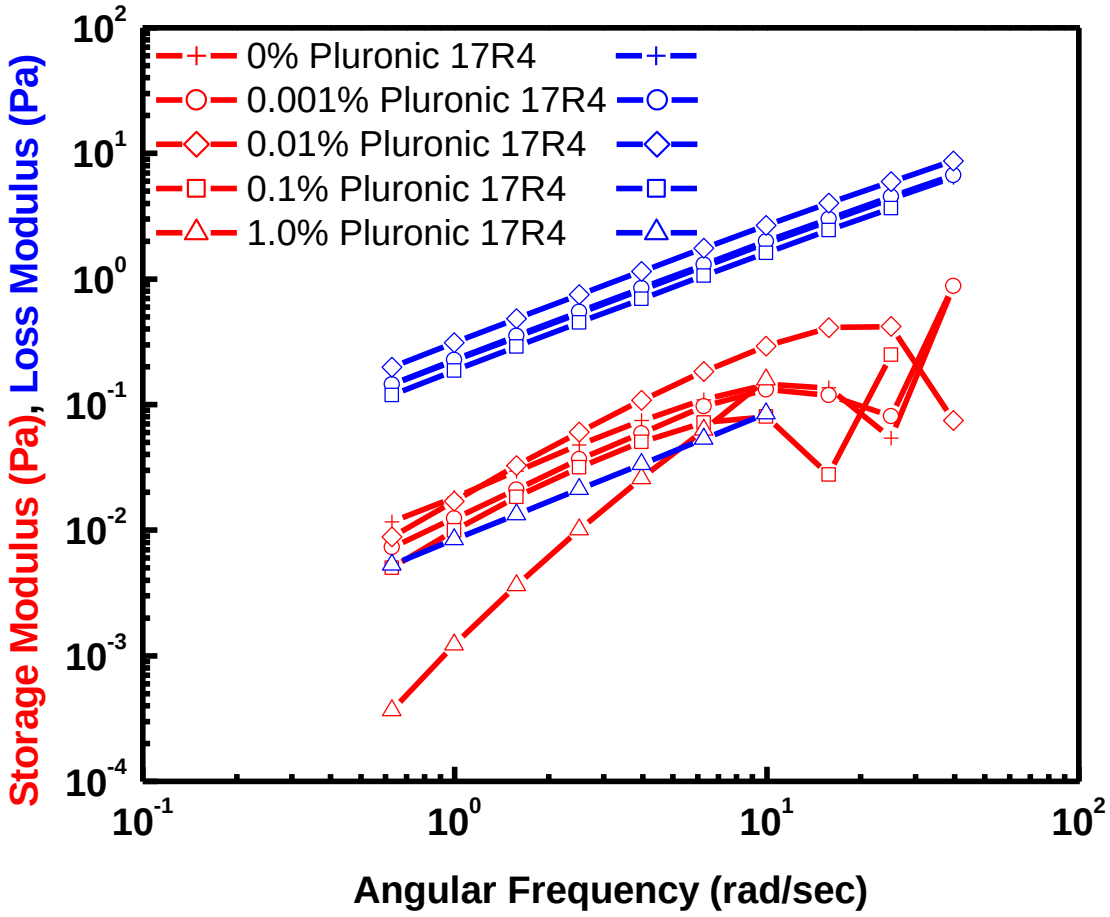

Figure 3. 4. Modulus versus Angular Frequency for 0% Pluronic 17R4(△), 0.001% Pluronic 17R4 (□),0.01% Pluronic 17R4 (○), 0.1% Pluronic 17R4 (◇) and 1.0% Pluronic 17R4 (+) at 2.0% Laponite suspensions. Red- Storage Modulus (Pa) and Blue- Loss Modulus (Pa). Frequency Sweep is within the Linear Viscoelastic Region.

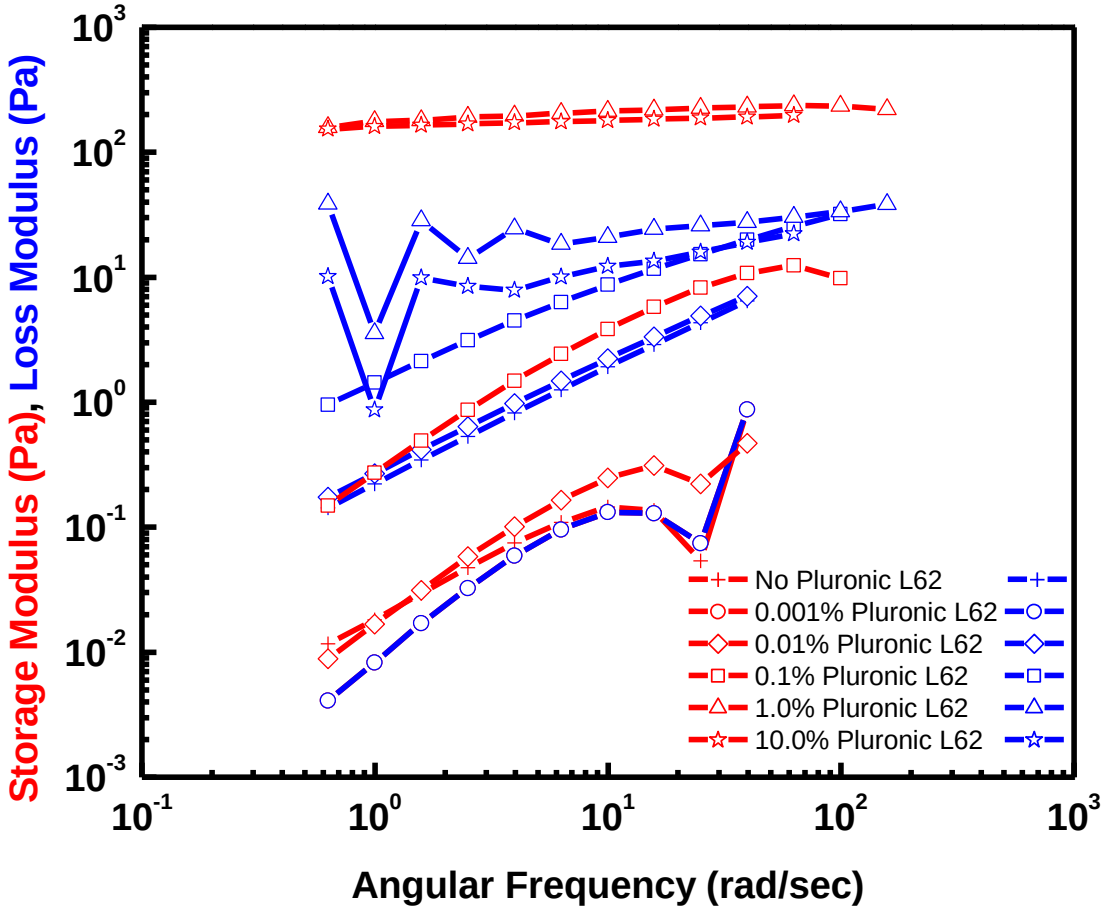

Figure 3. 5. Modulus versus Angular Frequency for 0% Pluronic L62(△), 0.001% Pluronic L62 (□),0.01% Pluronic L62 (○), 0.1% Pluronic L62 (◇) and 1.0% Pluronic L62 (+) at 2.0% Laponite suspensions. Red- Storage Modulus (Pa) and Blue- Loss Modulus (Pa). Frequency Sweep is within the Linear Viscoelastic Region.

Figure 3.6 shows a comparison of the elastic moduli to the polymer content for each polymer. As Pluronic L62 increases in concentration with the Laponite suspension, the viscoelastic properties shift from a viscous dominant fluid to an elastic dominant fluid. This synergistic effect is due to Pluronic L62's optimal adsorption, functionality,

geometric structure and synergistic contributions from polymeric repulsion. At concentrations as low as 0.1% Pluronic L62, there is an exponential increase in elastic modulus and continues for concentrations up to 10% Pluronic L62.

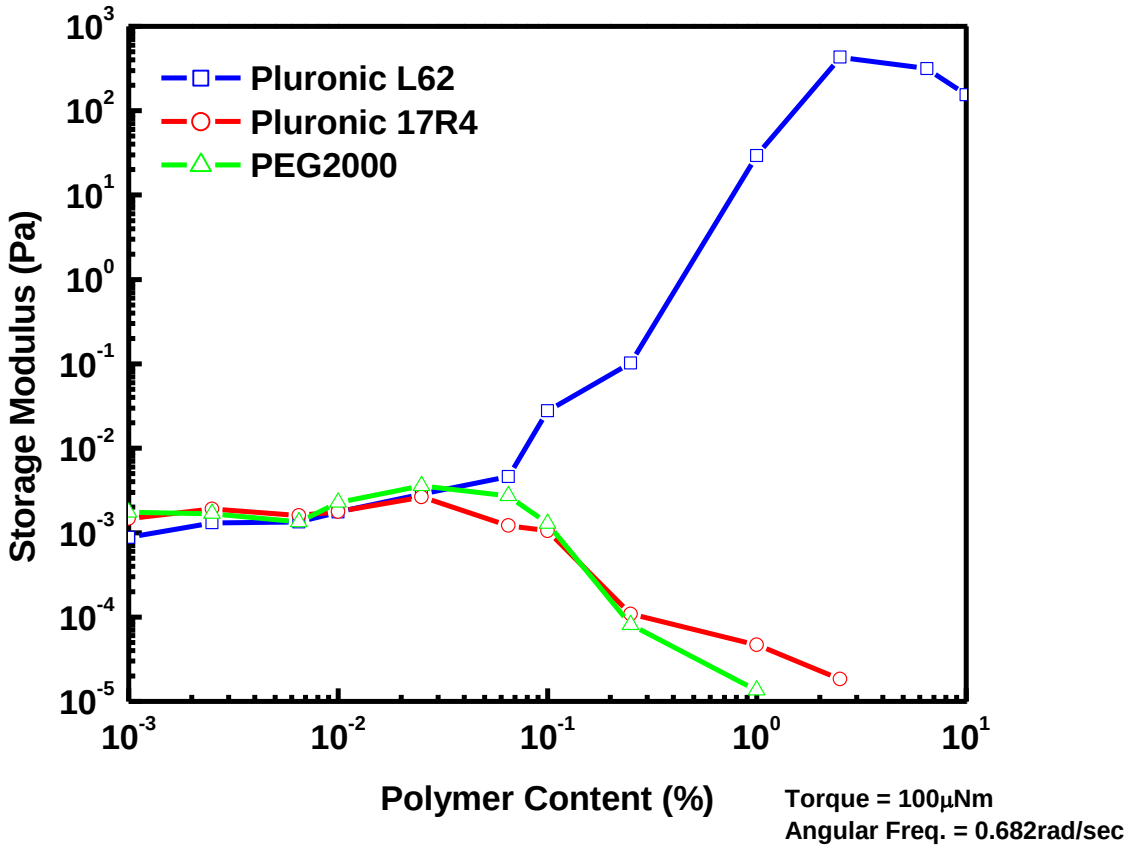

Figure 3. 6. Storage Modulus (Pa) versus % Polymer Content for Pluronic L62(□), Pluronic 17R4 (○) and PEG2000 (△) at 2.0% Laponite suspensions.

Figure 3.7, Figure 3.8 and Figure 3.9 show how the addition of polymer contributes to the flow for the 2% laponite suspensions of PEG2000, Pluronic 17R4 and Pluronic L62, respectively. Figure 3.10 shows the viscosity values relative to each

polymer. At 1.0% viscosity differentiation is observed for Pluronic L62 compared to the Pluronic 17R4 and PEG2000. Polymer saturation has occurred for the all suspensions, but no synergistic viscosity interactions occurs using PEG2000 and Pluronic 17R4.

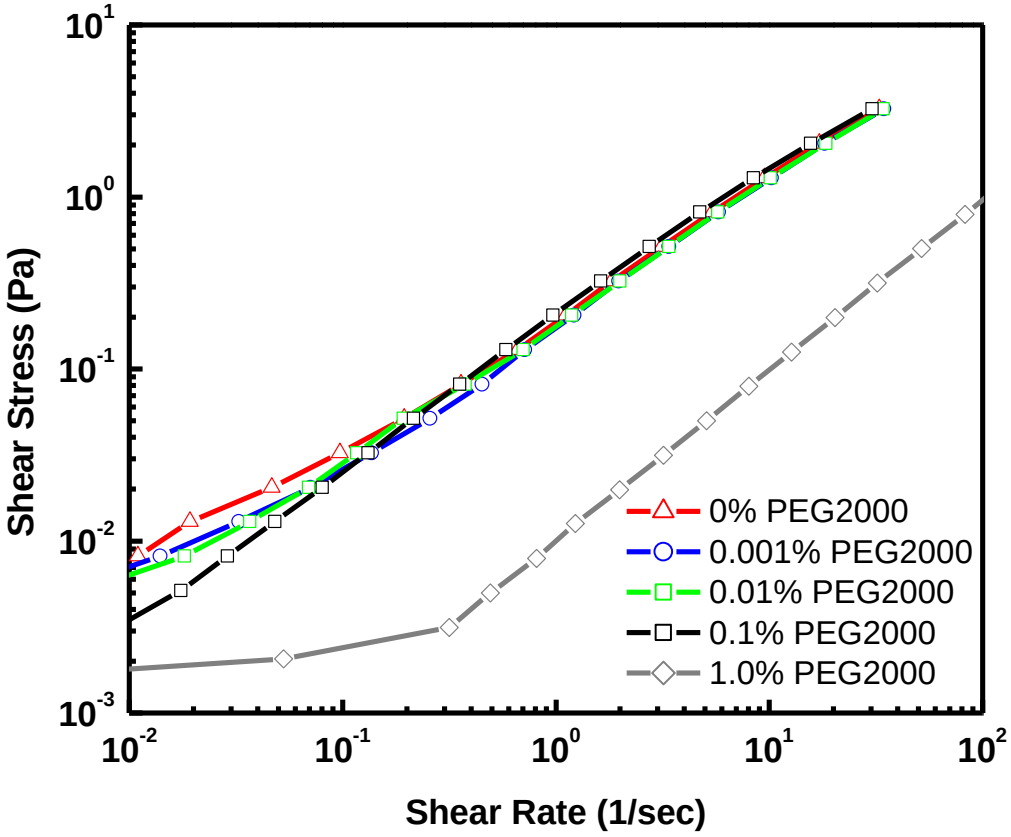

Figure 3. 7. Modulus versus Angular Frequency for 0% PEG2000(△), 0.001% PEG2000 (□),0.01% PEG2000(○), 0.1% PEG2000(◇) and 1.0% PEG2000(+) at 2.0% Laponite suspensions. Red- Storage Modulus (Pa) and Blue- Loss Modulus (Pa). Frequency Sweep is within the Linear Viscoelastic Region.

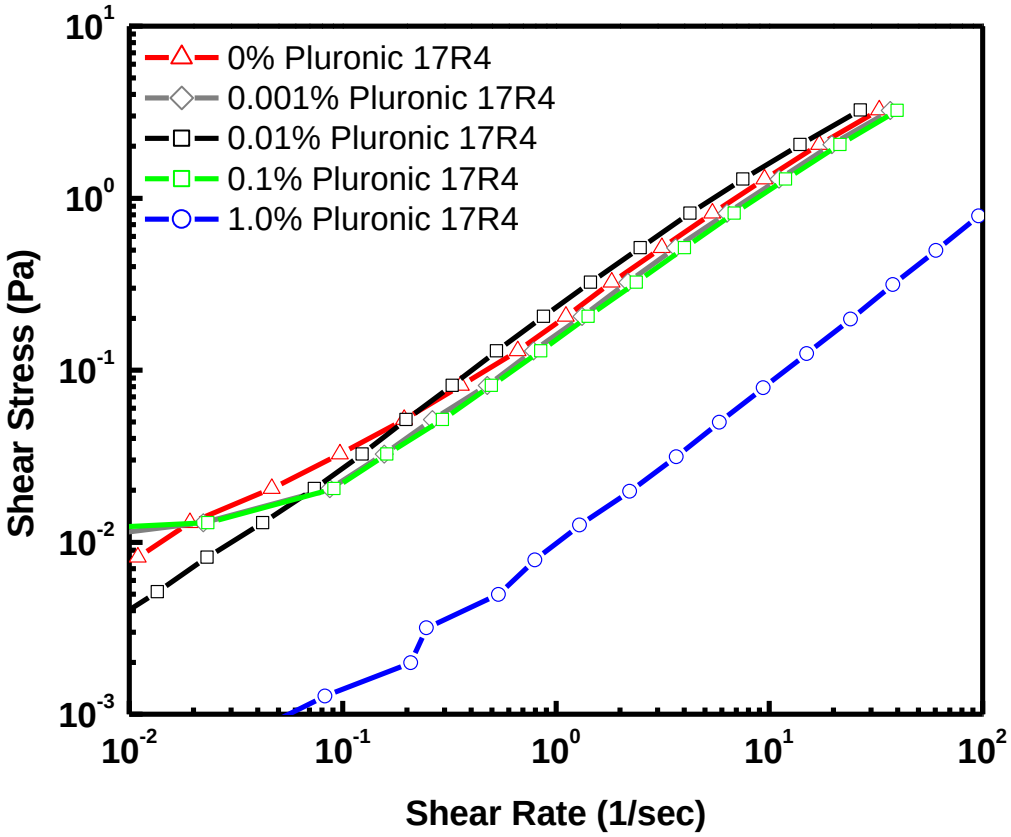

Figure 3. 8. Modulus versus Angular Frequency for 0% Pluronic 17R4(△), 0.001% Pluronic 17R4 (□),0.01% Pluronic 17R4 (○), 0.1% Pluronic 17R4 (◇) and 1.0% Pluronic 17R4 (+) at 2.0% Laponite suspensions. Red- Storage Modulus (Pa) and Blue- Loss Modulus (Pa). Frequency Sweep is within the Linear Viscoelastic Region.

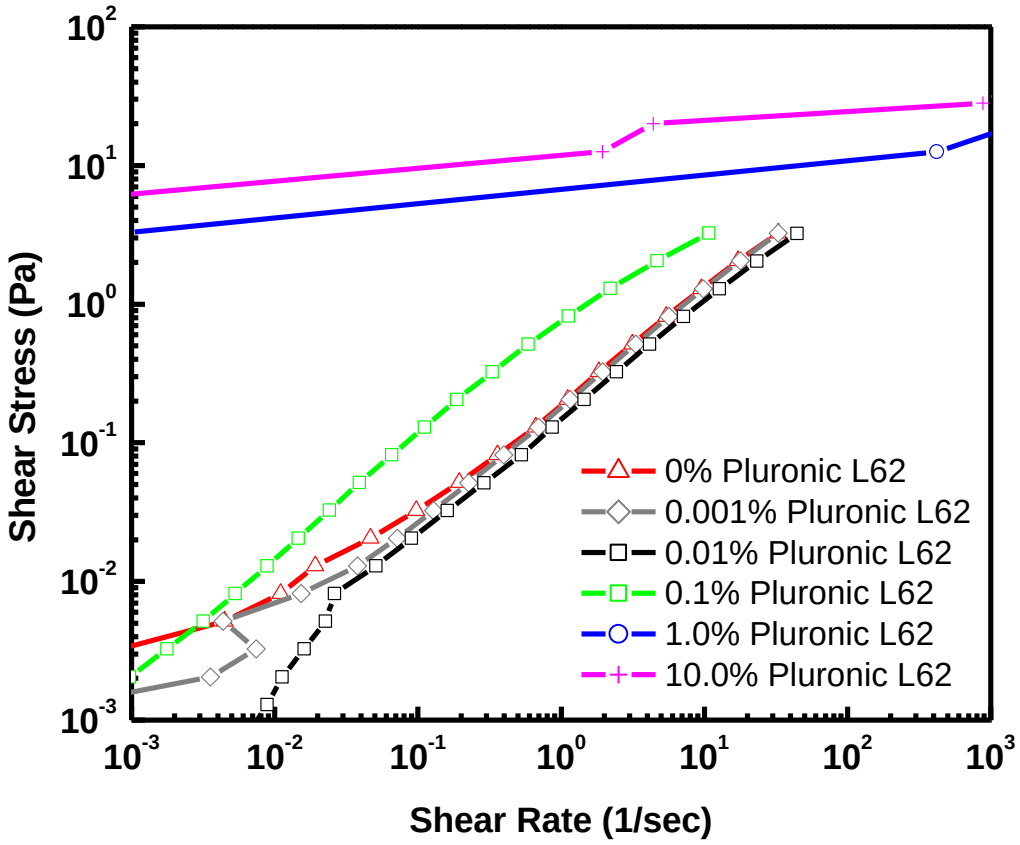

Figure 3. 9. Modulus versus Angular Frequency for 0% Pluronic L62(△), 0.001% Pluronic L62 (□),0.01% Pluronic L62 (○), 0.1% Pluronic L62 (◇) and 1.0% Pluronic L62 (+) at 2.0% Laponite suspensions. Red- Storage Modulus (Pa) and Blue- Loss Modulus (Pa). Frequency Sweep is within the Linear Viscoelastic Region.

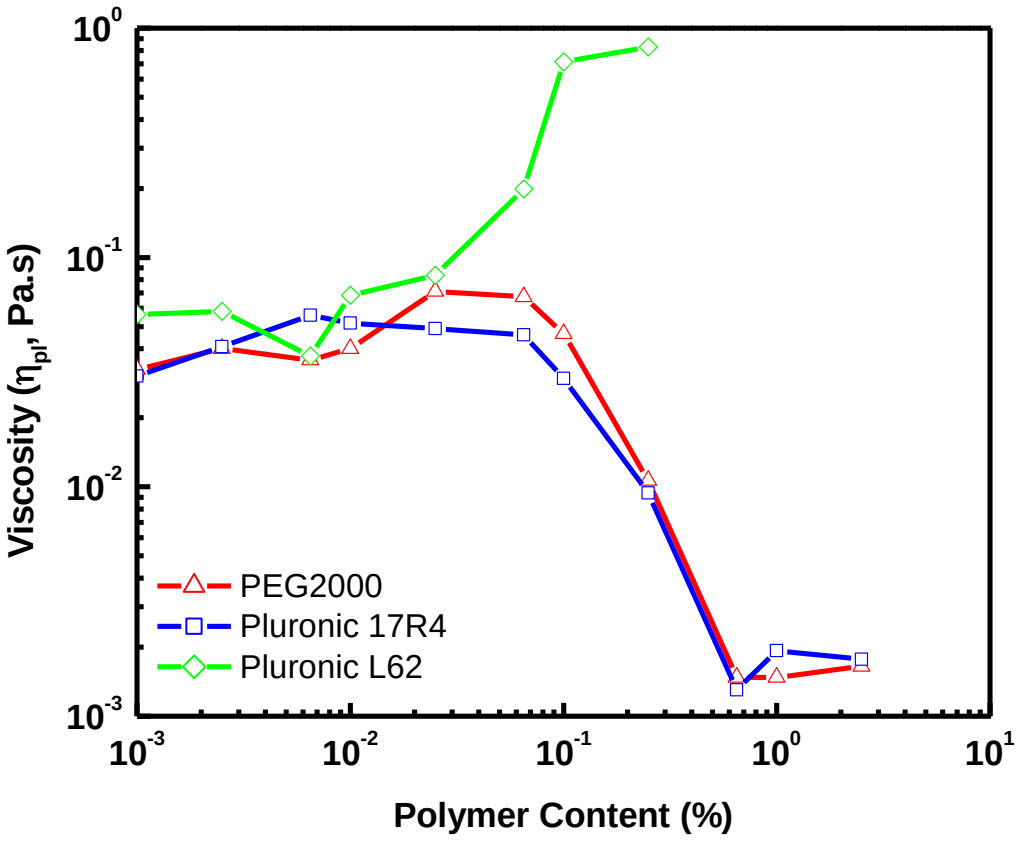

Figure 3. 10. Plastic Viscosity (η_{pl}, Pa.s) versus % Polymer Content for Pluronic L62(□), Pluronic 17R4 (○) and PEG2000 (△) at 2.0% Laponite suspensions.

To summarize, all three dispersions had similar rheological properties up to 0.1% polymer content. As the hydrophilic PEG2000 increased up to 10% polymer content, the structure and flow of the dispersion reduced significantly, the polymer destabilized the dispersion. A similar trend was observed with Pluronic 17R4 where a reduction in structure and flow was a result of the polymer steric effect destabilizing the dispersion. Pluronic L62 concentrations above 0.1% show increased storage modulus, loss

modulus and viscosity, as water content in the foam decreases by only 0.1%, the particle stabilized foam increases its bulk mechanical strength. The following work focuses on polymer concentrations of 0.1% and higher.

Figure 3.11 shows a temperature ramp was performed for 2% Laponite with 1.0% Pluronic L62 to characterize thermogelling effects up to 60°C. 60°C was the limit in temperature due to the testing environment. The polymer concentration of 1% was chosen due to differentiation of viscoelastic properties. The laponite suspension alone was viscoelastic throughout the temperature ramp. The shape of the curve is more dependent on the laponite structure as temperature increases. The addition of the Pluronic L62 only shifted the suspension to an elastic dominant fluid, but curvature was mainly influenced by Laponite. Polymer depletion has been observed with Laponite and Pluronic F127 as a function of temperature.[28] Polymer depletion of the Laponite Pluronic F127 suspensions displayed a synergistic thermogelling response. This was not observed for the 2%Laponite and 1% Pluronic L62. The lack of thermogelling is due to Pluronic L62 lower PEO length.

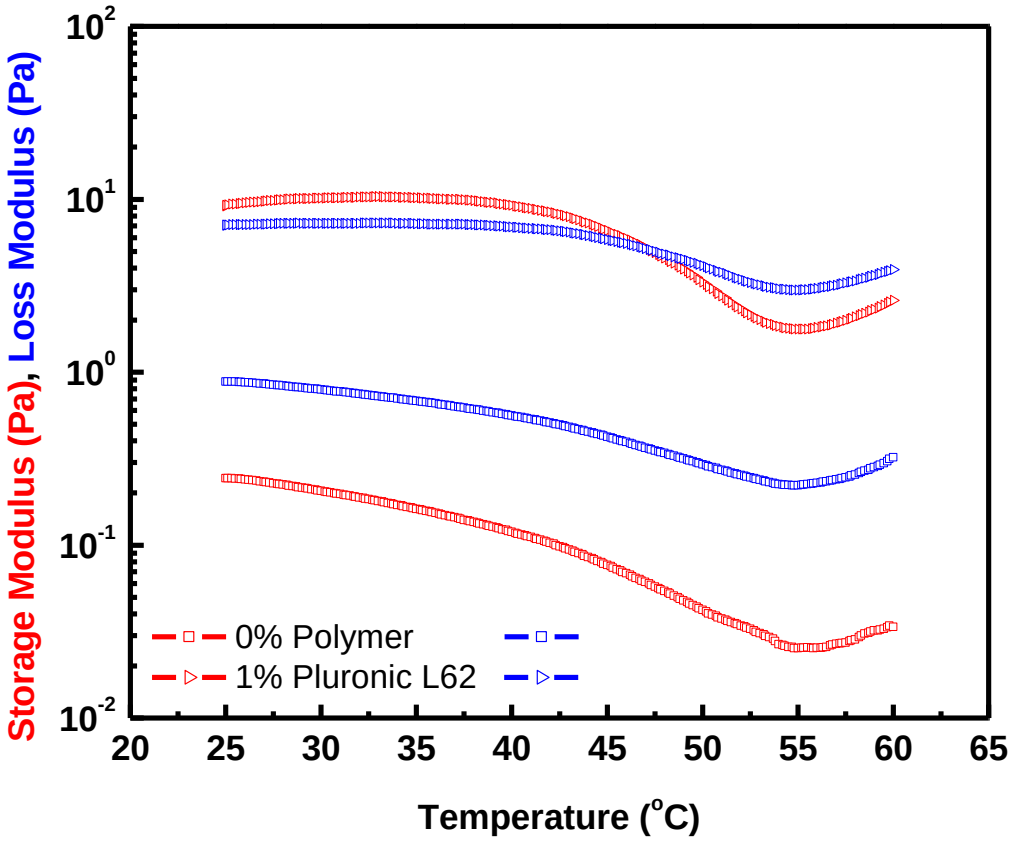

Figure 3. 11. Modulus versus Temperature for 0% Pluronic L62(○) and 1.0% Pluronic L62 (▷) at 2.0% Laponite suspensions. Red- Storage Modulus (Pa) and Blue- Loss Modulus (Pa). Temperature Sweep is within the Linear Viscoelastic Region.

3.3.2 Thermogravimetric Analysis

2% Laponite with Pluronic L62 Dose Response

Figure 3.12 is the full thermogram for the 2% Laponite with Pluronic L62.This was used to demonstrate the thermal contribution of Laponite and Pluronic L62. Figure 3.13 shows the derivative of the %weight/temperature as a function of temperature for water loss. As Pluronic L62 is added with Laponite, the water loss temperature is increased,

Table 3.1. Figure 3.14 shows the derivative of %weight/temperature as a function of temperature for Pluronic L62 loss. Laponite provides more themal at lower Pluronic L62 concentrations, Table 3.2. This suggests that thermal enhancement of the particle stabilized foam can be achieved with very little polymer added.

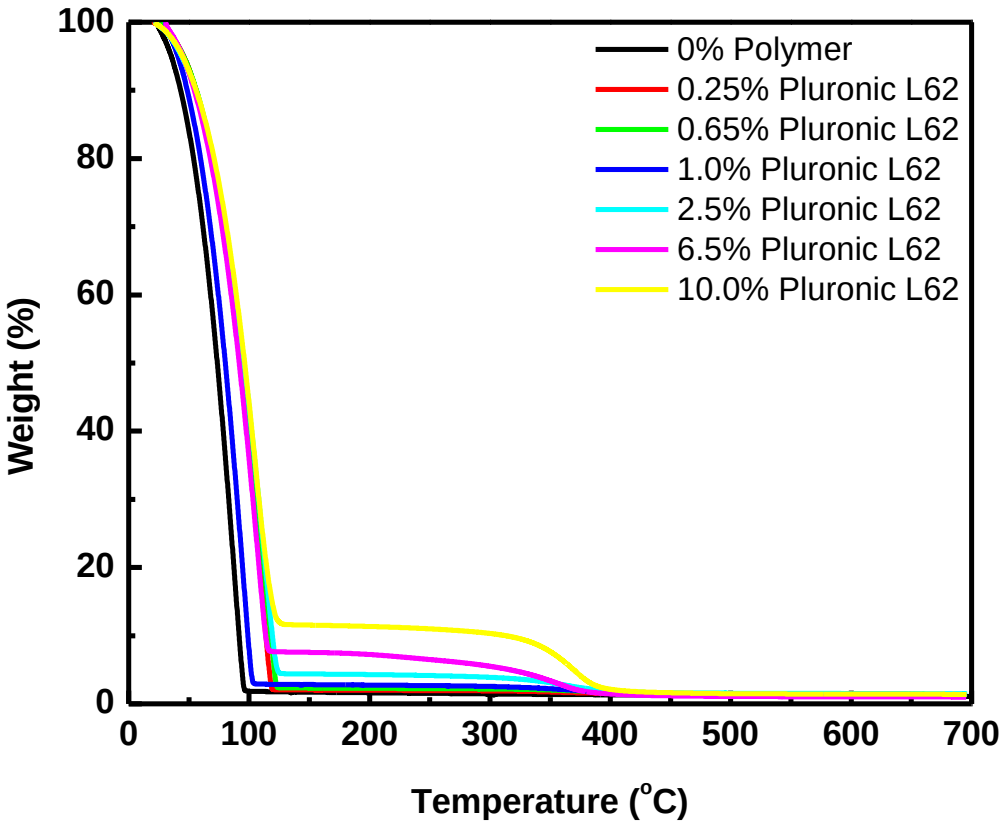

Figure 3. 12. % Weight versus Temperature for 0% (black), 0.25% (red),0.65% (green), 1.0% (blue), 2.5% (aqua), 6.5% (pink) and 10.0% (yellow) Pluronic L62 at 2.0% Laponite suspensions.

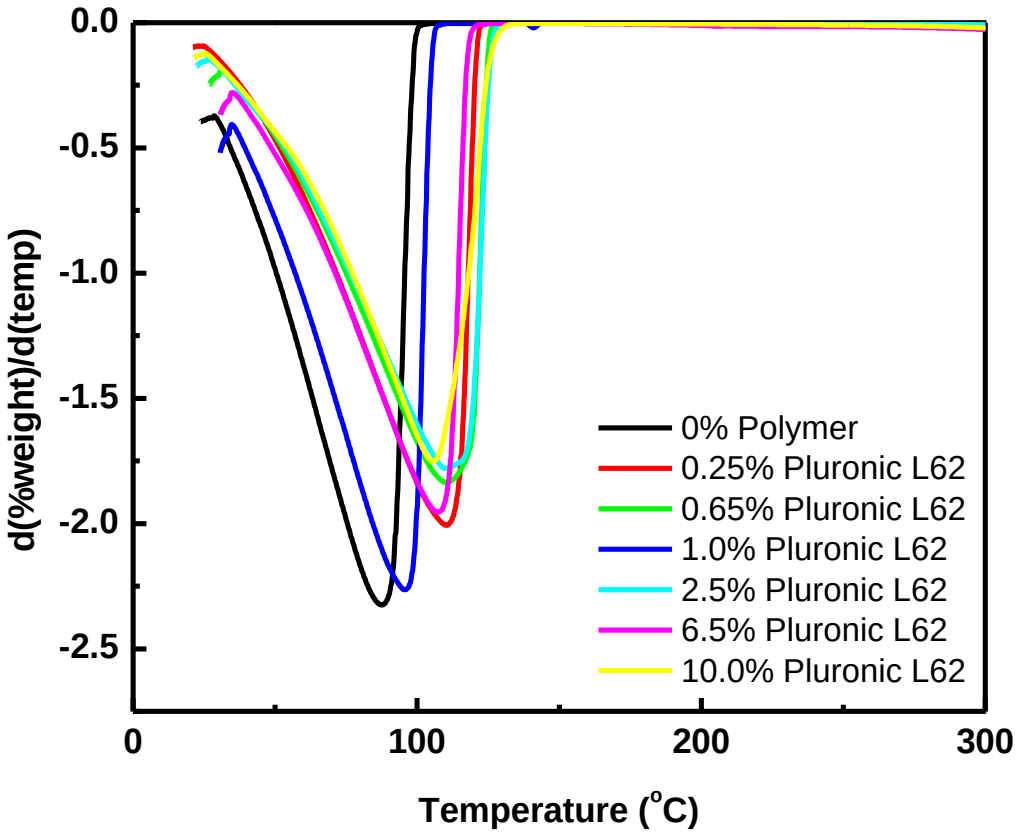

Figure 3. 13. d(%Weight)/d(temp) versus Temperature for 0% (black), 0.25% (red),0.65% (green), 1.0% (blue), 2.5% (aqua), 6.5% (pink) and 10.0% (yellow) Pluronic L62 at 2.0% Laponite suspensions. Water region.

Table 3. 1. Peak from d(%Weight)/d(temp) versus Temperature for 0%, 0.25%,0.65%, 1.0%, 2.5%, 6.5% and 10.0% Pluronic L62 at 2.0% Laponite suspensions. Water region.

% content	Peak Height
0% Pluronic L62	87.602 °C
0.25% Pluronic L62	110.209 °C
0.65% Pluronic L62	110.093 °C
1.0% Pluronic L62	95.877 °C
2.5% Pluronic L62	110.152 °C
6.5% Pluronic L62	107.333 °C
10.0% Pluronic L62	105.59 °C

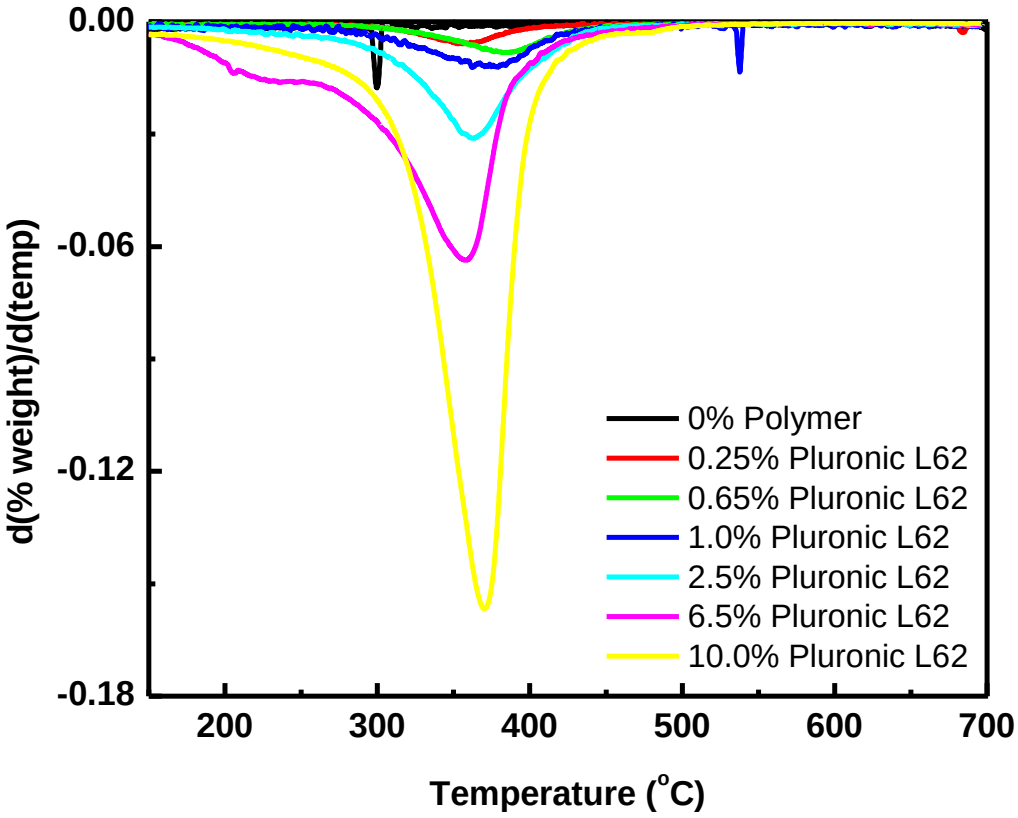

Figure 3. 14. d(%Weight)/d(temp) versus Temperature for 0% (black), 0.25% (red),0.65% (green), 1.0% (blue), 2.5% (aqua), 6.5% (pink) and 10.0% (yellow) Pluronic L62 at 2.0% Laponite suspensions. Pluronic L62 region.

Table 3. 2. Peak from d(%Weight)/d(temp) versus Temperature for 0%, 0.25%,0.65%, 1.0%, 2.5%, 6.5% and 10.0% Pluronic L62 at 2.0% Laponite suspensions. Pluronic L62 region.

% content	Peak Height
0% Pluronic L62	-
0.25% Pluronic L62	357.06 °C
0.65% Pluronic L62	385.303 °C
1.0% Pluronic L62	376.584 °C
2.5% Pluronic L62	363.016 °C
6.5% Pluronic L62	358.04 °C
10.0% Pluronic L62	370.44 °C

2% Laponite with and without 1% and10% Pluronic L62

Figure 3.15 shows the thermogram of Pluronic L62 with and without Laponite. Figure 3.16 shows the derivative of the %weight/temperature as a function of temperature for water loss. Addition of Laponite to Pluronic L62 does not increase the temperature peak but the peaks broaden at higher temperatures. Laponite provides a

limited amount of thermal stability for water compared to Pluronic L62. Pluronic L62 has more influence at increasing the temperature for water loss than Laponite, Table 3.3.

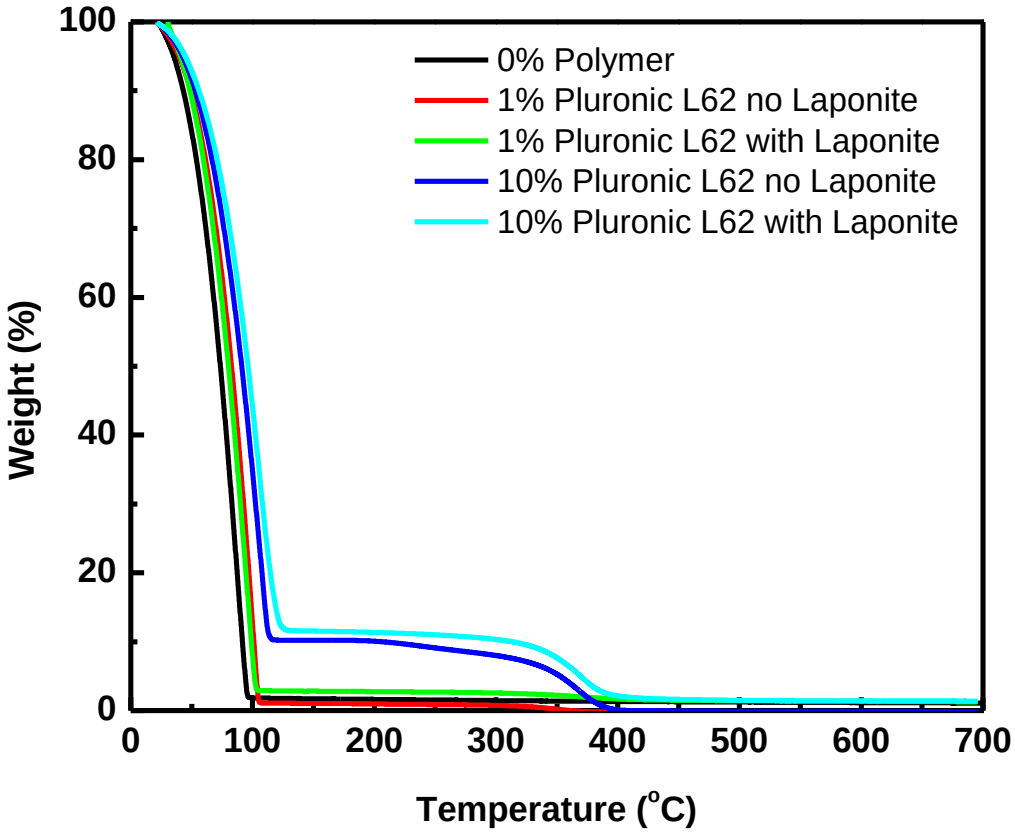

Figure 3. 15. % Weight versus Temperature for 0% Pluronic L62 (black),1% Pluronic L62 no Laponite (red), 1% Pluronic L62 with 2% Laponite (green), 10.0% Pluronic L62 no Laponite (blue) and 10% Pluronic L62 with Laponite (aqua).

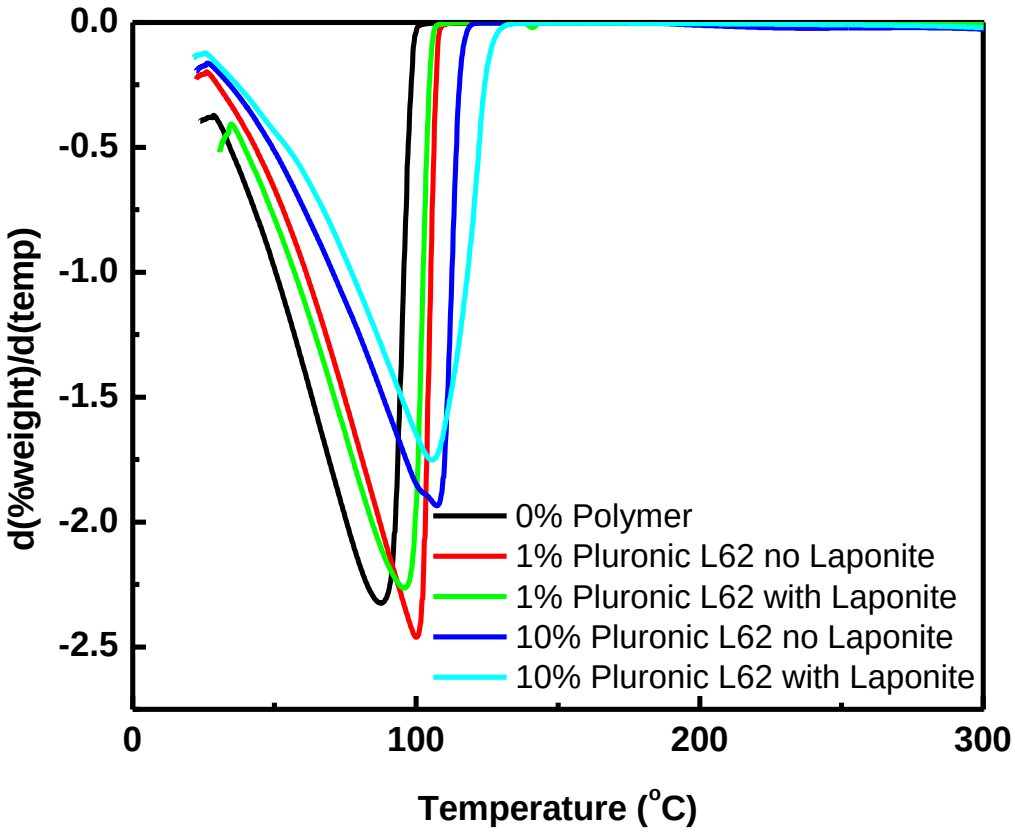

Figure 3. 16. d(%Weight)/d(temp) versus Temperature for 0% Pluronic L62 (black),1% Pluronic L62 no Laponite (red), 1% Pluronic L62 with 2% Laponite (green), 10.0% Pluronic L62 no Laponite (blue) and 10% Pluronic L62 with Laponite (aqua). Water region.

Table 3. 3. d(%Weight)/d(temp) versus Temperature for 0% Pluronic L62,1% Pluronic L62 no Laponite, 1% Pluronic L62 with 2% Laponite, 10.0% Pluronic L62 no Laponite and 10% Pluronic L62 with Laponite. Water region.

% content	Peak Height
Laponite only	87.602 °C
1% Pluronic L62	99.89 °C
Laponite and 1% Pluronic L62	95.877 °C
10% Pluronic L62	107.322 °C
Laponite and 10% Pluronic L62	105.59 °C

Figure 3.17 shows the derivative of the %weight/temperature as a function of temperature for Pluronic L62 loss. The incorporation of laponite with 1% Pluronic L62 shows a broader peak that is shifted to a higher temperature. Table 3.4 indicates the addition of Laponite to Pluronic L62 provides improved thermal degradation than without Laponite. Addition of laponite with 10% Pluronic L62 shows only a single peak shifted to higher temperature and without a lower degradation peak near 200 °C. This shows that Pluronic L62 has improved thermal resistance when incorporated with laponite. This also indicates there is a strong thermal interaction between Laponite and Pluronic L62 compared to Pluronic L62 alone.

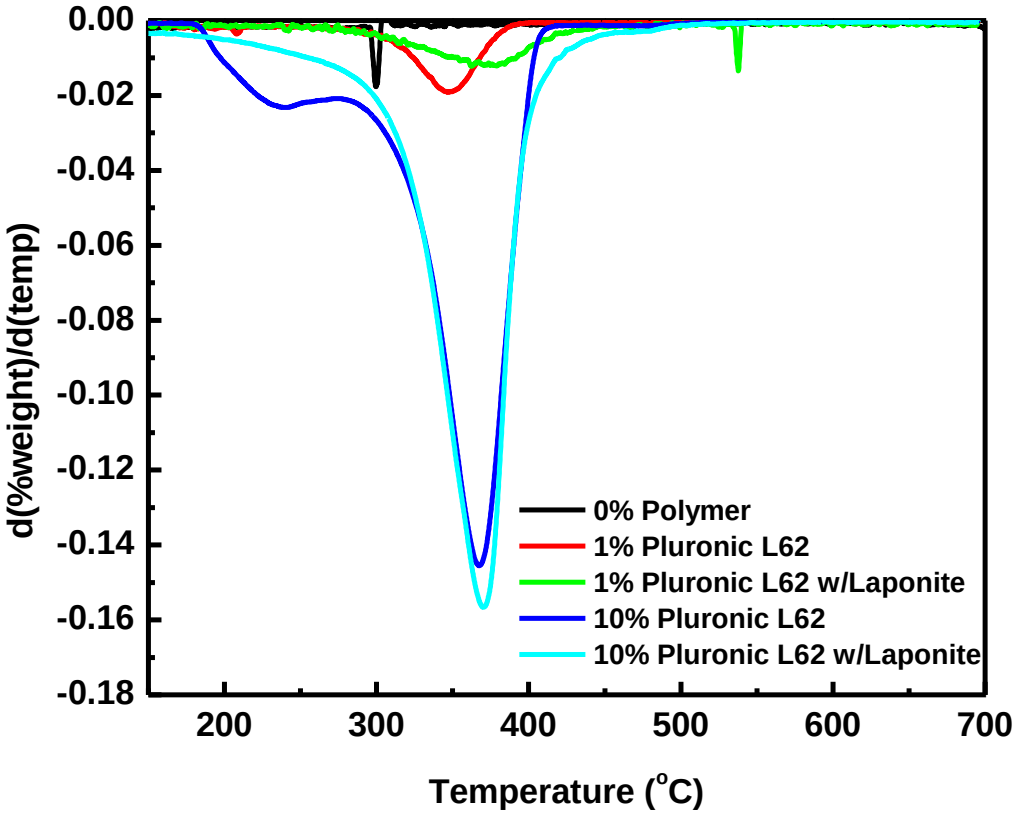

Figure 3. 17. d(%Weight)/d(temp) versus Temperature for 0% Pluronic L62 (black),1% Pluronic L62 no Laponite (red), 1% Pluronic L62 with 2% Laponite (green), 10.0% Pluronic L62 no Laponite (blue) and 10% Pluronic L62 with Laponite (aqua). Pluronic L62 region.

Table 3. 4. d(%Weight)/d(temp) versus Temperature for 0% Pluronic L62,1% Pluronic L62 no Laponite, 1% Pluronic L62 with 2% Laponite, 10.0% Pluronic L62 no Laponite and 10% Pluronic L62 with Laponite. Pluronic L62 region.

% content	Peak Height
Laponite only	-
1% Pluronic L62	346.941 °C
Laponite and 1% Pluronic L62	376.584 °C
10% Pluronic L62	367.495 °C
Laponite and 10% Pluronic L62	370.44C

3.3.3 Surface Charge

Surface Charge has been observed to impact foam stability using zeta potential.[29] Figure 3.18 shows that all polymers do impact zeta-potential in the dispersions. Then focus will be on the Laponite and Pluronic L62 dispersion for electrokinetic mobility using streaming potential. Comparison of both methods will be used to differentiate what interactions are occuring with Pluronic L62 adsorbing onto Laponite.

Electrophoretic Mobility- Zeta Potential

2% Laponite with Polymer Dose Response

Figure 3.18 demonstrates that all three types of polymer have a similar effect on the surface charge of Laponite. As polymer content increases, the zeta-potential approaches zero. Zeta-potential below 20mV change colloidal stability. Minimal polymer content quickly reduces the surface charge. Polymer content above 1% changes the colloidal stability. This was also observed more readily in the rheological characterization of both the frequency and flow curves. The reduction in zeta-potential of Laponite due to the polymer addition shows that Laponites electrostatic repulsion has dropped.

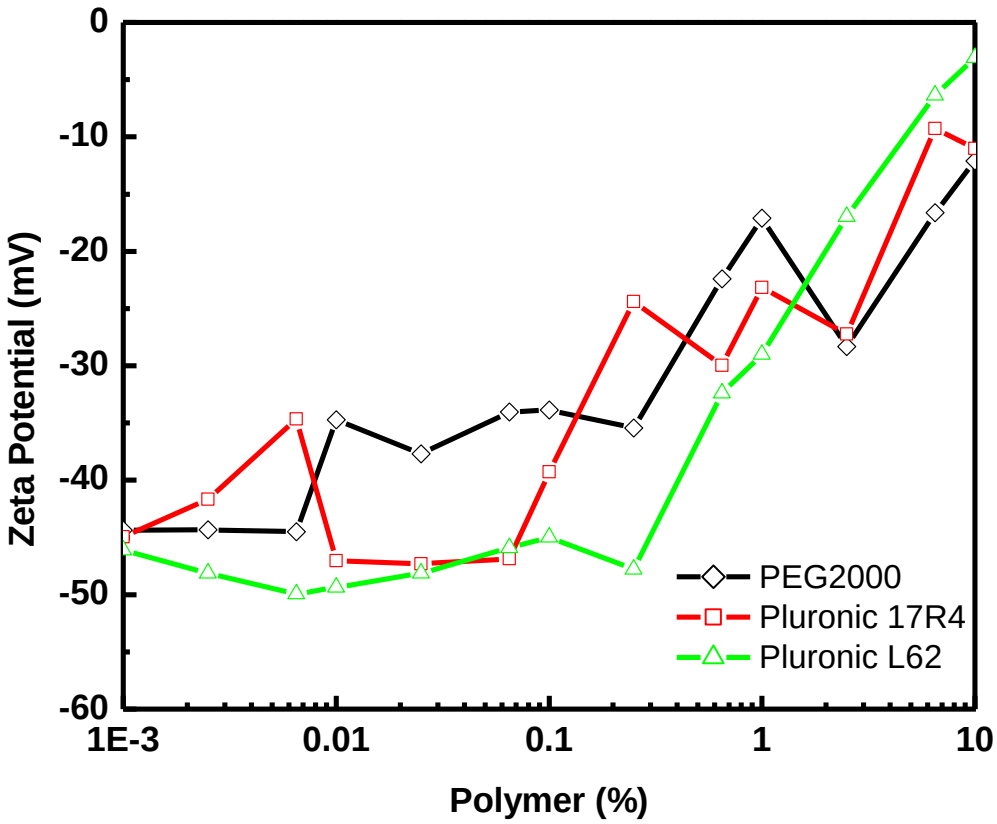

Figure 3. 18. Zeta Potential (mV) versus % Polymer Content for PEG2000 (◇), Pluronic 17R4 (□) and Pluronic L62 (△) at 2.0% Laponite suspensions.

Electrokinetic Mobility- Streaming Current Potential

Laponite with Polymer Dose Response (cationic vs nonionic)

Streaming current is a very well established technique in the pulp and water treatment industries.[30] Some new academic and industrial interest has been used for labile polyelectrolytes.[31] Streaming current potential has not been pursued for foaming

applications. A comparison will be made using a classic cationic polymer, poly(diallyldimethylammonium) chloride (PDADMAC), and Pluronic L62. Figure 3.19 shows the electrokinetic potential as a function of polymer content. In the case for PDADMAC, there is a small shift in charge between 0.1% and 2.25% polymer content. Then PDADMAC addition changes from negative to positive in potential. This indicates all the negatively charged sites on Laponite have interacted with the cationic sites of PDADMAC. Addition of Pluronic L62 shows an initial reduction in charge up to 1% polymer but begins to reach a plateau upon further addition of polymer. Addition of Pluronic L62 does not approach zero. The addition of both polymers show that electrostatic interactions impact surface charges at polymer concentrations above 1%. Polymer concentrations below 1% suggest that electrostatic interactions of PDADMAC are equivalent to the lipophilc properties of Pluronic L62.

For both surface charge techniques, at 1.0% Pluronic L62 saturation has occurred with the Laponite surface. The streaming current device is a simple setup that could potentially be used to study electrostatic interactions of clays and polymers by complementing zeta-potential. It is relatively easy to use and costs for instrumentation are much lower than that of sophisticated zeta-potential analyzers.

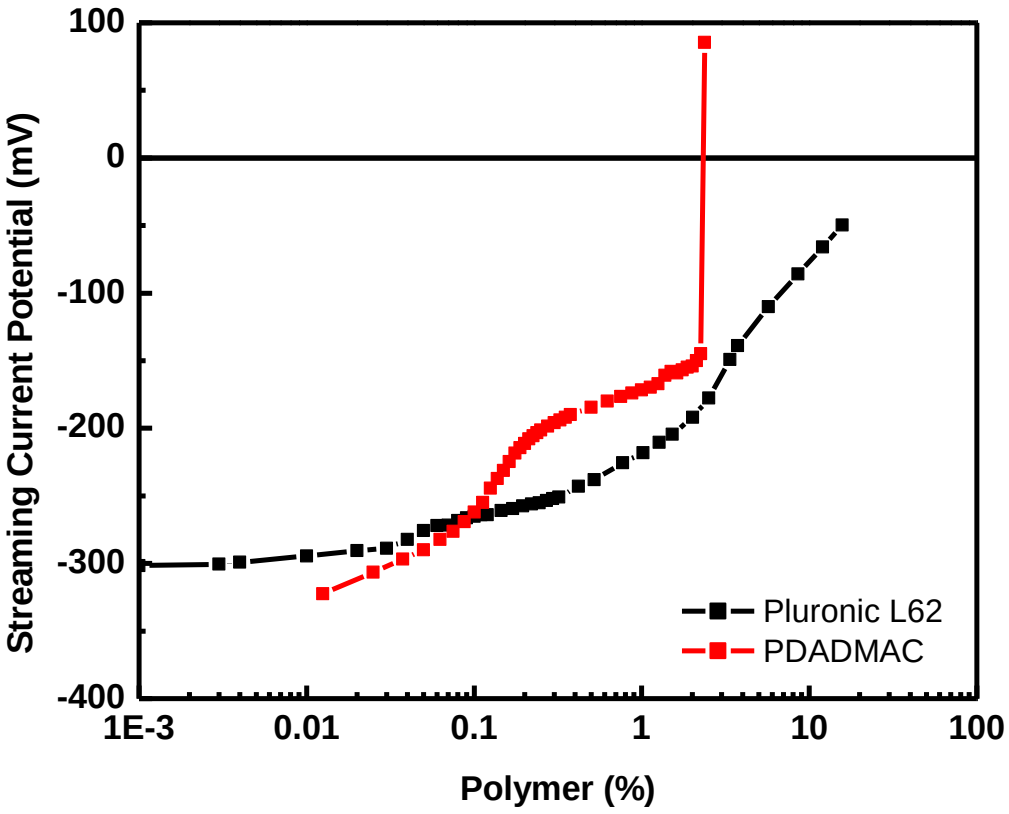

Figure 3. 19. Streaming Current Potential (mV) versus % Polymer Content for Pluronic L62 (red) and PDADMAC (black) at 2.0% Laponite suspensions.

3.3.4 Adsorption Isotherm

The adsorption profiles for each type of polymer displayed a Langmuir monolayer. Langmuir monolayer is a linear relationship between the adsorbed polymer amount and the total amount of polymer adsorbed. Differentiation between each polymer began with 0.1% Pluronic 17R4, 0.25% PEG2000 and 0.65% Pluronic L62. At these respective concentrations, laponite reaches its adsorption maxima with a monolayer of the polymers. Adsorption is greatest for Pluronic L62. Desorption to Laponite is highest for Pluronic 17R4, lower adsorbed value at 0.065%. Laponite has a higher affinity for Pluronic L62, highest adsorbed polymer. Laponite's interaction with Pluronic L62 is due to the functionality and geometry of the polymer.

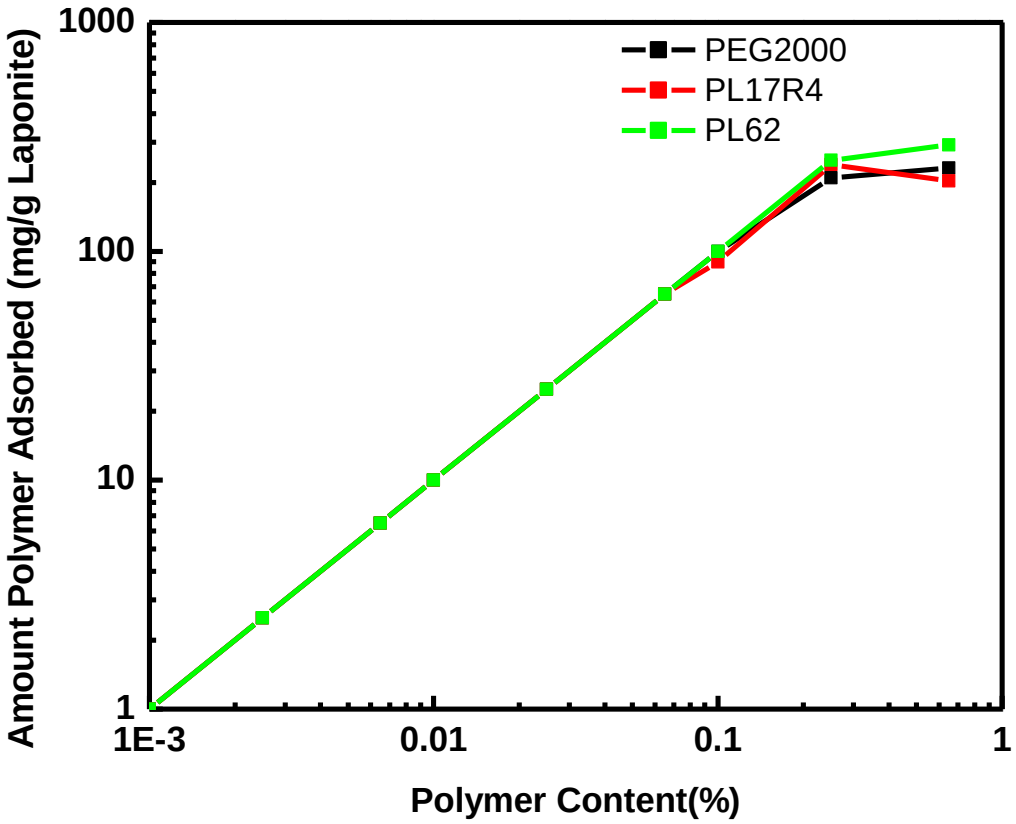

Figure 3. 20. Γ (mg adsorbed polymer / g Laponite) versus Polymer Content (%) on 1.0% Laponite suspensions.

3.3.5 Adsorption Layer Thickness- Dynamic Light Scattering

1% Laponite Suspensions with Pluronic L62 Dose Adsorption Layer thickness

Light scattering intensity for 1% Laponite suspensions displayed were within the range of the instrument. It is known that polyethyleneoxide polymers increase the layer thickness around Laponite particles. DLS complements rheological and surface charge work by showing particle changes due to Pluronic L62 interactions with Laponite through layer thickness. Figure 3.21 shows the scattering intensity vs decay time for Laponite and a dose response with Pluronic L62. The curvature of the graph is used to calculate the particles lognormal diameter. The correlation function changes curvature as Pluronic L62 is added to the Laponite suspension with the longest relaxation time at 0.01% Pluronic L62. The correlation function begins to relax faster upon addition of 1.0% Pluronic L62.

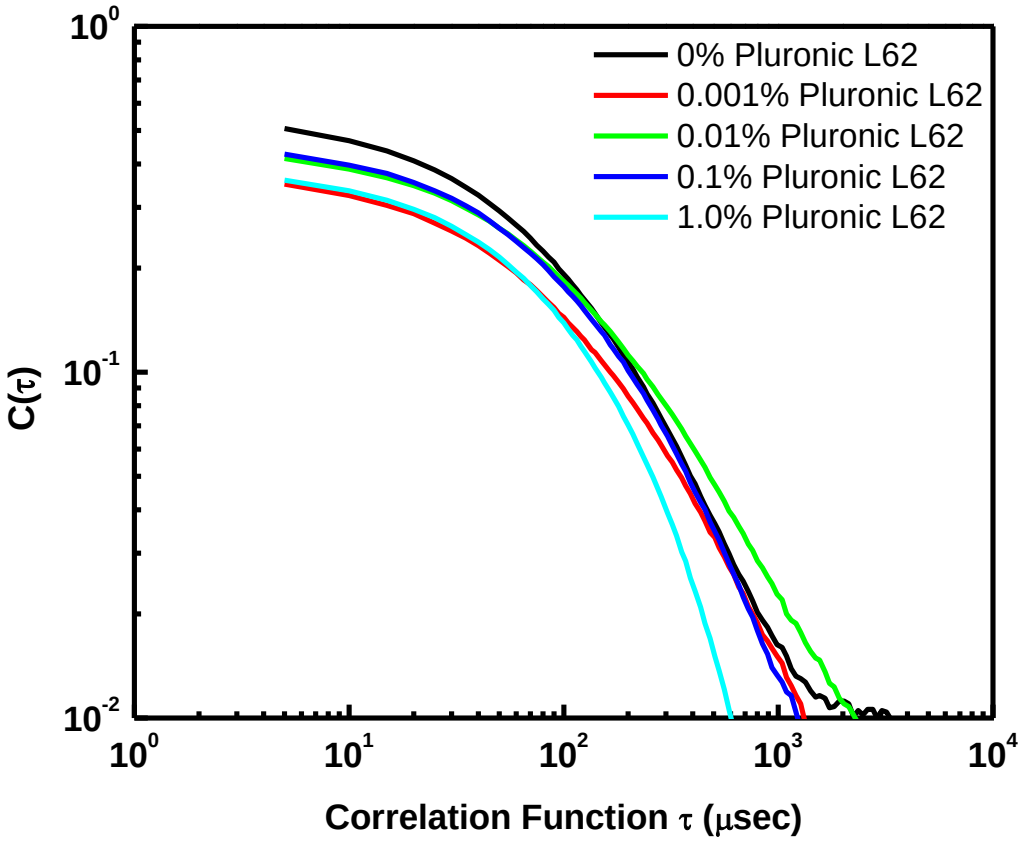

Figure 3. 21. C(τ) versus Correlation Function τ (sec) for 0% (black), 0.001% (red), 0.01% (green), 0.1% (blue) and 1.0% (aqua) Pluronic L62 at 1.0% Laponite suspensions.

Figure 3.22 shows the lognormal diameter of the Laponite and Pluronic L62 interactions. Figure 3.22 shows that 0.01% Pluronic has maximum interaction with Laponite by increasing the diameter from 32nm to 55nm. The maximum Pluronic L62 Layer thickness from DLS is calculated to be 11.5nm. High molecular weight PEO onto laponite was shown to only increase layer thickness by 4.7nm with a 43Kg/mol PEO.[32]

Pluronic F127 onto carbon black increased layer thickness by 7.1nm.[33] Pluronic L62 layer thickness by DLS is within reasonable agreement with other surfactants adsorbed onto different particles.

The optimal layer thickness increase for 0.01% Pluronic L62 is due to its packing onto Laponite. At concentrations below 0.01% Pluronic L62, the ratio of polymer to Laponite surface area is small. As the ratio increases, the Pluronic L62 begins to pack tighter and layer thickness drops. As the polymer concentration approaches 1.0% Pluronic L62, micellization of Pluronic L62 contributes to a lower diameter. Interfacial tension studies will be discussed in the next chapter. The change in layer thickness is similar to what was observed and proposed for Pluronic F127 and carbon black.

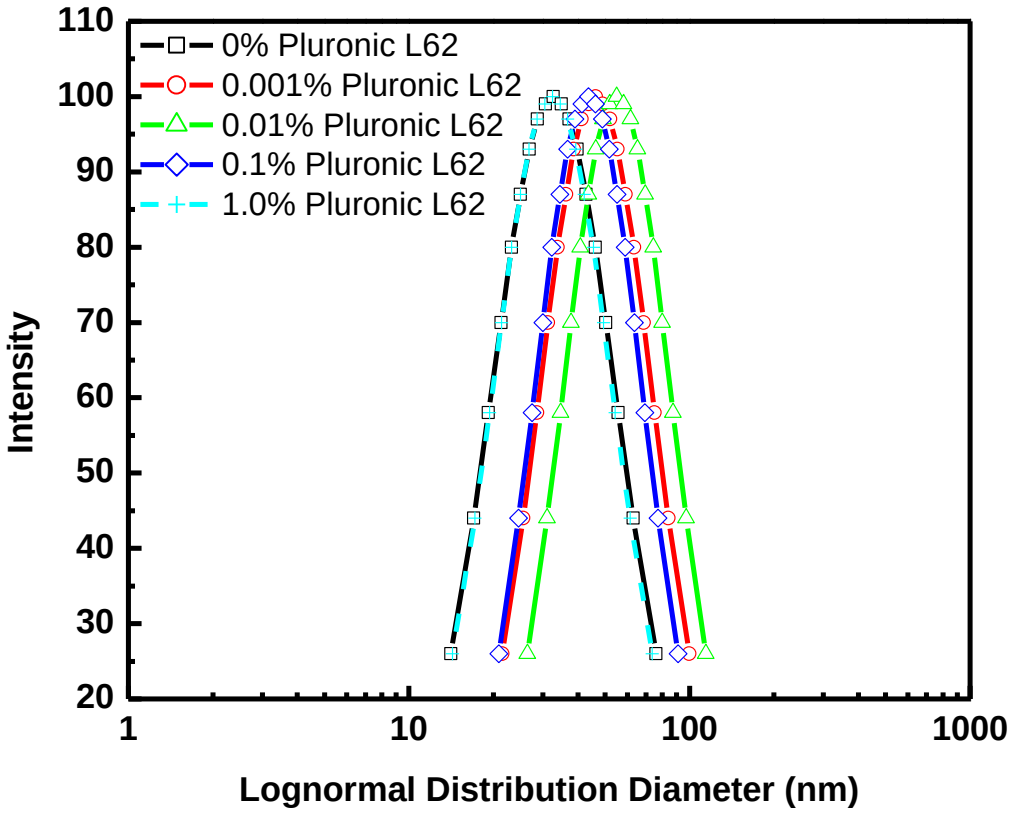

Figure 3. 22. Lognormal Distribution for 0% (black), 0.001% (red), 0.01% (green), 0.1% (blue) and 1.0% (aqua) Pluronic L62 at 1.0% Laponite suspensions.

3.3.6 Adsorption Layer thickness- Viscometry

Figure 3.23 shows the relative viscosity as a function of volume fraction of Pluronic L62. In Figure 3.23, low volume fractions had higher relative viscosities. This same trend is observed with the light scattering data. This is due to the polymer not packed tightly onto the Laponite. Theoretically, the relative viscosity should approach 1. In Figure 3.24, the slope from a volume fraction beginning at 0.005 can give a linearity with R^2=0.8054. Knowing the volume fraction and relative viscosity are related to the

layer thickness, a layer thickness of 13.1nm was calculated (discussed in Chapter 2). Even though at low volume fractions of Pluronic L62, the viscometric method (13.1 nm) and DLS analysis (11.1 nm) are in good agreement for the hydrodynamic adsorbed layer thickness of Pluronic L62 onto Laponite.

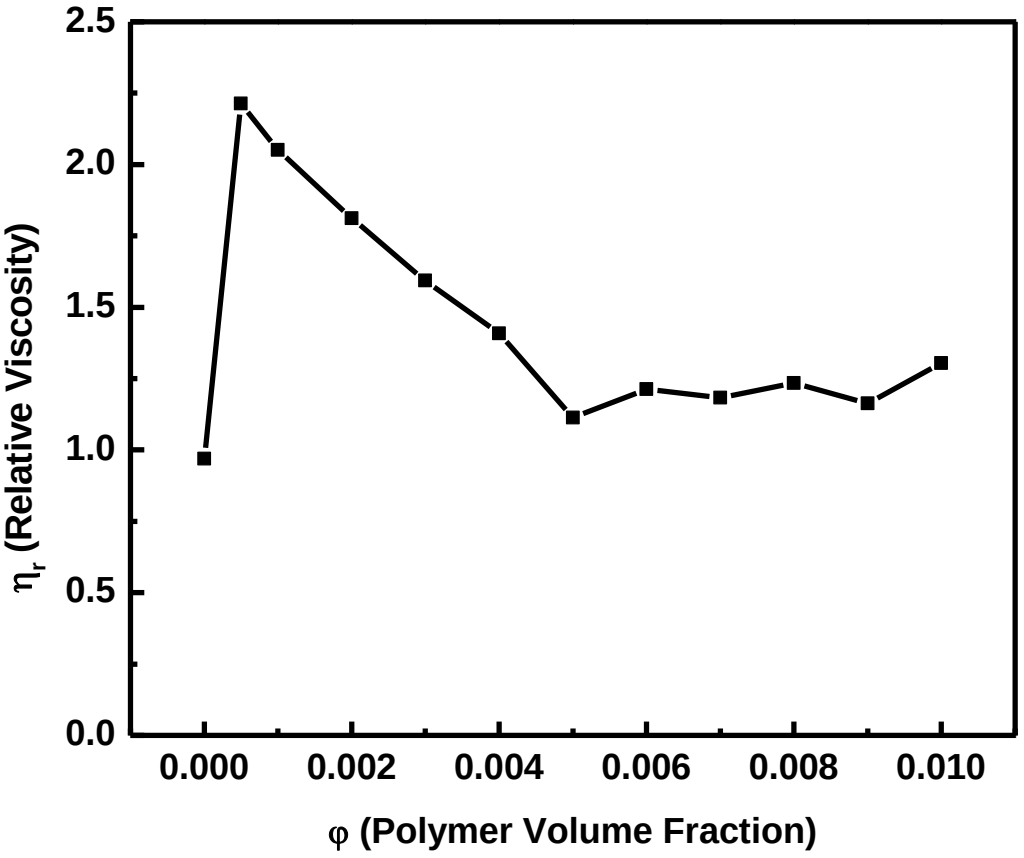

Figure 3. 23. Relative viscosities of 1.0% Laponite suspensions versus Pluronic L62 volume fraction.

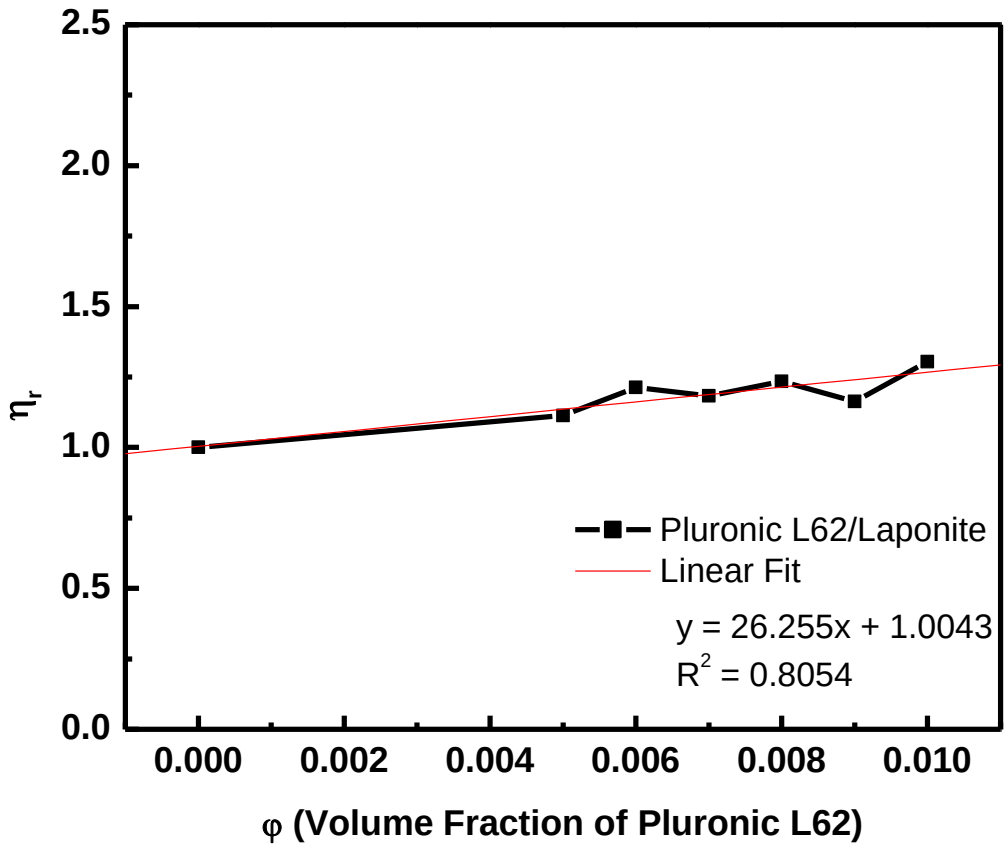

Figure 3. 24. Relative viscosities of 1.0% Laponite suspensions versus Pluronic L62 volume fraction. Adsorbed layer thickness can be calculated from the slope by eq 2.5.

3.4 Chapter Conclusion

Dispersion stability between polymer colloid interactions of Pluronics and PEG2000 with Laponite in aqueous media is an important parameter for the mechanism and preparation of firefighting foam technology. Initially, to understand the dispersion behavior rheological and surface charge characterizations were performed. Next a thermal characterization looking at the mass loss and derivatives of the suspension was

performed to understand how the dispersion affected water removal and polymer degradation. Finally, the adsorption isotherm and adsorption layer thickness were determined on the Laponite particles. These studies provide a fundamental understanding and practical application in designing firefighting foam formulations.

The rheological characterizations of elasticity and flow show that 0.1% of polymer is needed to affect these parameters. Electrostatic contributions were the major contributor in all three polymeric systems up to 0.1%. Pluronic L62 showed increased rheological responses in both experiments, the steric buildup increased repulsion leading to increases in structural and flow values. Optimal rheological properties were within 2.5% and 6.5% Pluronic L62 with Laponite.

Both zeta-potental and streaming current potential showed the electrostatic repulsion dropped as all polymeric systems were added to Laponite. This trend demonstrated as the polymer was added, the electrostatic repulsion dropped significantly by a reduction in potential. Most literature has used zeta potential using DLS. In this work, streaming current potential was used to demonstrate feasibility. Pluronic L62 was compared to a common cationic polyelectrolyte, PDADMAC, to gain better insight into how a nonionic surfactant behaves to a common electrolyte. Initially, both show a drop in potential. In PDADMAC's case the charge is neutralized and turns positive. In Pluronic L62's case the charge plateaus out beyond 1% addition.

TGA studies showed that there is an optimal and synergistic contribution of the Pluronic L62 with Laponite in regards to thermal stability. The incorporation of Laponite and Pluronic L62 increases the thermal resistance of water by shifting the peaks to

higher values. Addition of Laponite significantly improves the thermal stability of Pluronic L62, from 346.9 °C for a 1% Pluronic L62 solution to 376.6 °C for 1.0% Pluronic L62 with 2.0% Laponite. This practical experiment suggests that for firefighting foam formulations, the optimal range of Laponite is between 1% and 2% where as Pluronic L62, minimal ranges should be between 1% and 2.5%. Values above 2.5% Pluronic L62 with Laponite are only affected from polymer addition.

The adsorption isotherm for Pluronic L62, Pluronic 17R4 and PEG2000 onto Laponite was determined using a centrifugation technique and a colorimetric method developed to determine the unbound polymer concentration water. Laponite was saturated by 0.65% polymer content. Pluronic L62 had the highest affinity to Laponite. High affinity of polymer systems may provide advantages in firefighting applications. This demonstrated that the hydrophobicity and geometry of Pluronic L62 are significant parameters for adsorption onto Laponite for firefighting formulations.

Viscometry and DLS provided similar results to the adsorbed layer thickness for Pluronic L62 onto Laponite, 13.1 nm and 11.2 nm respectively. Viscometric data allowed for determination of layer thickness at higher polymer content above 0.5%. At lower surfactant concentration, DLS demonstrated that the adsorbed layer thickness increases. At 1.0% Pluronic, the layer thickness begins to drop showing bimodal behavior from the polymer micelle. The micelle hydrodynamic layer for Pluronic L62 is 14 nm compared to the hydrodynamic radius of Laponite at 32 nm. The changes in particle size distribution correlates with what was observed for the zeta-potential for Pluronic L62. The radius size demonstrates how the polymer can pack in order to

provide more structure at the Laponite interface and optimal thermal properties for firefighting application.

3.5 References

(1) Iurascu, B.; Siminiceanu, I.; Vione, D.; Vicente, M. A.; Gil, A. *Water Research*, **2009**, *43(5),* 1313-1322.

(2) Sabino, M.C; Glen, M.A.; Rabe, T.E. U.S. Patent, **2005**, US 20050244355 A1 20051103.

(3) Seydibeyoglu, M.O.; Isci, S.; Guengoer, N.; Ece, O.I.; Guener, F.S. *Journal of Applied Polymer Science*, **2010**, *116(2),* 832-837.

(4) Doyle, J.; Barlas, J. *Polymers Paint Colour Journal*, **1995**, *185, 4369,* 15-17.

(5) Haraguchi, K.; Song, L. *Macromolecules*, **2007**, *40, 15,* 5526-5536.

(6) Mourchid, A.; Delville, A.; Lambard, J.; LeColier, E.; Levitz, P. *Langmuir,* **1995,** *11, 6,* 1942-1950.

(7) Willenbacher, N. *Journal of Colloid and Interface Science*, **1996**, *182, 2,* 501-510.

(8) Stefanescu, E.A.; Schexnailder, P.J.; Dundigalla, A.; Negulescu, I.I.; Schmidt, G. *Polymer*, **2006**, *47, 21,* 7339-7348.

(9) Saunders, J.M.; Goodwin, J.W.; Richardson, R.M.; Vincent, B. *The Journal of Physical Chemistry B,* **1999**, *103, 43,* 9211-9218.

(10) Barron, W.; Murray, B.S.; Scales, P.J.; Healy, T.W.; Dixon, D.R.; Pascoe, M. *Colloids and Surfaces A: Physicochemical and Engineering Aspects*, **1994**, *88, 2–3,* 129-139.

(11) Nicolai, T.; Cocard, S. *Langmuir,* **2000**, *16, 21,* 8189-8193.

(12) Bohmer, M.R.; Koopal, L.K.; Janssen, R.; Lee, E.M.; Thomas, R.K.; Rennie, A.R. *Langmuir*, **1992**, *8,* 2228-2239.

(13) Bergaya, F.; Theng, B.K.G.; Lagaly, G*. Handbook of Clay Science, Developments in Clay Science*, **2006**, Wiley VCH, New York, 1, 141-245.

(14) Mourchid, A.; Delville, A.; Lambard, J.; LeColier, E.; Levitz, P. *Langmuir,* **1995**, *11*, *6,* 1942-1950.

(15) Macosko, C. W. *Rheology: Principles, Measurements and Applications*, **1994**, Wiley VCH, New York, 461-464.

(16) Boucenna, I.; Royon, L.; Colinart, P. *Journal of Thermal Analysis and Calorimetry*, **2009**, *98*, 119–123.

(17) Castelletto, V.; Ansari, I.A.; Hamley, I.W. *Macromolecules,* **2003**, *36,* 1694-1700.

(18) Nelson, A.; Cosgrove, T. *Langmuir,* **2004**, *20,* 10382-10388.

(19) De Lisi, R; Lazzara, G.; Milioto, S.; Murator, N. *Journal of Thermal Analysis and Calorimetry,* **2007***, 87, 1,61–67.*

(20) De Lisi, R.; Lazzara, G.; Lombardo, R.; Milioto, S.; Muratore S.; Turco Liveri, M. L. *Physical Chemistry Chemical Physics*, **2005**, *7*, 3994 –4001.

(21) Nelson, A.; Cosgrove, T. *Langmuir,* **2004**, *20,* 2298-2304.

(22) Bohmer, M.R.; Koopal, L.K.; Janssen, R.; Lee, E.M.; Thomas, R.K.; Rennie, A.R. *Langmuir*, **1992**,*8*, 2228-2239.

(23) Lal, J.; Auvray, L. Journal Applied Crystallography, **2000**, *33*, 673-676.

(24) Nelson, A.; Cosgrove, T. *Langmuir*, **2005**, *21,* 9176-9182.

(25) Lin, Y.; Smith, T.W.; Alexandridis, P. *Langmuir,* **2002**, *18,* 6147-6158.

(26) Ghebeh, M.; Corrigan, A. H.; Butler, M. *Anal. Biochem.* **1998**, *262,* 39-44.

(27) Van Olphen, H. *An Introduction to Clay Colloid Chemistry*, Wiley, New York, **1977**.

(28) Sun, K.; Raghavan, S.R.; *Langmuir*, **2010**, *26, 11*, 8015–8020.

(29) Umemura, Y.; Yamagishi, A.; Schoonheydt, R.; Persoons, A.; De Schryver, F. *Thin Solid Films*, **2001**, *388*, 5–8.

(30) Pelton, R.; Cabane, B.; Cui, Y.; Ketelson, H.A. *Analytical Chemistry*, **2007**, *79*, 8114-8117.

(31) Cui, Y.; Pelton, R.; Ketelson, H.A. *Macromolecules,* **2008**, *41*, 8198-8203.

(32) Nelson, A.; Cosgrove, T. *Langmuir,* **2004**, *20,* 2298-2304.

(33) Lin, Y.; Smith, T.W.; Alexandridis, P. *Langmuir,* **2002**, *18,* 6147-6158.

CHAPTER 4

FILM AND AIR-LIQUID SURFACE PROPERTIES OF LAPONITE POLYMER INTERACTIONS

4.1 Introduction

Film and interface properties are a topic of much interest. Many end-use applications for film and interface properties include medical[1], pharmaceutical[2], optical[3], electronic[4] and packaging[5] fields. Clay polymer films provide an improved barrier response to mechanical[6], retentive[7], conductivity[8] or gas diffusion[9]. Particle polymer systems have shown to improve film and interface structural and mechanical properties observed when in combination.

Surface Energy of particle surfactant interfaces has focused on clays with cationic surfactants for particle stabilized foams by looking only at the contact angle of water.[10] The surface energy is associated with barrier properties of interfaces.[11,12] In general all three phases of matter have surface force components. Derjaguin-Landau-Verwey-Overbeek (DLVO) interactions recognizes there is a balance of competing forces for colloid (suspension) stability in regards to potential net energy (Gibbs free energy) of the colloidal system. Contact angle is a measurement of a liquid droplet on a surface that provides the information necessary to give surface energy. The following work will provide a more complete picture of the Laponite Polymer interactions of films and how this impacts firefighting foam technology. Another advantage of looking at different liquids is that surface energy calculations look at solvents that have apolar and a broad range of liquid interfacial energies. In other words, varying the organic liquids for surface energy calculations provides direct applicability for which particle stabilized foam would be compatible for organic fires, Class B type.

X-Ray Diffraction of nanocomposites has shown structural changes in Laponite by intercalation of a polymer into the silicate matrix.[13] Many cationic polymers are intercalated into clay matrices, driven mainly by ion exchange from the clay surface anions and the surfactant cations.[14,15] Other work has investigated nonionic polymers such as polyethyleneoxides, driven through hydrogen bonding mechanism of hydroxyl groups from both the clay and polymer.[16,17] This work will focus on how the functionality and geometry are additional factors that attribute to this mechanism of Laponite and Pluronic system providing enhanced structural properties for firefighting foam applications.

Particle stabilized foams have increased structural properties formed at the air water interface that are linked to retarding foam drainage.[18,19] The dilatational response is a common way to characterize the foam properties in food and foaming applications.[20,21] This technique is typically a pendant drop method using an expanding and contracting bubble. Very few observations have been obtained due to difficulty in instrumentation using a shearing mechanism[22], more realistic to foam drainage. The following work will optimize the most relevant ratio of of Pluronic L62 to Laponite for firefighting foam technology.

This chapter discusses the film and air-liquid surface properties of Laponite aqueous dispersions with Pluronic L62, a wetting and foaming nonionic surfactant, Pluronic 17R4, a wetting and defoaming nonionic surfactant, and a Polyethyleneoxide, a hydrophilic homopolymer with wetting and no foaming properties. This chapter provides a better understanding of the interfacial properties of Laponite and Pluronic L62. In

addition this chapter describes how the different types of polymer structure and hydrophilicity impact particle stabilized foams.

4.2 Experimental

The Laponite Polymer films were characterized with an OCA 20 by placing 10 drops of Laponite Polymer dispersions onto glass slides. Samples were dried in an oven overnight at 60°C and placed in a dry chamber until use. A 500 µL Hamilton Syringe with a 22 gauge flat tip needle was used to place 5 µL of liquid on the films. Analytical grade water, glycerol and dichloromethane were the three liquids used for the complete surface energy calculation of each Laponite-polymer film. All contact angles were taken at equilibrium, not more than 5 seconds. The contact angles were measured at 20°C under ambient conditions. The film was covered with at least a monolayer of water, which would be a reasonable environment for the type of application. Table 4.1 shows the surface tension parameters for the liquids used in this work.

Table 4. 1. Surface Tension and Surface Energy values in (mN/m) for Water, Glycerol and Dichloromethane.

Liquid[23]	γ_L	γ_L^D	γ_L^P
Water	72.8	29.1	43.7
Glycerol	64	37.4	26
Dichloromethane	28.6	26.5	2.1

Sample films were also analyzed by Small angle XRD by placing 10 drops of Laponite Polymer dispersions onto glass slides. The samples were dried overnight at

60°C and placed in a dry chamber until use. All XRD were collected using a Siemens D-500 Powder X-Ray Diffractometer coupled to a copper anode source. The diffractometer was equipped with a diffracted beam flat graphite monochromator, a CuKα x-ray tube and a scintillation detector. Diffraction patterns were collected in reflection mode geometry from 2-40° 2θ at a scan rate of 0.05° and a dwell time of 2.00 seconds.

The interfacial rheology experiments are performed using a double wall ring (DWR) geometry attached to a stress-controlled rheometer (AR G-2, TA Instruments). The details of the governing equations have been described elsewhere,[24] as well as chapter 2. Two types of experiments were performed 1. Oscillation, i.e. stress and frequency sweeps, and 2. Steady state flow. The stress sweep parameters are as follows: equilibration of 10 minutes after the gap was set to the air-liquid interface, the stress swept from 0.01 μNm to 100 μNm with 5 steps each decade in logarithmic mode and the frequency was set at 0.1 Hz. Once the Linear Viscoelastic Region was determined, a frequency sweep was performed as follows: equilibration of 10 minutes after the gap was set at the air-liquid interface, frequency sweep was from 0.1 Hz to 10 Hz at at stress of 1.0 μNm. In the steady state flow experiments, there was a ramp up and ramp down in torque. The ramp up (ramp down was in opposite order) torque was from 0.1 μNm to 10 μNm with 5 steps per decade in logarithmic mode. Each step was allowed 5 minutes to equilibrate 3 shear values within 5% of the previous shear value for 30 seconds each.

4.3 Results and Discussion

4.3.1 Surface Energy of Laponite Films

Contact angle from sessile droplet has been used to differentiate particle stabilized foams. Water has both a polar and dispersive contribution to surface energy. This is useful but more value can be distinguished looking at the total surface energy of the particle stabilized foam. This work looks at the full picture of the surface energy of the laponite polymer systems and how the total surface energy impacts particle stabilized foams.

Figures 4.1 through Figures 4.3 show the actual snapshot of a Sessile Drop experiment on a 2% Laponite dried film on a glass substrate. An explanation on how the contact angles are used for surface energy values follows by looking at the untreated Laponite film. Contact angles and surface energy of the Laponite film is consistent to other clays of Laponite[25] and hectorite[26]. The droplet upon contact with the surface drops from the needle and a picture is taken upon equilibrium, contact angle does not change. Figure 4.1 is a water droplet at a contact angle of 42.5° ± 0.2°. This value is agreement with previous work on Laponite powders as a function of cation exchange. Table 4.1 shows the common interfacial energy values for the three liquids used to determine the dispersive and polar forces of the Laponite polymer composites. Water has the highest surface energy values with moderate polar energy values. In general like attracts like, when the surface energy of the liquid is high and the surface energy of the film is high low contact angles are expected. This is generally termed as a wettable surface with the respective liquid.

Figure 4.2 is a sessile droplet using Glycerol. One noticeable difference is the lower contact angle of 26.2° ± 1°. Glycerol has a lower surface energy. The Laponite

surface shows more affinity to Glycerol resulting in a lower contact angle. Table 4.1 also shows that the polar components γ^P is close to half the value of water and the γ^D is relatively higher to water. Figure 4.3 is a sessile droplet of Dichloromethane with a contact angle of 12.2° ± 0.1°. Dichlormethanes surface energy is the lowest of the three test liquids. Dichloromethane has only a dispersive energy component γ^D of 26.5 mN/m. Dichloromethane's contact angle is only associated with the dispersive component of the Laponite film.

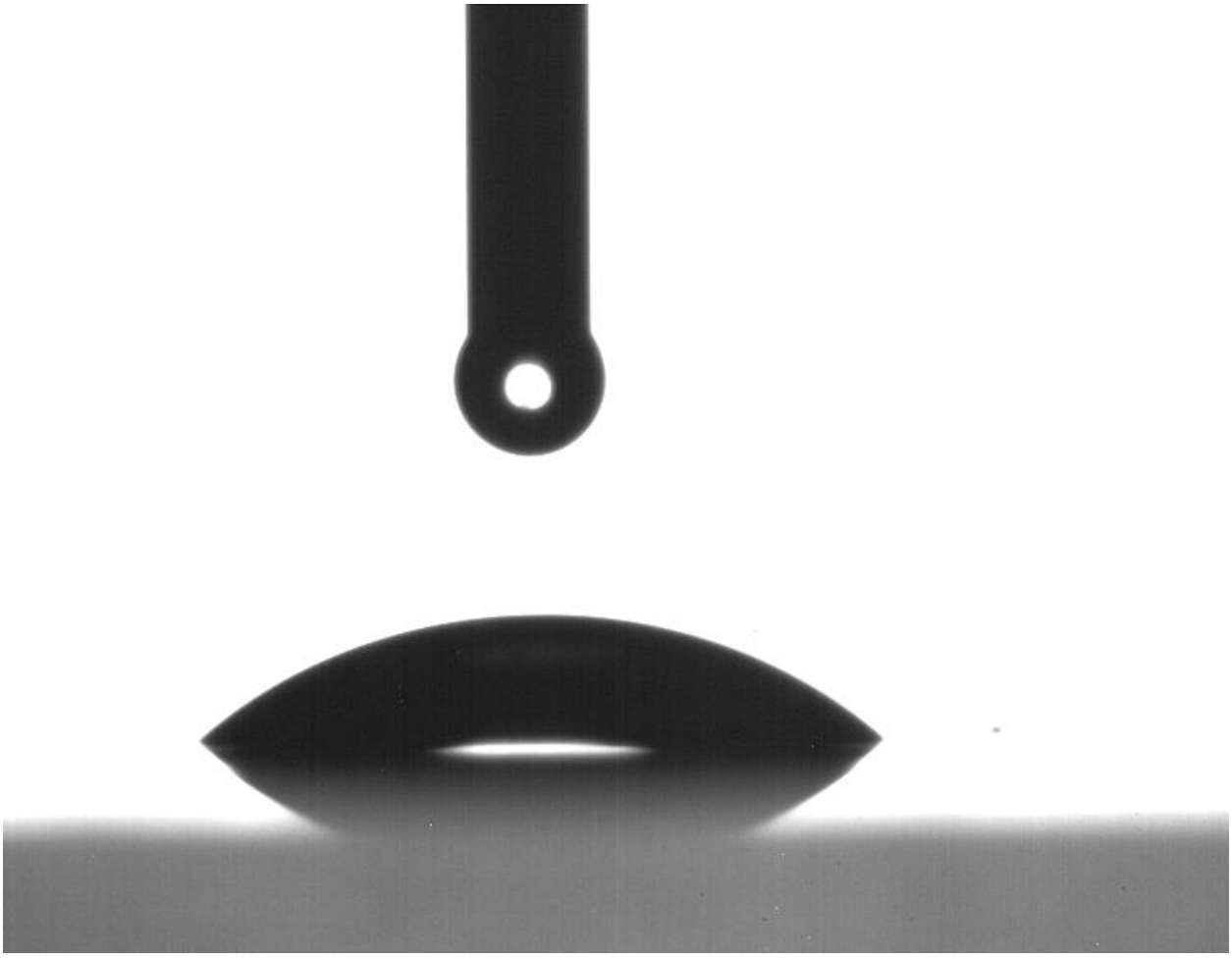

Figure 4. 1. Sessile Droplet on a 2% Laponite Film from 5 µL Water.

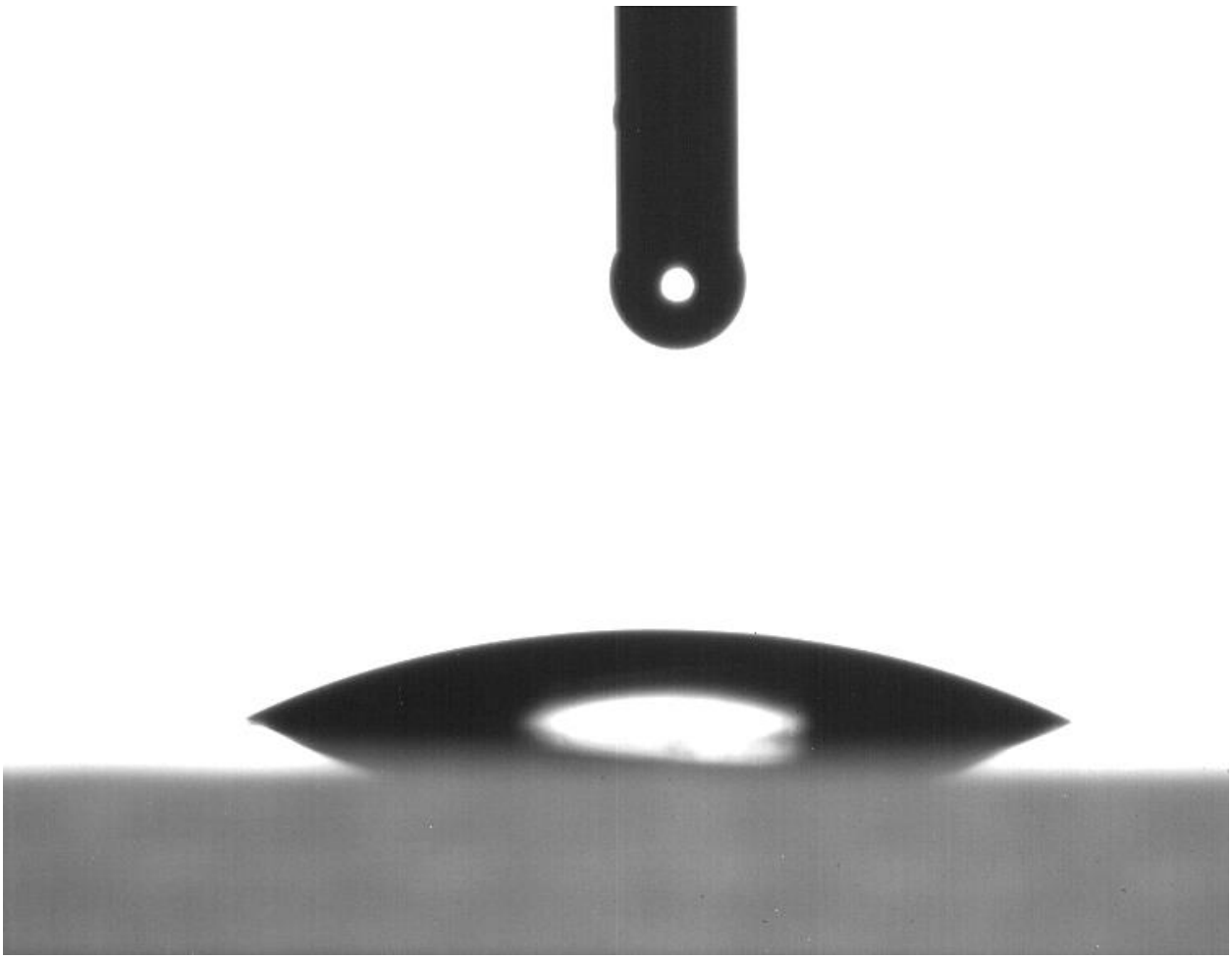

Figure 4. 2. Sessile Droplet on a 2% Laponite Film from 5 µL Glycerol.

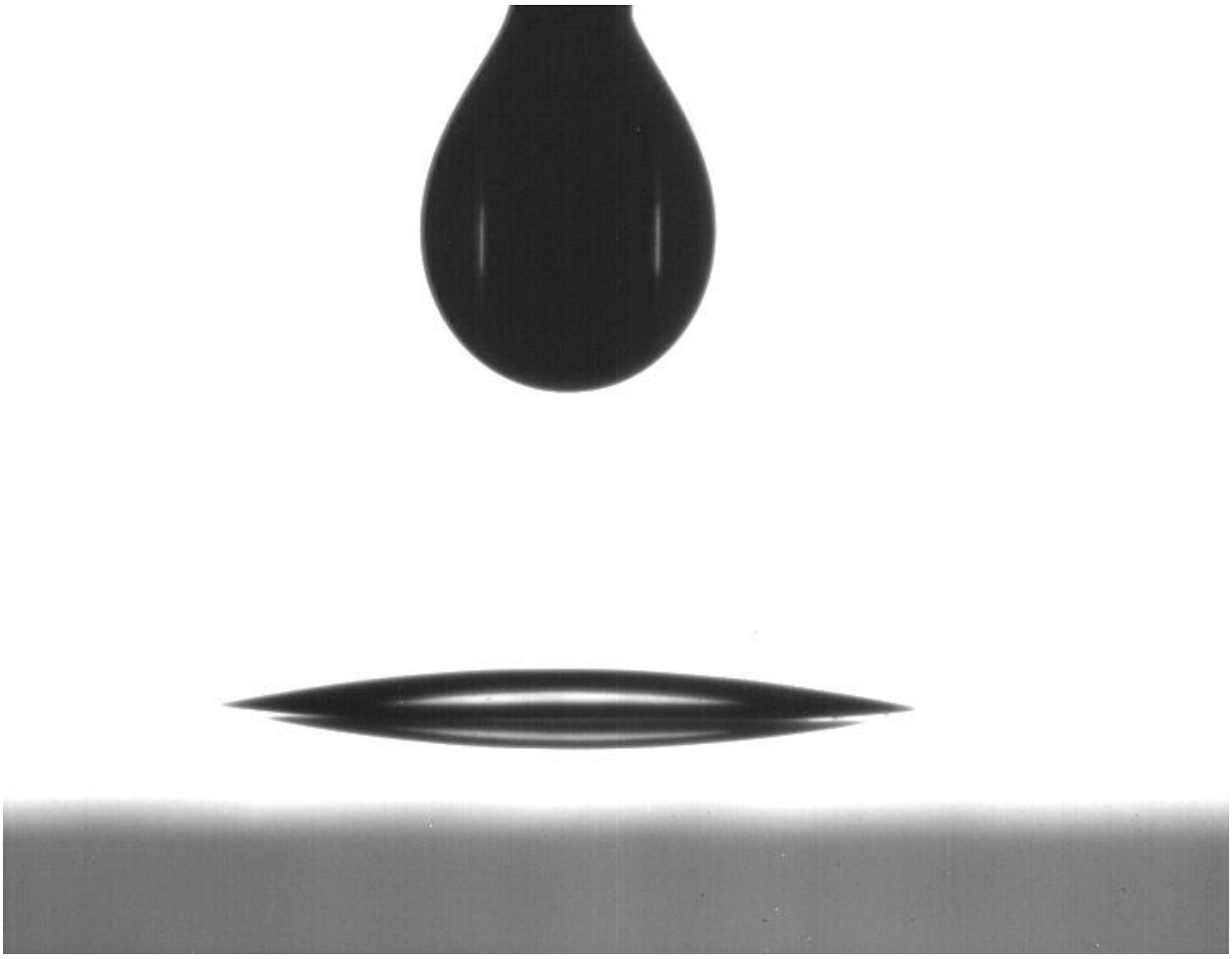

Figure 4. 3. Sessile Droplet on a 2% Laponite Film from 5 µL Dichloromethane.

The contact angles from each liquid are used to determine the surface free energy of the films. Figures 4.4 through Figure 4.6 show the calculated dispersive, polar and total surface free energy of the Laponite films with respective polymer. Figure 4.4 shows the polymer response of PEG2000 with 2% Laponite films. The polar surface free energy is the major contributor for total surface energy. At 0.25% PEG2000 content there is a reduction in polar surface energy of the Laponite film, a minima occurs. At 1.0% PEG2000 content, a maxima occurs in polar surface energy of the Laponite film.

The dispersive free energy has minimal contribution to the total surface energy for the Laponite films. The dispersive energy is consistent in value up to 1.0% PEG2000. Beyond 1.0% PEG2000, the dispersive free energy values drop in half. The total surface free energy for Laponite and PEG2000 films follow the same trend as the polar surface free energy values.

The surface free energy diagram demonstrates that the Laponite film is consistently the same up to 0.25% PEG2000. Saturation of the Laponite particles occurs at 0.25% PEG2000, due to minima in surface free energy. A maxima is reached at 1.0% PEG2000 and plateaus. Higher PEG2000 concentrations have saturated the Laponite surface resulting in an increase of polarity and reduction in dispersivity.

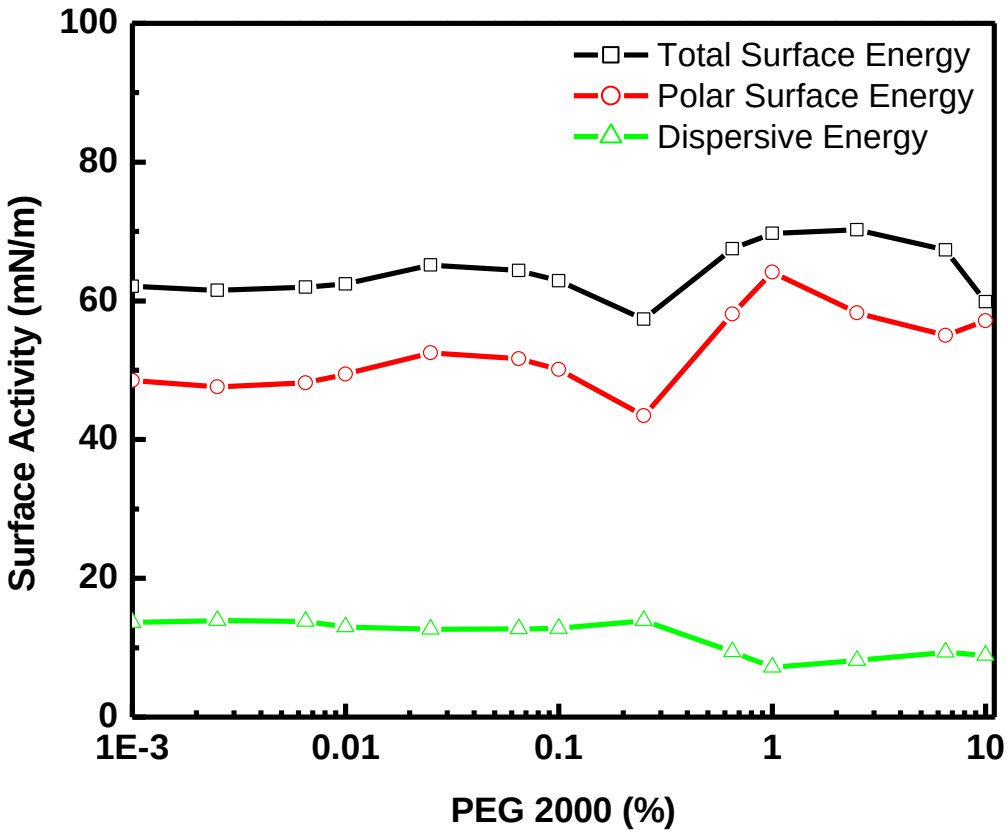

Figure 4. 4. Surface Energy Components for dried 2% Laponite Films with PEG2000 dose response. Total Surface Energy (□, black), Polar Surface Energy Component (○, red) and Dispersive Surface Energy Component (△, green).

Figure 4.5 is the surface free energy diagram for Laponite films with Pluronic 17R4, a defoamer/film destabilizer, the same trend is observed to that of the Figure 4.4. But there is a difference in surface energy approaching 0.25% Pluronic 17R4, a reduction in total and polar surface free energy. The hydrophobic character of Pluronic 17R4 impacts the reduction in polar surface energy. This can be interpreted as the

Laponite and Pluronic 17R4 have a more intimate interaction causing the polar surface energy to reach a minimum at 0.25% Pluronic 17R4. There is a similar increase in both the total and polar surface energies for the Laponite films at concentrations above 1.0% Pluronic 17R4. Additionally, the dispersive surface free energy follows the same trend as does the Laponite PEG2000 films. The hydrophobicity has a significant impact on polar surface free energy up to 0.25% Pluronic 17R4. At higher Pluronic 17R4 content the hydrophilicity of the polymer contributes more, deduced from the results obtained for the Laponite PEG2000 films in Figure 4.4. The following conclusion can be also be deduced for Figure 4.6 with Laponite Pluronic L62 films, differences are between polymer architecture of Pluronic L62 and Pluronic 17R4.

Figure 4.6 is the surface free energy diagram for Laponite films with Pluronic L62, a foamer/film stabilizer, the same trend is observed to that of the Figure 4.5. There is a difference in surface energy approaching 0.25% Pluronic L62, a reduction in total and polar surface free energy. The hydrophobic character of Pluronic L62 impacts the reduction in polar surface energy. This can be interpreted as the Laponite and Pluronic L62 have a more intimate interaction causing the polar surface energy to reach a minimum at 0.25% Pluronic L62. There is a similar increase in both the total and polar surface energies for the Laponite films at concentrations above 1.0% Pluronic L62. Additionally, the dispersive surface free energy follows the same trend as does the Laponite Pluronic 17R4 films. The hydrophobicity has a similar impact on polar surface free energy up to 0.25% for both Pluronic 17R4 and Pluronic L62. At higher Pluronic L62 content the hydrophilicity of the polymer contributes more, deduced from the results obtained for the Laponite PEG2000 films in Figure 4.4.

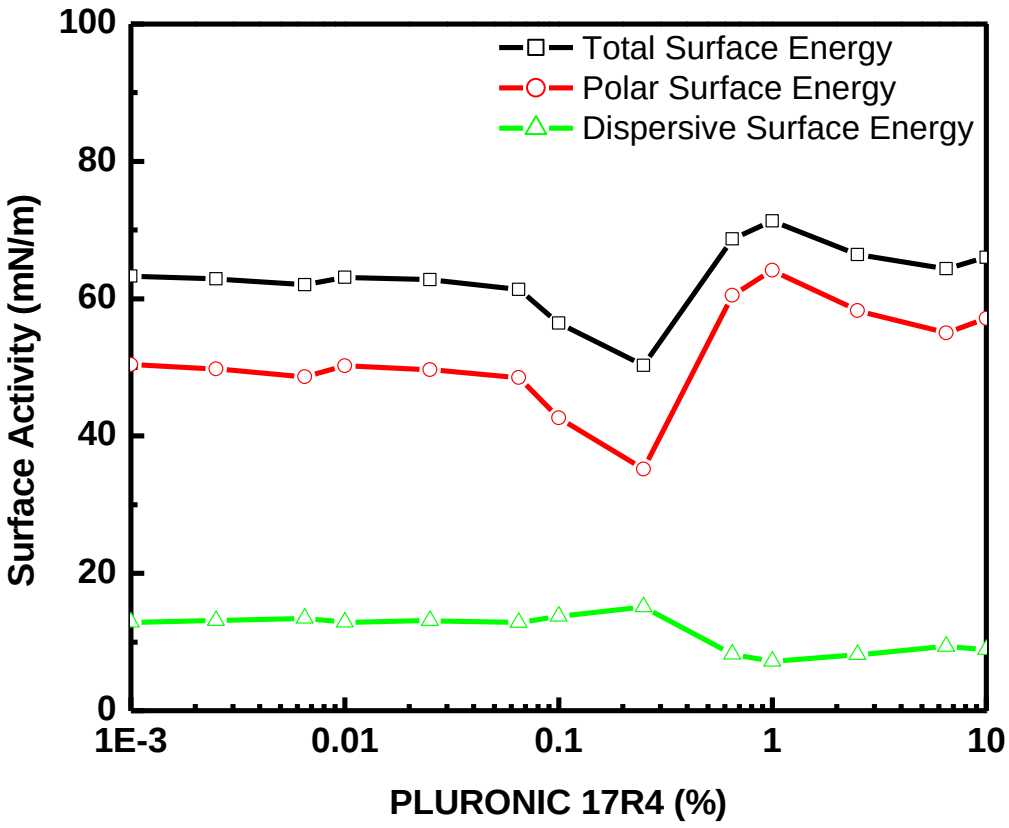

Figure 4. 5. Surface Energy Components for dried 2% Laponite Films with Pluronic 17R4 dose response. Total Surface Energy (□, black), Polar Surface Energy Component (○, red) and Dispersive Surface Energy Component (△, green).

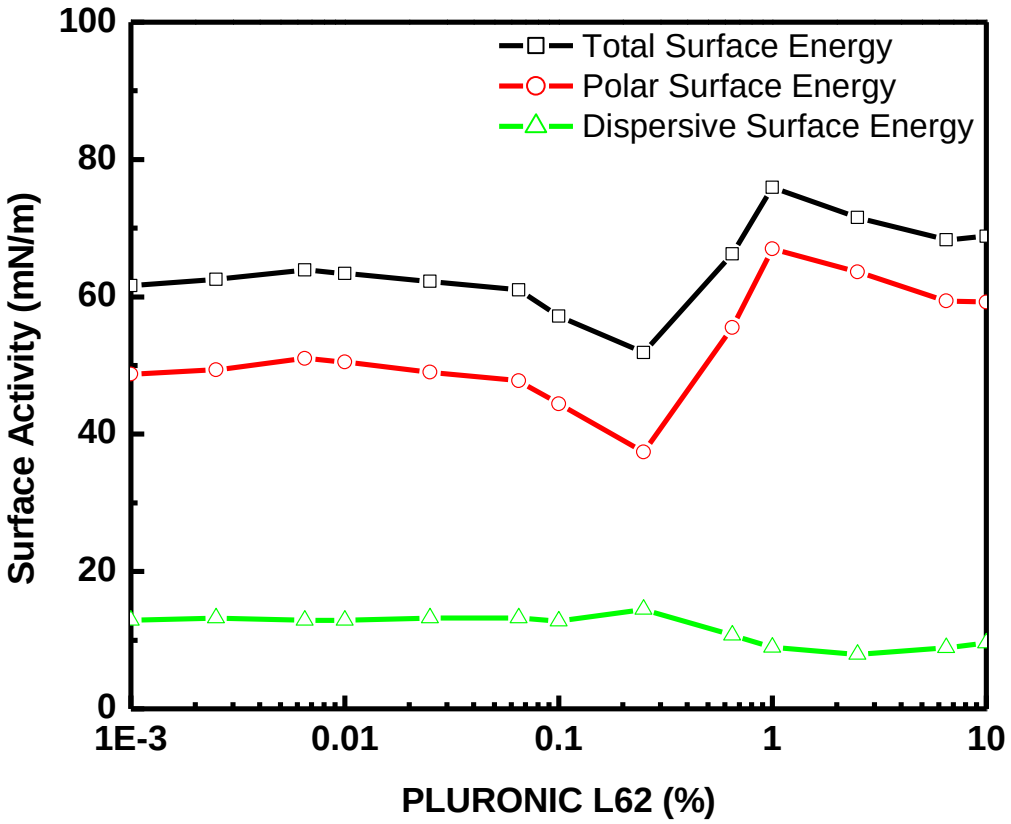

Figure 4. 6. Surface Energy Components for dried 2% Laponite Films with Pluronic L62 dose response. Total Surface Energy (□, black), Polar Surface Energy Component (○, red) and Dispersive Surface Energy Component (△, green).

Summary of Laponite films with Polymers

All surface energy components were dominated mainly from Laponite up to 0.25% polymer content. For all Laponite polymer films, the polar surface energy component contributed most with minima at 0.25% polymer and maxima at 1.0% polymer. The dispersive energy contributed minimally, but reduced in surface energy at 0.25% polymer. Figure 4.7 is the total surface free energies for the Laponite films with

three polymer systems. Laponite total surface energy is the major contributor up to 0.1% polymer content. The external oxygen atoms have not been saturated with the polymers. Differences begin to show up at 0.01% polymer, Laponite approaches polymer saturation. Films begin to differentiate as low as 0.01% PEG2000, with higher total surface energies. The hydrophilic portion of the polymer saturates the Laponite surface with its hydroxyl groups.

Both films using Pluronic 17R4, a defoamer, and Pluronic L62, a foamer, show lower total surface energy values at 0.01% polymer. This infers the functionality of the propylene oxide group to contribute to lower surface energies from 0.1% polymer up to 1.0% polymer. The propylene oxide portion of the Pluronics increases the hydrophobicity of the Laponite Polymer films up to 0.25% polymer. As more polymer concentration increases to 1.0% the hydrophilic portion contributes more to Laponite total surface energy.

The surface energy of the Laponite surfaces with polymer contribution shows how dispersions will behave in different types of liquids. Having particles that are more equivalent in surface energy provides more valuable information than just looking at sessile droplet of water contact angle. Looking at surface energy also is a more useful and easy to use tool to characterize components for particle stabilized films.

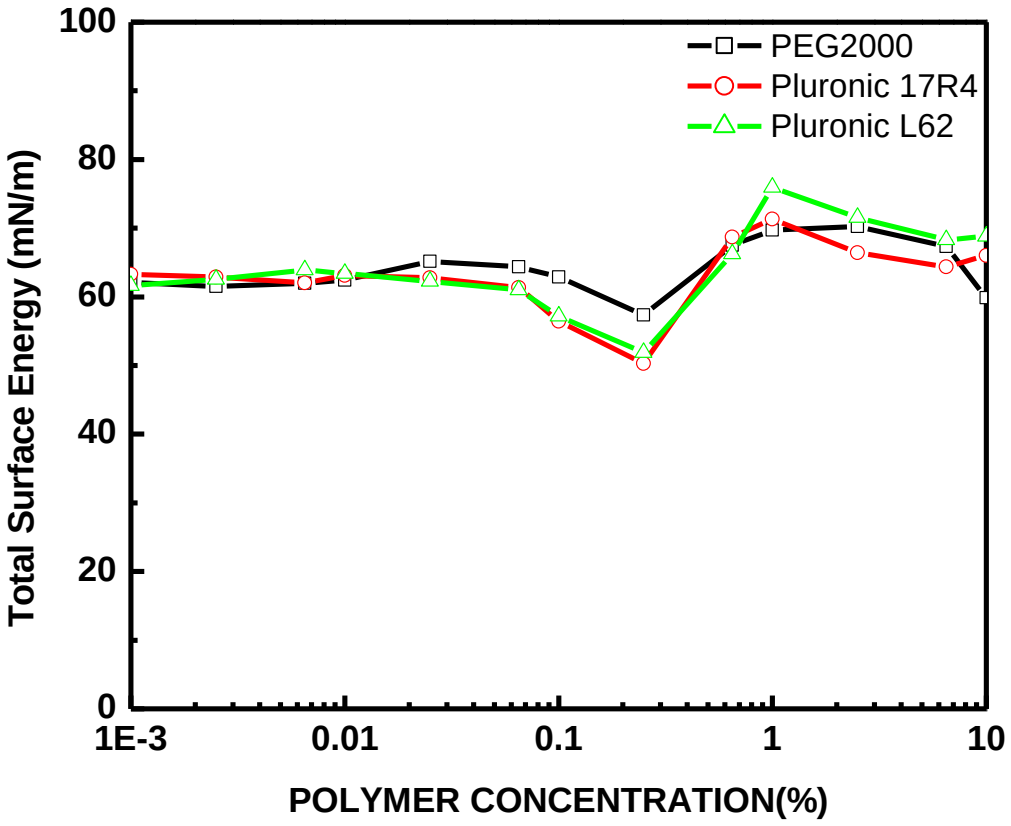

Figure 4. 7. Total Surface Energy for dried 2% Laponite Films with PEG2000, hydrophilic polymer, (□, black), Pluronic 17R4, defoamer, (○, red) and Pluronic L62, foamer, (△, green).

4.3.2 XRD of Laponite Films

From the surface free energy data, further analysis was performed using X-Ray diffraction at low angles for the Laponite polymer systems. In Figures 4.8 through 4.10, there are some general trends in regards to structure. First, Laponite alone has a broad peak for the (001) basal spacing at 14.2 Å, 2θ near 8°. The (001) basal spacing is similar to literature values previously reported.[27,28] Upon addition of 0.25% polymer the (001) basal spacing increases and FWHM decreases. Increasing further to 1.0% polymer content a more oriented structure of the Laponite with polymer occurs due to additional 2θ peaks appearing in the XRD patterns and decrease of FWHM for the (001) reflection. Table 4.2 shows the (001) basal plane spacing for Laponite and polymer content. Intercalation into the silicate matrix is evident for all polymer investigated. The degree of intercalation is similar for both PEG2000 and Pluronic 17R4 at both 0.25% and 1.0% polymer content. At 0.25% Pluronic L62, the spacing increased the most. This is most likely due to the architecture of the propylene oxide group in the middle of the copolymer instead of the outside as in Pluronic 17R4. Saturation of Laponite occurs at 1.0% polymer addition and basal spacings are the same.

The XRD figures reveal the relationship between intercalation and surface free energy for a foaming polymer and the molecularly equivalent, Pluronic 17R4, and hydrophilic polymer component, PEG2000. Pluronic L62 shows more structuring relative to PEG2000 and Pluronic L62. A relationship is noted between the surface free energy and the XRD data. There is a relationship of increased d-spacing and 2θ peaks with the

surface free energy minima. Differentiation of intercalation into the silicate matrix and reduction of total surface energy occurs at 0.25% polymer, most prevalent with Pluronic L62 with highest d-spacing value and lowest total surface energy. Intercalation and total surface energy is equivalent for all 1.0% polymer addition. Others literature values using higher molecular weight Pluronics and a similar PEG2000 have not shown the increased order, mainly due to differences in method preparation.[29]

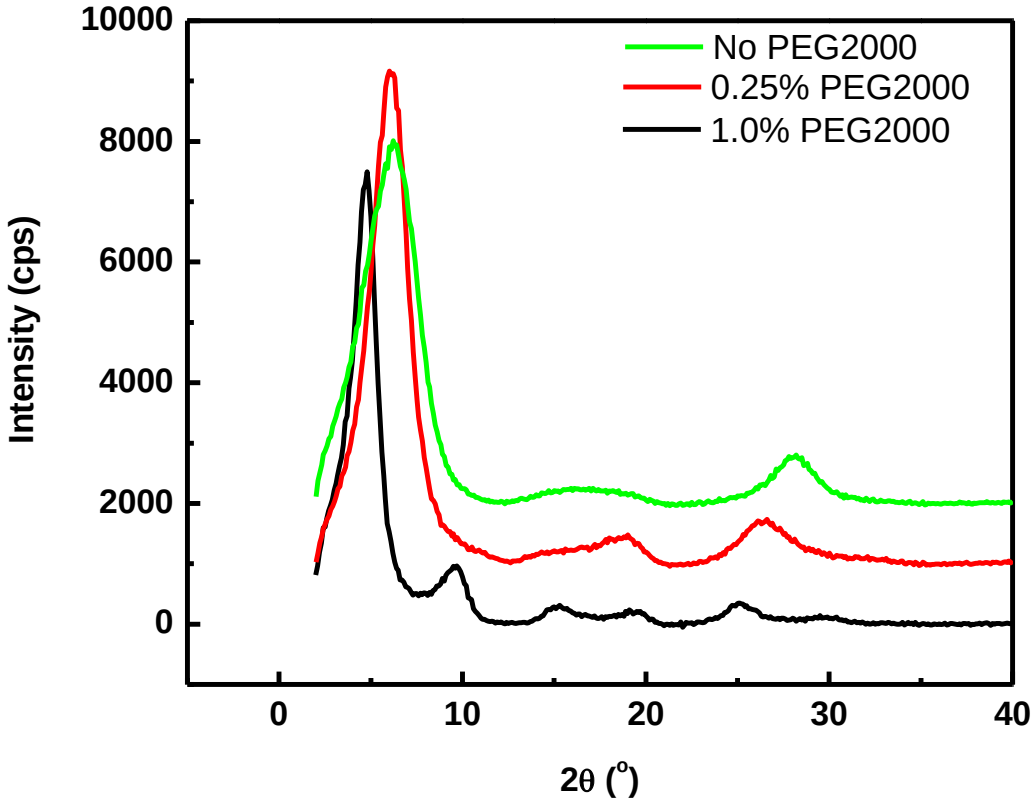

Figure 4. 8. XRD pattern for of 2% Laponite films on glass no PEG2000 (green), 0.25% PEG2000 (red) and 1.0% PEG2000 (black).

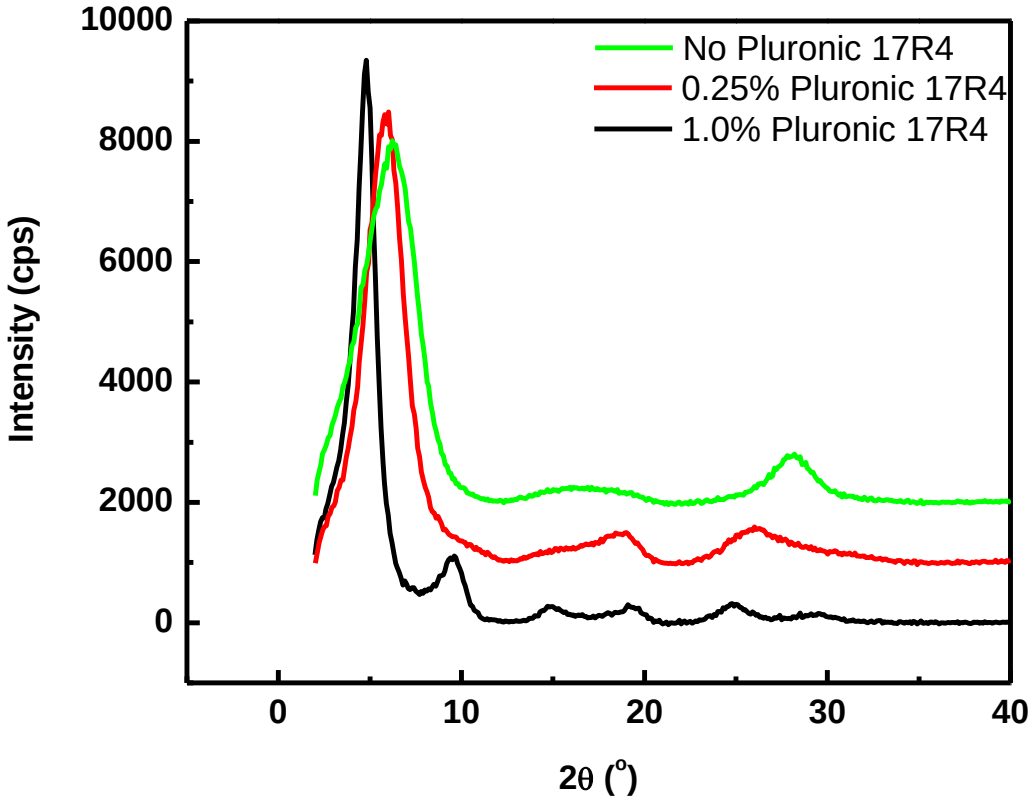

Figure 4. 9. XRD pattern for of 2% Laponite films on glass no Pluronic 17R4 (green), 0.25% Pluronic 17R4 (red) and 1.0% Pluronic 17R4 (black).

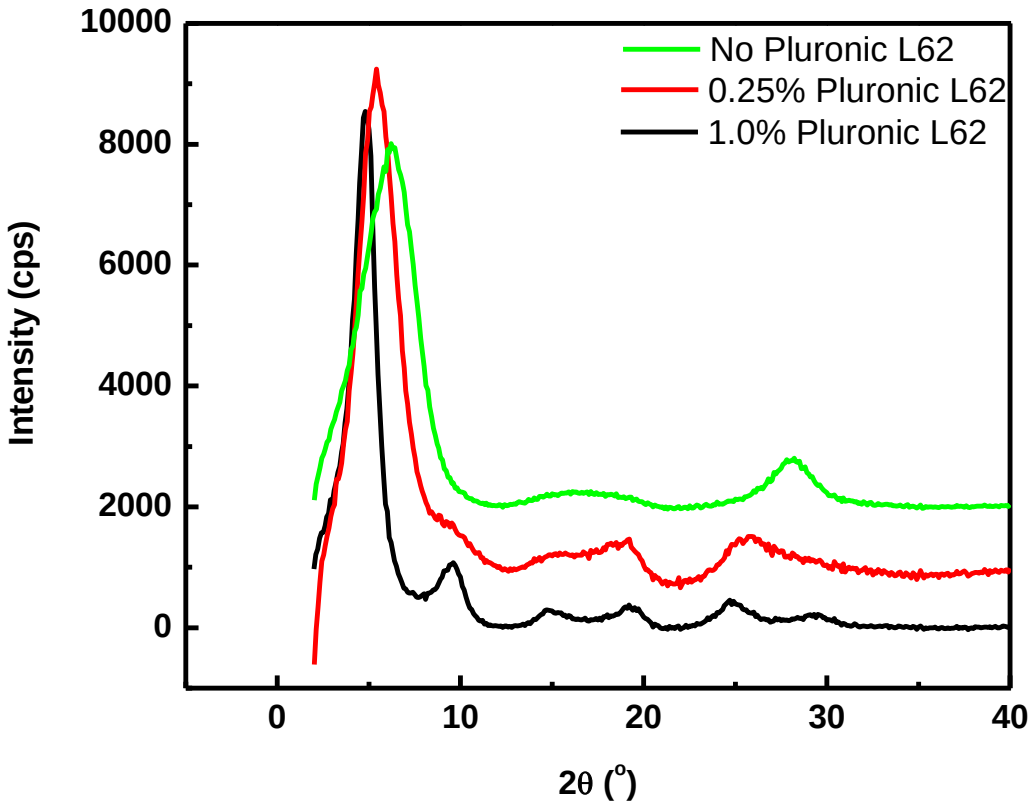

Figure 4. 10. XRD pattern for of 2% Laponite films on glass no Pluronic L62 (green), 0.25% Pluronic L62 (red) and 1.0% Pluronic L62 (black).

Table 4. 2. 2% Laponite films with various polymers and the (001) basal spacings (in Å).

% Polymer	(001) Basal spacing (Å)
0%	14.2
0.25% PEG2000	14.7
1.0% PEG2000	18.4
0.25% Pluronic 17R4	14.7
1.0% Pluronic 17R4	18.4
0.25% Pluronic L62	16.3
1.0% Pluronic L62	18.4

4.3.3 Interfacial Surface Tension of Laponite Suspensions with Pluronic L62

Figure 4.11 reveals the importance of Laponite's interaction with Pluronic L62 at the air-liquid interface, in relation to surfactant adsorption on the Laponite surface by the interfacial tension values. At low polymer concentration, the Laponite depletes Pluronic L62 from the liquid interface up to 0.1% Pluronic L62. A minima in interfacial tension is reached at 0.65% Pluronic L62. What is also revealed is that at 0.65% Pluronic L62 with Laponite the interfacial tension is equivalent to that of the Pluronic L62 alone, critical micelle concentration of Pluronic L62 is 0.5%. At 1.0% Pluronic L62, the liquid interface now has adsorbed Laponite interacting with the Pluronic L62. The next section provides structural characterization that is linked to this Laponite Pluronic L62 layer at the air-liquid interface.

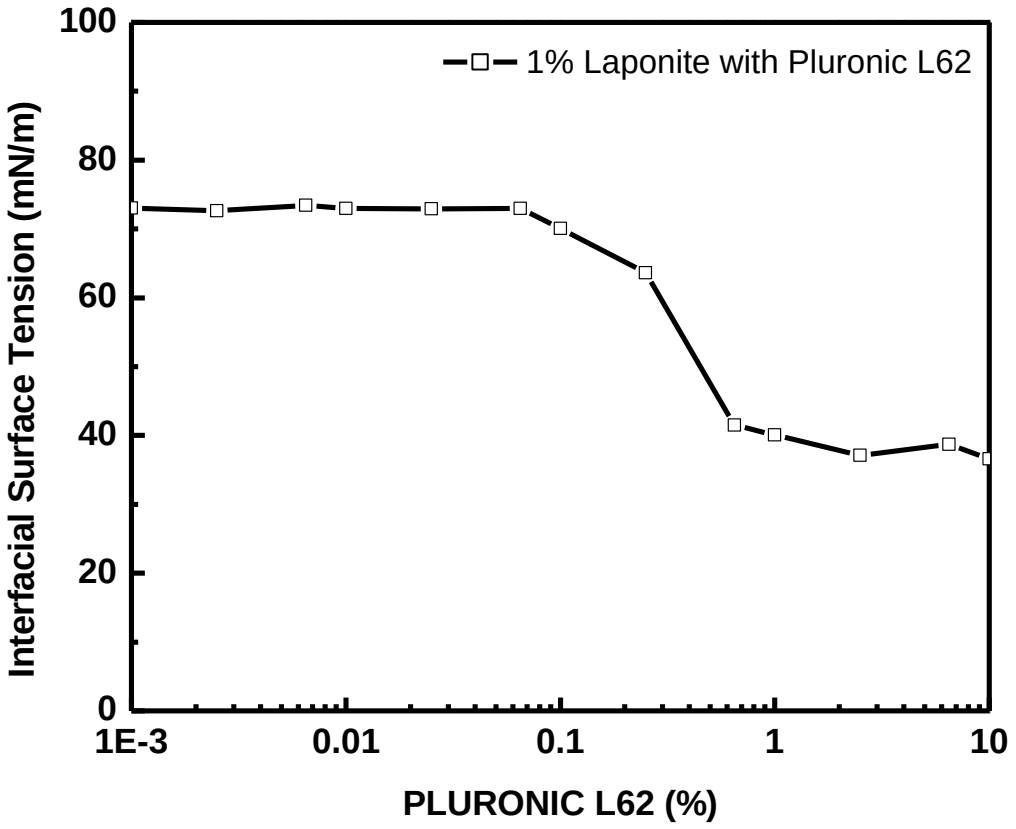

Figure 4. 11. Interfacial Surface Tension of 1% Laponite Dispersion with Pluronic L62 Dose Response.

4.3.4 Interfacial Rheology of Laponite with Polymers

The following is a discussion of the viscoelastic properties for the Laponite polymer films at the air-liquid interface as it may relate to foam stability. The Laponite films reveal how the polymer interactions and functionality changes the film structure at the air-water interface. This frequency range was chosen to demonstrate how the hydrophobic and architectural differences of Pluronic L62 provide enhanced structure to the Laponite films. Laponite alone at the air-water interface shows only a viscous modulus response with minimal storage modulus. Figure 4.12 shows the interfacial storage and loss modulus for 2.0% Laponite with PEG2000 dose response. All are viscous dominant at the interface, there is little elastic contribution of the PEG2000 upon an increase in concentration. This dose response shows that Laponite is depleting the liquid surface of PEG2000. At 1.0% PEG2000 the loss modulus has dropped significantly. Figure 4.13 shows the interfacial storage and loss modulus for 2.0% Laponite with Pluronic 17R4, similar to that shown in Figure 4.12.

Figure 4.14 shows the interfacial storage and loss modulus for 2.0% Laponite with Pluronic L62. The Pluronic dose response is similar to both PEG2000 and Pluronic 17R4 up to 0.01% polymer. At 0.1% Pluronic L62, there is an exponential increase in storage and loss moduli, still viscous dominant. There is another increase in modulus response at 1.0% Pluronic L62. At 1.0% Pluronic L62, a highly elastic interface is formed. Increased interfacial storage modulus may provide enhanced foam stability for particle stabilized foams using Pluronic L62 and Laponite. Laponite with polymer

concentrations of 2.5% Pluronic L62 were difficult to handle and ensure an even liquid layer to obtain results.

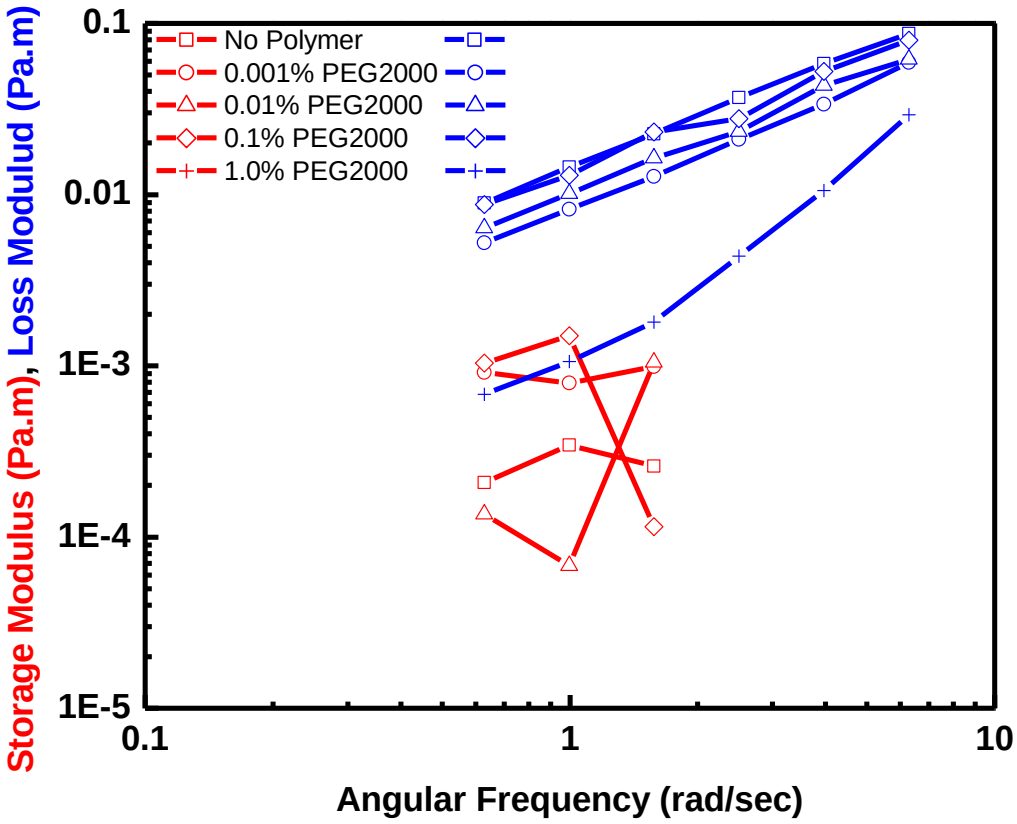

Figure 4. 12. Interfacial Modulus (Pa) versus Angular Frequency (rad/sec) for 0% PEG2000(□), 0.001% PEG2000 (○),0.01% PEG2000(△), 0.1% PEG2000(◇) and 1.0% PEG2000(＋) at 2.0% Laponite suspensions. Red- Storage Modulus (Pa) and Blue- Loss Modulus (Pa).

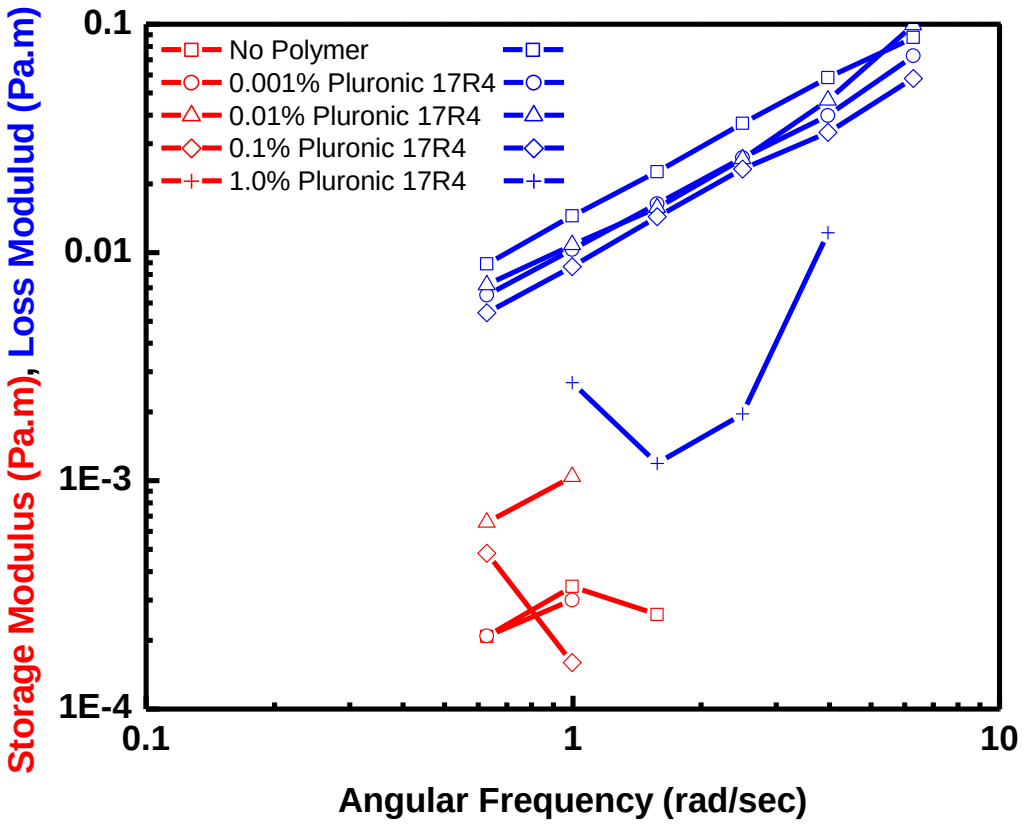

Figure 4. 13. Interfacial Modulus (Pa) versus Angular Frequency (rad/sec) for 0% Pluronic 17R4 (□), 0.001% Pluronic 17R4 (○), 0.01% Pluronic 17R4 (△), 0.1% Pluronic 17R4 (◇) and 1.0% Pluronic 17R4 (+) at 2.0% Laponite suspensions. Red- Storage Modulus (Pa) and Blue- Loss Modulus (Pa).

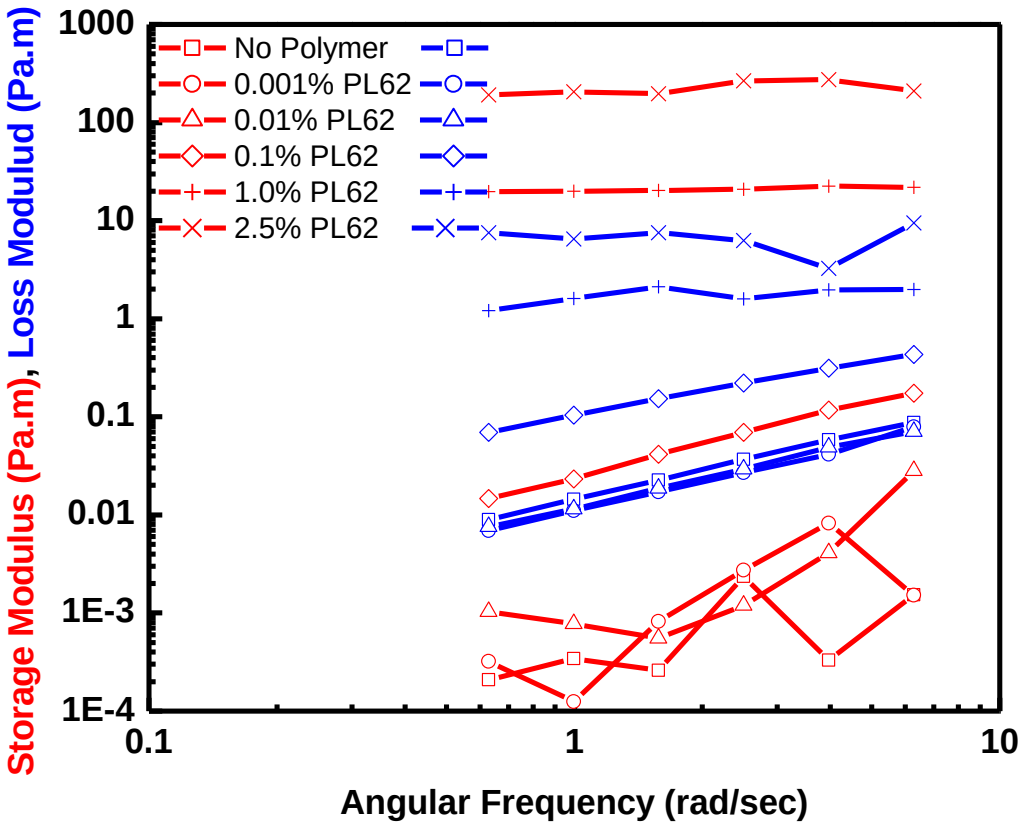

Figure 4. 14. Interfacial Modulus (Pa) versus Angular Frequency (rad/sec) for 0% Pluronic L62 (□), 0.001% Pluronic L62 (○), 0.01% Pluronic L62 (△), 0.1% Pluronic L62 (◇) and 1.0% Pluronic L62 (+) at 2.0% Laponite suspensions. Red- Storage Modulus (Pa) and Blue- Loss Modulus (Pa).

Interfacial Shear of Laponite with Polymers

Foam drainage may be characterized by interfacial shear viscosity. Figure 4.15 and 4.16 demonstrate how the addition of the PEG2000 and Pluronic 17R4 to Laponite incrementally reduces the interfacial shear viscosity. In this instance,as polymer increases, the Laponite is depleted from the surface. The most notable difference is at 1.0% polymer addition where shear rate increases dramatically at equivalent shear stresses.

Figure 4.17 shows a much different interfacial shear stress profile for 0.1% and 1.0% Pluronic L62, shear rates are reduced for equivalent shear stresses. This is an indication that the Pluronic L62 and Laponite have enhanced the interfacial structure from shearing. More stress is needed to reach higher shear rate values. At concentrations above 2.5% Pluronic L62, the shear rate values timed out and were well below 1.0×10^{-4} sec^{-1}. This may be related to the reduction in foam drainage by slowing down the viscosity for the liquid to pass through the filament capillary.

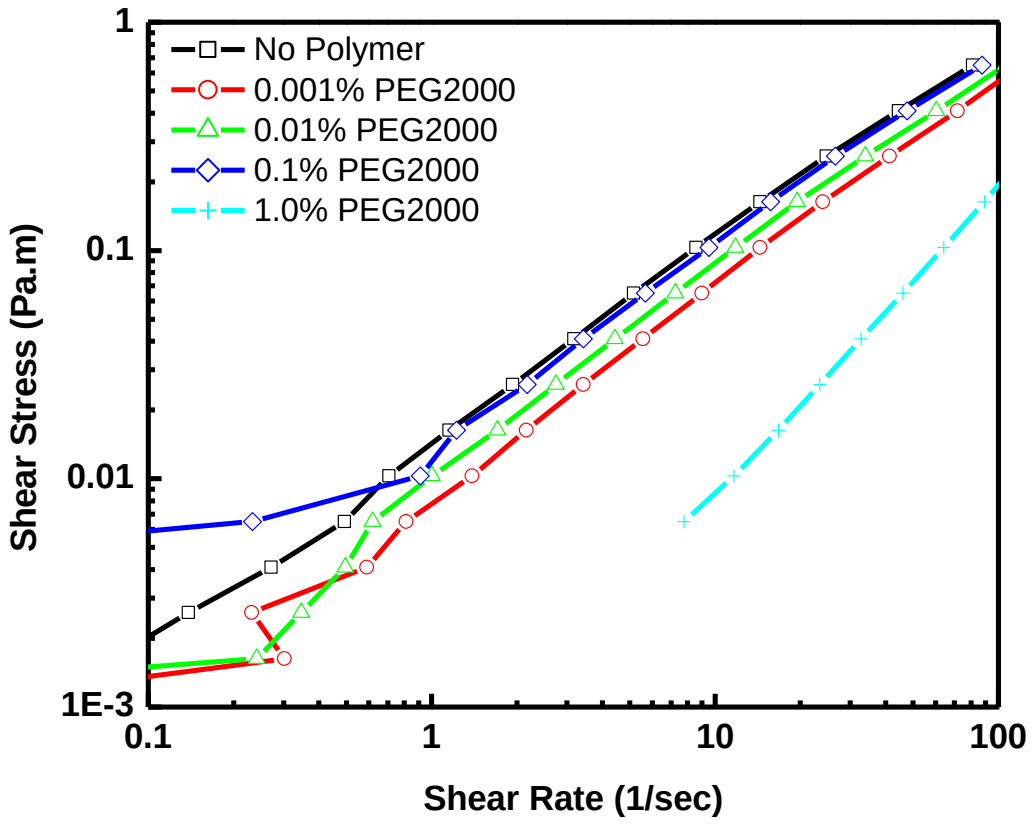

Figure 4. 15. Interfacial Shear Stress (Pa.m) vs Shear Rate (1/sec) for 0% PEG2000 (□), 0.001% PEG2000 (○), 0.01% PEG2000 (△), 0.1% PEG2000 (◇) and 1.0% PEG2000 (+) at 2.0% Laponite suspensions.

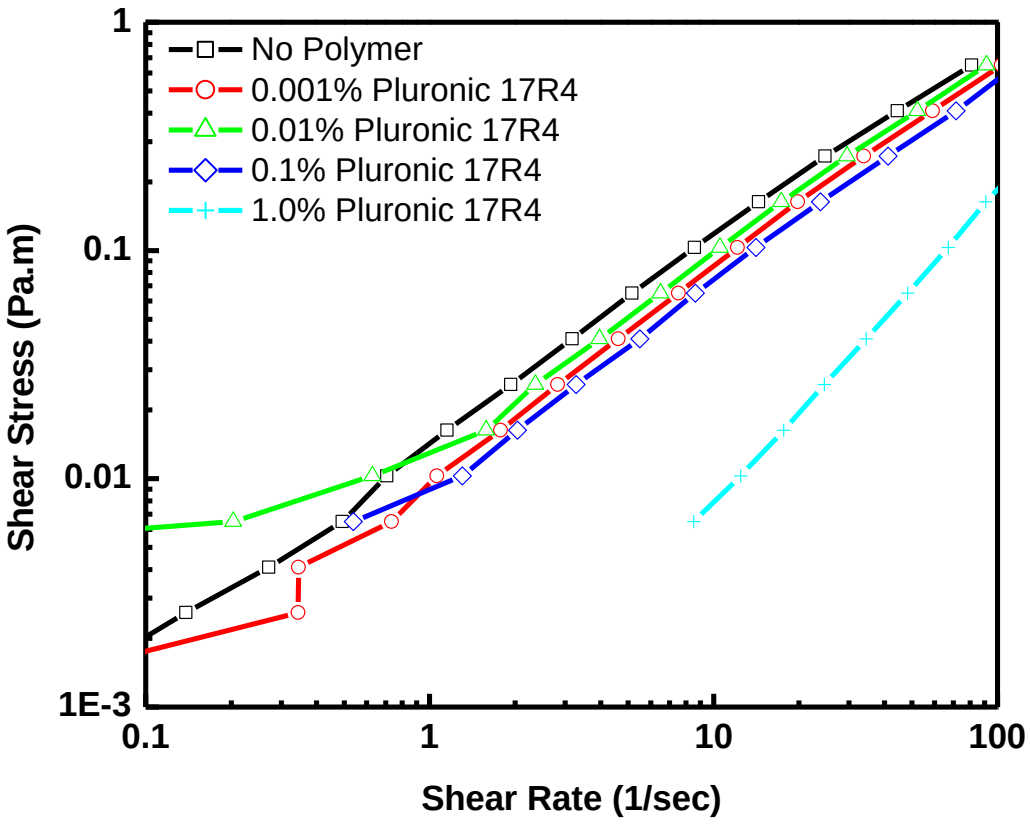

Figure 4. 16. Interfacial Shear Stress (Pa.m) vs Shear Rate (1/sec) for 0% Pluronic 17R4 (□), 0.001% Pluronic 17R4 (○), 0.01% Pluronic 17R4 (△), 0.1% Pluronic 17R4 (◇) and 1.0% Pluronic 17R4 (+) at 2.0% Laponite suspensions.

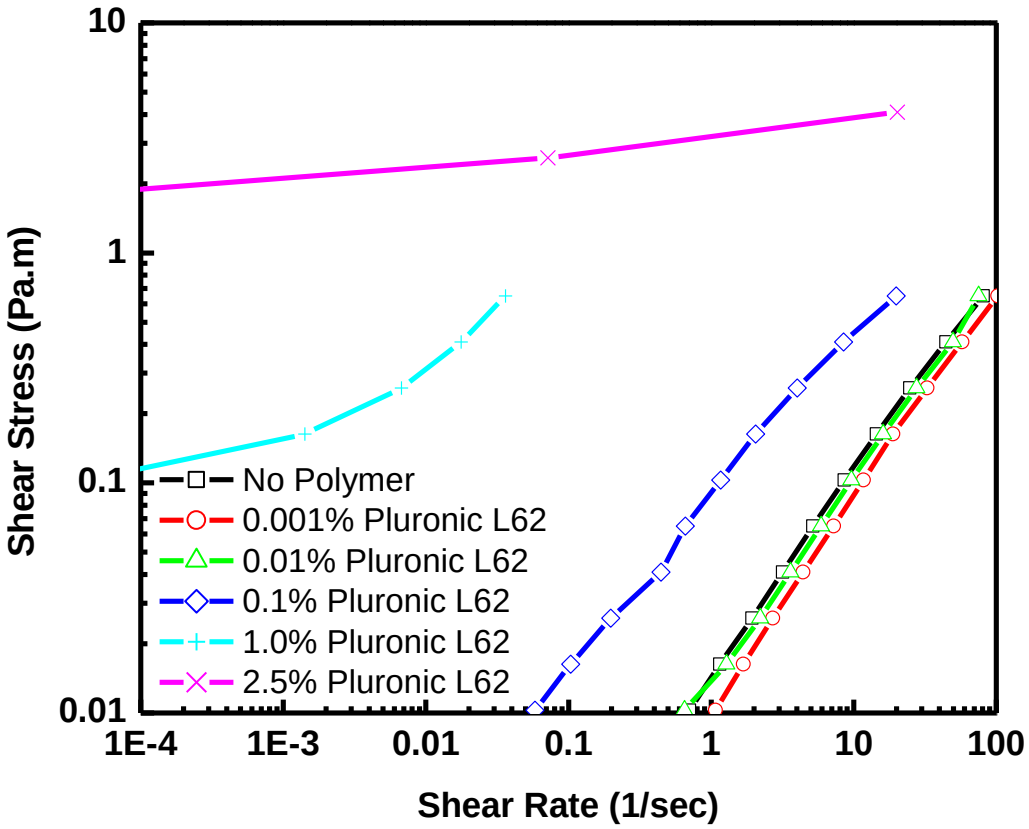

Figure 4. 17. Interfacial Shear Stress (Pa.m) vs Shear Rate (1/sec) for 0% Pluronic L62 (□), 0.001% Pluronic L62 (○), 0.01% Pluronic L62 (△), 0.1% Pluronic L62 (◇) and 1.0% Pluronic L62 (+) at 2.0% Laponite suspensions.

4.4 Conclusions

The Laponite/polymer composite film and air-liquid interfaces were studied using novel characterization techniques in this work. This work provided a more complete picture for the mechanism of Laponite/Pluronic L62 composites through film and air-liquid techniques. Laponite interacts with each polymer in different ways, mainly through H-bonding for the PEG2000. Laponite interacts in a dynamic way with both Pluronic

17R4 and Pluronic L62. Pluronic 17R4 the defoamer has an empirical structure of propylene oxide-ethylenoxide-propylene oxide, whereas Pluronic L62 has an empirical structure of ethylene oxide-propylene oxide- ethylene oxide. The hydrophilic block of the polymers will interact with the hydrophilic Laponite.

Surface energies for the Laponite films showed to contribute to the majority of the forces up to 0.01% polymer content. The major contributor to the total surface energy was the polar surface energy component. As the Laponite/polymer film approached 0.25% polymer, the surface energy reached a minimum. The surface energy minimum was accounted for by the hydrophobicity of the polymer. Lower surface energies were found for Laponite films with the foamer, Pluronic L62, relative to the Laponite films with the defoamer, Pluronic 17R4, due to molecular architecture. At 1.0% polymer content, the films reached a surface energy maximum, attributed to the hydrophilic component of the polymers. A reduction in the dispersive surface energy and increase in the polar surface energy component is accounted for this rise in total surface energy for the Laponite polymer composites.

X-ray diffraction confirmed intercalation of all polymers into the silicate matrix at 0.25% polymer for the (001) basal spacing. A relationship showed that d-spacing increases as the concentration increases. At 0.25% Pluronic L62, molecular architecture had a larger d-spacing of Laponite than 0.25% Pluronic 17R4, defoamer. Additionally, an increase in the polymer content reduced the full width half height, a reflection of increased order of the silicate matrix.

The surface tension experiments demonstrated that Laponite depletes the surface active Pluronic L62 from the surface up to 0.65% Pluronic L62. Most Laponite

and polymer films at the air-liquid interface are viscous dominant with very little storage modulus present. Both interfacial frequency and flow demonstrated that Laponite is depleted from the interface by a reduction in modulus and stress. Both PEG2000 and Pluronic 17R4 with Laponite lose all storage modulus by 1.0% polymer. Laponite at 0.1% Pluronic L62 has an enhanced viscoelastic response with an increase in interfacial storage modulus, loss modulus and shear stresses. Laponite with polymer concentrations above 1.0% Pluronic L62, change to an elastic dominant interface with an even higher increase in interfacial storage modulus, loss modulus and shear stresses. Laponite enhances Pluronic L62 interfacial properties above 1.0% Pluronic L62.

4.5 References

(1) Bayer, I.S.; Steele, A.; Martorana, P.J.; Loth, E., Fabrication of Superhydrophobic Polyurethane/Organoclay Nano-Structured Composites from Cyclomethicone-in-water Emulsions, *Applied Surface Science*, **2010**, *257*, 823-826.

(2) Ruiz-Hitzky, E.; Aranda, P.; Darder, M.; Rytwo, G., Hybrid Materials Based on Clays for Environmental and Biomedical Applications, *Journal of Materials Chemistry*, **2010**, *20*, 9306-9321.

(3) Heinz, H.; Clay Minerals for Nanocomposites and Biotechnology: Surface Modification, Dynamics and Responses to Stimuli, *Clay Minerals*, **2012**, *47 (2)*, 205-230.

(4) Ranade, A.; D'Souza, N.A.; Gnade, B., Poly(amine-imide) Nanocomposites for high-Temperature Wire Coatings, *Polyimides and Other high Temperature Polymers*, **2005**, *3*, 283-298.

(5) Svagan, A.J.; Åkesson, A.; Cárdenas, M.; Bulut, S.; Knudsen, J.C.; Risbo, J.; Plackett, D., Transparent Films Based on PLA and Montmorillonite with Tunable Oxygen Barrier Properties, *Biomacromolecules*, **2012**, *13*, 397-405.

(6) Ranade, A.; Nayak, K.; Fairbrother, D., D'Souza, N.A., Maleated and Non-Maleated Polyethylene-Montmorillonite Layered Silicate Blown Films: Creep, Dispersion and Crystallinity, *Polymer*, **2005**, *46*, 7323-7333.

(7) DeLeon, V.H.; Nguyen, T.D.; Nar, Mangesh; D'Souza, N.A.; Golden, T.D., Polymer Nanocomposites for Improved Drug Delivery Efficiency, *Materials Chemistry and Physics*, **2012**, *132*, 409-415.

(8) Huang, Y.P.; Lee, M.J.; Yang, M.K.; Chen, C.W., Montmorillonite Particle Alignment and crystallization and ion-conducting Behavior of Montmorillonite/Poly (Ethylene Oxide) Nanocomposites, *Applied Clay Science*, **2010**, *49*, 163-169.

(9) Priolo, M. A.; Gamboa, D.; Grunlan, J. C., Transparent Clay-Polymer Nano Brick Wall Assemblies with Tailorable Oxygen Barrier, *Applied Material Interfaces*, **2010**, *2 (1)*, 312−320.

(10) Zhang, S.; Lan, Q.; Liu, Q.; Xu, J.; Sun, D.; Aqueous Foams Stabilized by Laponite and CTAB, *Colloids and Surfaces A: Physicochemical Engineering Aspects*, **2008**, *317*, 406-413.

(11) Norris, J.; Giese, R.F.; Costanzo, P.M.; Van Oss, C.J., The Surface Energies of Cation Substituted Laponite, *Clay Minerals*, **1993**, *28*, 1-11.

(12) Kamal, M.R.; Calderon, J.U.; Lennox, R.B., Surface Energy of Modified Nanoclays and Its Effect on Polymer/Clay Nanocomposites, *Journal of Adhesion Science and Technology*, **2009**, *23*, 663-688.

(13) Dundigalla, A.; Lin-Gibson, S.; Ferreiro, V.; Malwitz, M.M.; Schmidt, G., Unusual Multilayered Structures in Poly(ethylene oxide)/Laponite Nanocomposite Films, *Macromolecules Rapid Communication*, **2005**, *26* ,143-149.

(14) Stefanescu, E.A; Stefanescu, C.; Donose, B.C.; Garno, J.C; Daly, W.H.; Schmidt, G.; Negulescu, I.I., Polymer/Clay Nanocomposites: Influence of Ionic Strength on the Structure and Adhesion Characteristics in Multilayered Films, *Macromolecular Materials and Engineering*, **2008**, *293*, 771-780.

(15) Gerstmans, A.; Urbanczyk, L.; Jérome, R.; Robert, J.-L., Grandjean, J., XRD and NMR Characterization of Synthetic Hectorites and the Corresponding Surfactant-Exchanged Clays, *Clay Minerals*, **2008**, *43 (2)*, 205-212.

(16) Loyens, W.; Jannasch, P.; Maurer, F.H.J., Poly(ethylene oxide)/Lapnite Nanocomposites via Melt-Compounding: Effect of Clay Modification and Matrix Molar Mass, *Polymer*, **2005**, *46*, 915-928.

(17) Doeff, M.M; Reed, J.S., Li Ion Conductors Based on Laponite/Poly(ethylene oxide) Composites, *Solid State Ionics*, **1998**, *113-115*, 109-115.

(18) Carn, F.; Colin, A.; Pitois, O.; Vignes-Adler, M.; Backov, R., Foam Drainage in the Presence of nanoparticle-Surfactant Mixtures, *Langmuir*, **2009**, *25 (14)*, 7847-7856.

(19) Monteux, C.; Fuller, G.G.; Bergeron, V.; Shear and Dilational Surface Rheology of Oppositely Charged Polyelectrolyte/Surfactant Microgels Adsorbed at the Air-Water Interface. Influence on Foam Stability, *Journal of Physical Chemistry B*, **2004**, *108 (42)*, 16473-16482.

(20) Noskov, B.A., Dilational Surface Rheology of Polymer and Polymer/Surfactant Solutions, *Current Opinion in Colloid & Interface Science*, **2010**, *15*, 229-236.

(21) Perez, O.E.; Sánchez, C.C.; Pilosof, A.M.R.; Patino, J.M.R., Dynamics of Adsorption of Hydroxypropyl Methylcellulose at the Air-Water Interface, *Food Hydrocolloids*, **2008**, *22*, 387-402.

(22) Vandebrill, S.; Franck, A.; Fuller, G.G.; Moldenaers, P.; Vermant, J., A Double Wall-Ring Geometry for Interfacial Shear Rheometry, *Rheologica Acta*, **2010**, *49*, 131-144.

(23) Owen, Wendt, Kaelble Method from OCA Software, Future Digital Scientific, v22, 2012.

(24) Fuller, G.G.; Aloyse, F.; Vermant, J., System and Method for Interfacial Rheometry, **2009**, US Patent 20090056423.

(25) Norris, J.; Giese, R.F.; Costanzo, P.M.; Van Oss, C.J., The Surface Energies of Cation Substituted Laponite, *Clay Minerals*, **1993**, *28*, 1-11.

(26) Van Oss, C.J.; Giese, R.F.; Costanzo, P.M., DLVO and Non-DLVO Interactions in Hectorite, Clay Minerals, **1990**, 38 (2), 151-159.

(27) Blanton, T.N.; Majumdar, D.; Melpolder, S.M., Microstructure of Clay-Polymer Composites, *Advances in X-Ray Analysis*, **2000**, *42*, 562-568.

(28) Daniel, L.M.; Frost, R.L.; Zhu, H.Y., Edge Modification with Dimethyl-octylmethoxysilane, *Journal of Colloid and Interface Science*, **2008**, *321 (2)*, 302-309.

(29) Lazzara, G.; Millioto, S.; Gradzielski, M.; Prevost, S., Small Angle Neutron Scattering, X-ray Diffraction, Differential Scanning Calorimetry and Thermogravimetry Studies to Characterize the Properties of Clay Nanocomposites, *Journal of Physical Chemistry C*, **2009**, *113*, 12213-12219.

CHAPTER 5

LAMELLA AND EXTENSIONAL FILAMENT PROPERTIES OF LAPONITE POLYMER FOAMS

5.1 Introduction

There are many great reviews on foams[1] and particle stabilized foams. [2, 3,4] Foam production and drainage properties rely heavily on the particle-polymer interaction that impact many foam applications, i.e. food colloids[5,6], oil recovery[7], consumer products[8] and fire fighting technology[9]. Research has focused on understanding the synergy of the particle polymer interactions in solution which includes depletion[10], adsorption[11], aggregation[12], XRay Diffraction, Small Angle Nuetron Scattering, rheology[13] and Nuclear Magnetic Resonance spectroscopy[14]. Although there is important synergy of particle stabilized foams, there are some unresolved areas in foam stability due to specific mechanisms for each component.[15] The design of experimentation is not fully resolved in looking at the contributions of polymer to the particle. Particle size, geometry and contact angle of quartz and hydrophobic graphite have been have shown to improve foam stability in the presence of Pluronic F108 for food, pharmaceutical and mining applications[16] but not components of the polymeric system, i.e. hydrophobicity, architecture and hydrophilicity.

Foams have unique bulk and interfacial viscoelastic properties that provide some mechanism for foam stability.[17,18,19] Two other important mechanisms for foam stability include lamella films and extensional filament formed. There is a need to understand the lamella film break up and extensional filament in regards to particle stabilized foam mechanisms. The challenge with lamella films are in the elaborate experimental designs using optical measurements, like interferometry.[20,21] A very simple method used in this

work comes from the classic du Nouy ring method of just pulling the liquid at a very slow rate until it breaks apart. The value of lamella properties to an extent can directly relate interfacial elasticity for film drainage. This work utilizes a simple lamella break point apparatus that can provide this information. In addition this work will provide a more complete understanding of the polymeric components of the Laponite –polymer films as it related to foam stability.

Foams have characteristic filaments (plateau bridges), where the fluid drains through.[22] Extensional flow experiments have been recently simplified using the CaBER1® for simple polymeric solutions.[23] The extensional flow of polymeric solutions has been investigated using the CaBER1® for food colloids.[24] Extensional flow is an important parameter in the ink industry for dispersions to prevent misting.[25] In the oil industry extensional flow is vital for enhanced oil recovery.[26] Filament stability has not been resolved as it relates to foam properties. A simple extensional technique is used to characterize how the filaments are formed, and further characterize the mechanism by which the particle-polymer systems can enhance foam stability.

In this work, lamella films and extensional filaments will be used as new tools to understand the mechanism between lamella film strength and extensional filament strength for foam production and stability on Laponite with Pluronic L62, a foamer, Pluronic 17R4, a defoamer, and PEG2000, a hydrophilic polymer. A series of foam production and stability experiments will be used to correlate the lamella film and extensional filament properties of the Laponite-polymer systems.

5.2 Experimental

The lamella film break point of Laponite with PEG200, Pluronic 17R4 and Pluronic L62 were characterized using a tensiometry attached with a platinum du Nouy ring for the film drainage tests from Future Digital Scientific. For each measurement, the platinum ring was thoroughly rinsed with deionized water and flame treated to a dull red heat. The ring was set aside to equilibrate to ambient temperatures then attached to the tensiometer. A 50 mL Teflon cup is thoroughly cleaned and air dried before placing 25 mL of Laponite polymer suspension into the Teflon cup. The du Nuoy ring is lowered 5 mm below the surface of the liquid, the rate is not a critical factor at this point only immersion is important. The rate of the motor pulling from the liquid was 10 mm/sec. The weight of the tension of the film formed was recorded as a function of time.

The filament stability of the Laponite polymer suspensions were characterized using a Capillary Breakup Extensional Rheometer (CaBER1®) from ThermoScientific. The plate diameter was 6mm using a linear stretch profile of 25 seconds starting at 3 mm for the base plate and ending at 12 mm after the stretch was completed. A laser follows the filament change as a function of time once the initial stretch is made. A video follows the curvature of the filament as it is being stretched. The video is linked and is synchronized to the actual experiment.

Foam stability measurements were optimized and characterized using an IKA T25 Ultra Turrax dispenser. Foam production using a high shear mixer is dependent on many factors, such as volume (including dimensions), mixing speed (rpm), depth of mixer in beaker, time and temperature. In all foam production experiments, volume was

set at 50mL in a 250mL borosilicate glass beaker, depth was submerged at the same height at 10cm and temperature was maintained at 22°C. Mixing speed and time were varied to obtain optimal processing conditions. It was found many had very similar foam production rates, as well as, overprocessing conditions. The high shear mixer was meticulously cleaned and air dried between each run with three mix rinse cycles for 1 minute at 10,000 rpm using a 500mL beaker with 400mL deionized water and air dried. Foam drainage experiments were performed for a series of Laponite Pluronic systems and followed in 100mL and 250mL graduated cylinders made from polymethylpentene (PMP). PMP is a low surface energy material with contact angles using deionized water greater than 90°. This is important because many experimental setups use glass equipment. The liquid portion of the foam has an affinity with the glass leading to an unnecessary interaction with the column wall. PMP will not have this effect. Both foam height and drainage levels were followed up to steady state.

5.3 Results

5.3.1 Lamella Break Point

The lamella is a thin film that is created from the immersion of the DuNouy ring in the liquid. It is slowly pulled back at a constant rate. There are two main points to consider, maximum weight on ring and dstance of lamella film formed from stretch. First, there is a maximum weight from the liquid on the ring that gives the surface tension of the liquid. Second, there is the film that is formed after the maximum weight pulled until it breaks (becomes unstable) that is characteristic to the components in the

liquid. Knowing these two criteria can give valuable information on how stable films are formed for foaming applications.

Figure 5.1 shows the lamella break point for a series of 2.0% Laponite Dispersions with PEG2000 dose response. At 2.0% Laponite only, there is a maximum reached at 0.9 grams, then drops to 0.8 grams and tapers off up to the breakpoint of 7.6 mm. Even though Laponite is not surface active, this experiment demonstrates surface elasticity of the film. As PEG2000 is added the maxima is lowered to 0.75 grams and is maintained at higher PEG2000 content. In all cases with added PEG2000 the lamella film breaks very quickly, near 4 mm. The shorter distance of the lamella breaking indicates that the PEG2000 removes Laponite from the surface and compromises the film elasticity. The hydrophilic PEG2000 destabilizes the Laponite lamella.

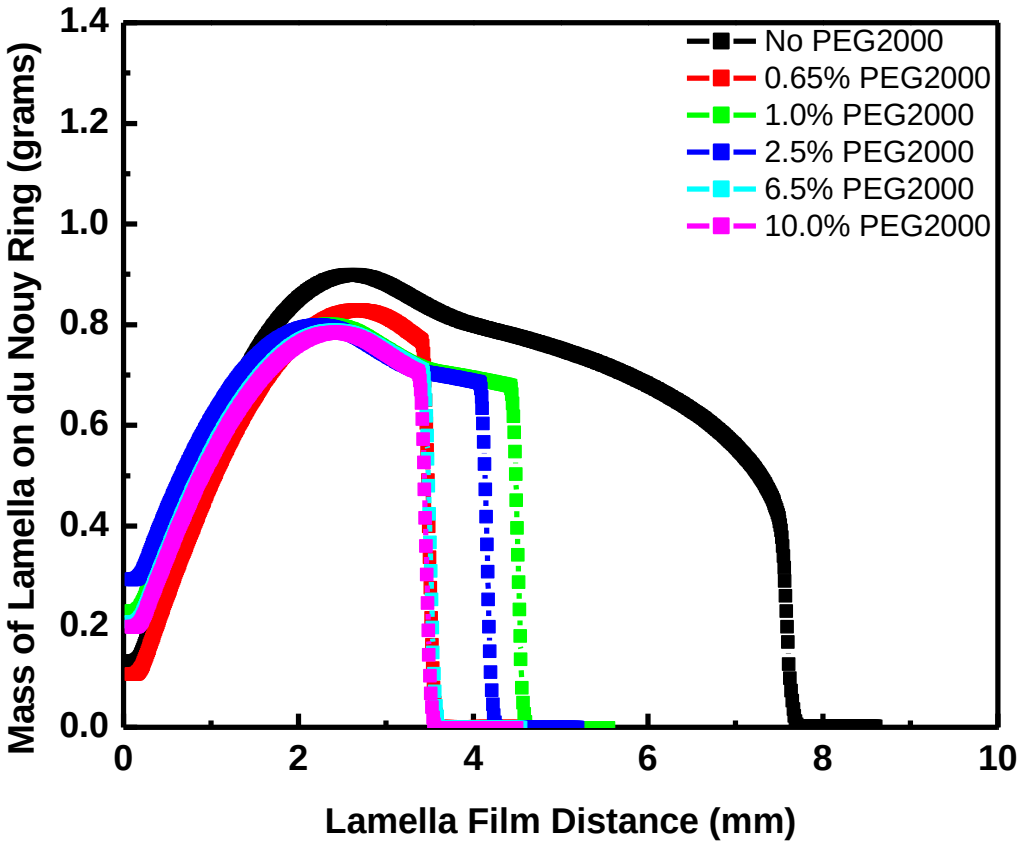

Figure 5. 1. Lamella Break Point for 2% Laponite dispersions with no PEG2000 (black), 0.65% PEG2000 (red), 1.0% PEG2000 (green), 2.5% PEG2000 (blue), 6.5% PEG2000 (aqua) and 10.0% PEG2000 (magenta).

Figure 5.2 shows the lamella break point for a series of 2.0% Laponite Dispersions with Pluronic 17R4 (a defoamer) dose response. Pluronic 17R4 shows a similar trend as with the PEG2000 series in reducing the lamella break point. The addition of Pluronic 17R4 quickly drops the maxima to 0.6 grams and approaches 0.45 grams. The lamella break points are generally less than 4 mm. The hydrophobicity of

Pluronic 17R4 contributes more to destabilizing the Laponite lamella compared to PEG2000.

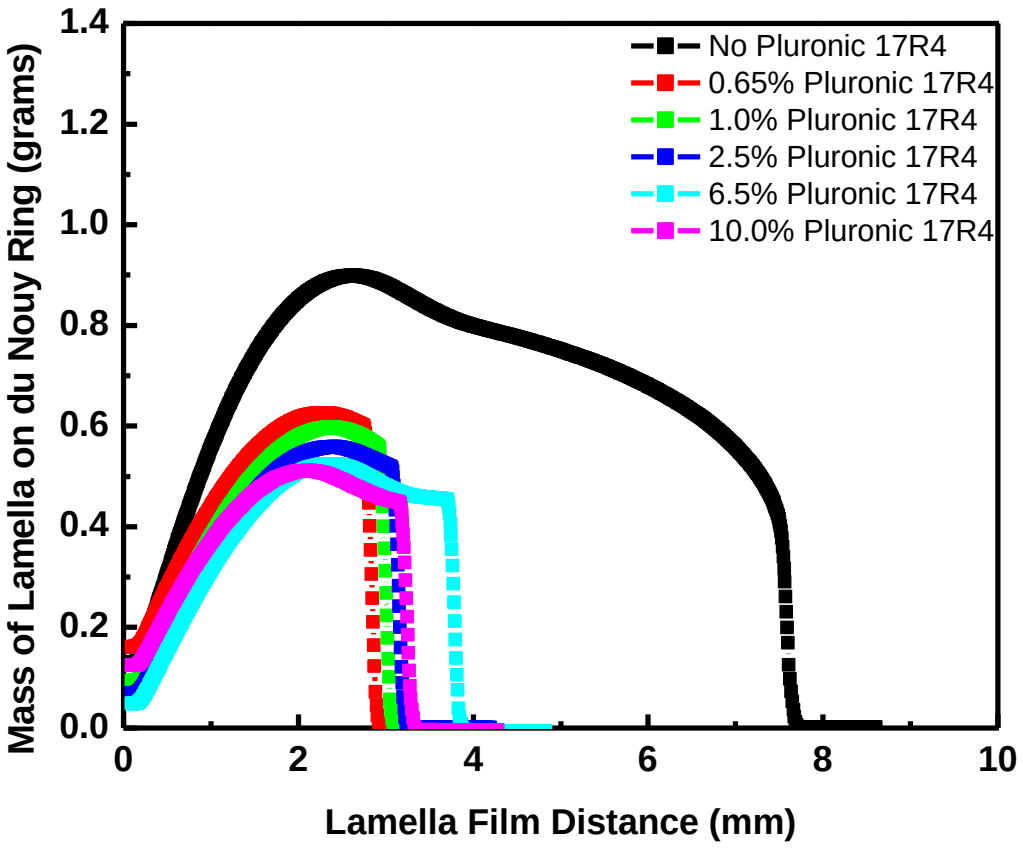

Figure 5. 2. Lamella Break Point for 2% Laponite dispersions with no Pluronic 17R4 (black), 0.65% Pluronic 17R4 (red), 1.0% Pluronic 17R4 (green), 2.5% Pluronic 17R4 (blue), 6.5% Pluronic 17R4 (aqua) and 10.0% Pluronic 17R4 (magenta).

Figure 5.3 shows the lamella break point for a series of 2.0% Laponite Dispersions with Pluronic L62 (a foamer) dose response. Addition of 0.65% Pluronic

L62 reduces the maximum weight to 0.7 grams but the lamella film extends beyond 8 mm. Addition of 1.0% Pluronic L62 shows a similar reduction in weight and a long lamella extension up to 8 mm. At 2.5% Pluronic L62 the maximum weight increases up to 1.1 grams and the lamella breaks off near 3.5 mm. An additional note is that at this concentration, the maximum weight begins to shift to lower lamella film distances. The maximum weight for 6.5% and 10.0% Pluronic L62 incrementally lower in value to 0.82 grams and 0.55 grams, respectively. The lamella break point for 6.5% and 10.0% Pluronic L62 both quickly approach 1.7 mm. As the Pluronic L62 concentration increases up to 1.0% the maximum weight decreases and lamella film is stable up to 8 mm. This indicates that Pluronic L62 adds more structure to the Laponite lamella structure. A shift in lamella film break point occurs at concentrations higher than 2.5% Pluronic. This indicates that the rate of the pull is too fast for the film to stabilize due to the both the increase in bulk and interfacial previously characterized in chapters 3 and 4. This experiment demonstrated the value and limits of how the functionality and architecture of the PEG2000, Pluronic 17R4 and Pluronic L62 play a role in lamella film structure as it may provide a link to foam stability.

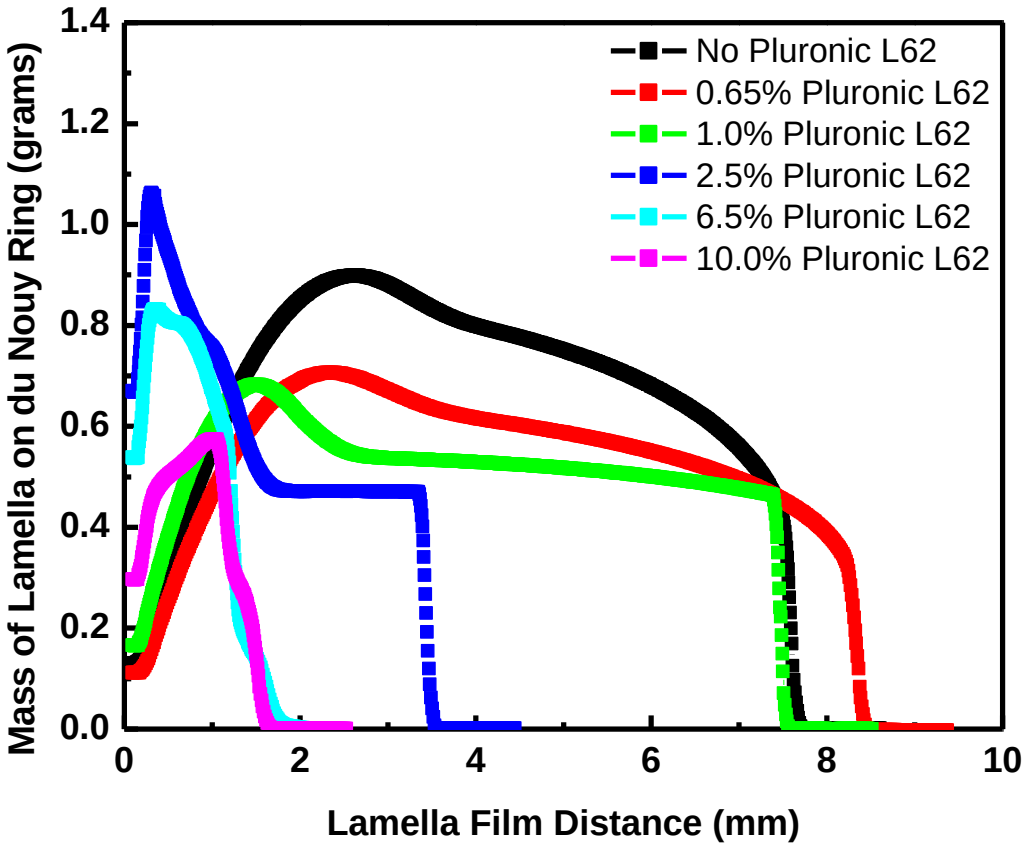

Figure 5. 3. Lamella Break Point for 2% Laponite dispersions with no Pluronic L62 (black), 0.65% Pluronic L62 (red), 1.0% Pluronic L62 (green), 2.5% Pluronic L62 (blue), 6.5% Pluronic L62 (aqua) and 10.0% Pluronic L62 (magenta).

5.3.2 Extensional Filament Strength

There are two competing forces in this extensional experiment. First there is the viscoelastic property as the fluid filament is stretched. Second, there is the surface tension that forces the fluid to pinch or break apart as the filament is stretched. A characteristic hump is seen for all dispersions, characteristic of rounding due to the surface tension of the fluid. Figure 5.4 shows the reduction of filament diameter as the fluids are stretched resulting in a breakup time for 2.0% Laponite dispersions with a PEG2000 dose response. Addition of PEG2000 increases the breakup time from 0.006 seconds with no PEG to 0.008 seconds with the addition of PEG2000. The initial filament diameter is lower upon addition of PEG2000.

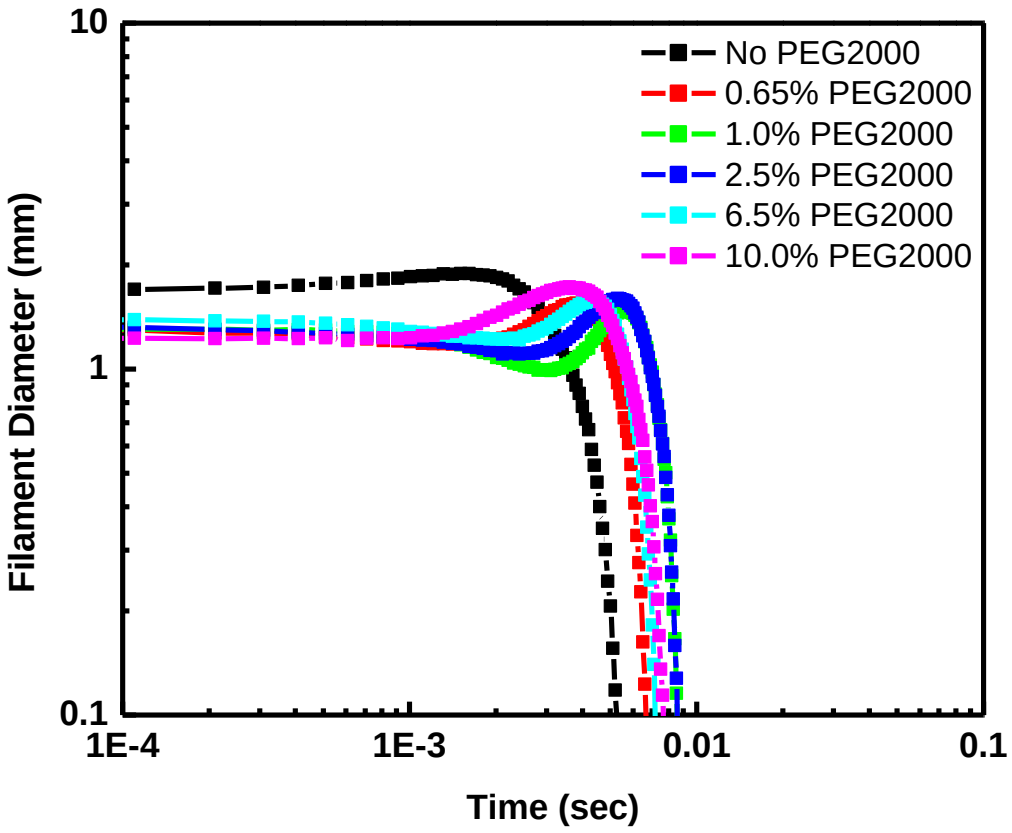

Figure 5. 4. Filament Breakup Time for 2% Laponite dispersions with no PEG2000 (black), 0.65% PEG2000 (red), 1.0% PEG2000 (green), 2.5% PEG2000 (blue), 6.5% PEG2000 (aqua) and 10.0% PEG2000 (magenta).

Figure 5.5 shows the apparent extensional viscosities for the 2.0% Laponite dispersions with PEG2000 dose response. The viscosity and strain both increase for all fluids. Addition up to 6.5% PEG2000 reduces the apparent extensional viscosity compared to Laponite alone. There is an increase in apparent extensional viscosity for 10.0% PEG2000 with Laponite. This shows that PEG2000 depletes Laponite's

extensional viscosity. Addition of 10.0% PEG2000 is a polymer dose effect. No synergy is observed between the hydrophilic PEG2000 and Laponite.

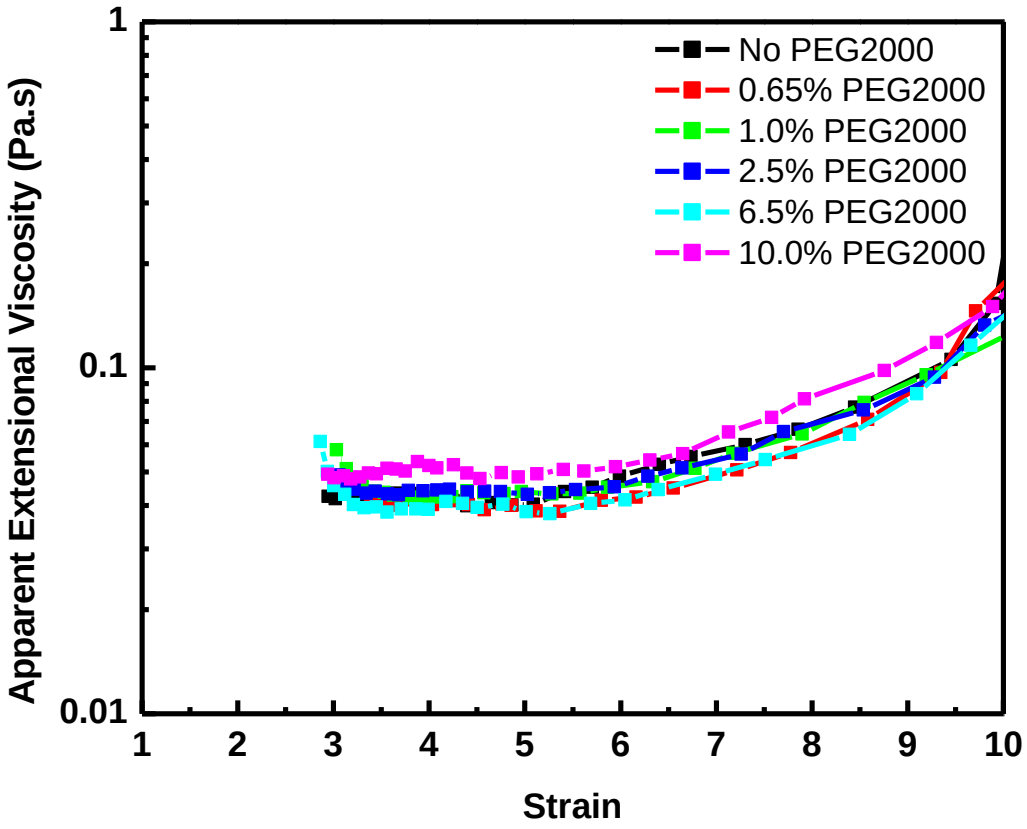

Figure 5. 5. Apparent Extensional Viscosities for 2% Laponite dispersions with no PEG2000 (black), 0.65% PEG2000 (red), 1.0% PEG2000 (green), 2.5% PEG2000 (blue), 6.5% PEG2000 (aqua) and 10.0% PEG2000 (magenta).

The CaBER experiment is linked to a video program that demonstrates what the image of the fluid looks like as the filament is stretched. Figure 5.6 shows the 2.0% Laponite with 1.0% PEG2000 frame and filament graph. The frame on the left is linked to a filament experiment on the right in Figure 5.6. The red line is used to correlate the

frame and filament diameter together in the experiment. Below the frame is a time and frame stamp along with the diameter of the fluid. The curvature of the fluid is very round and pronounced for the PEG2000 sample. Near the top portion of the liquid, there are some droplets that are formed. These droplets show up as small humps in the filament diameter graphs. This particular Laponite and PEG2000 dispersion has a very rapid breakup time along with a low apparent extensional viscosity profile.

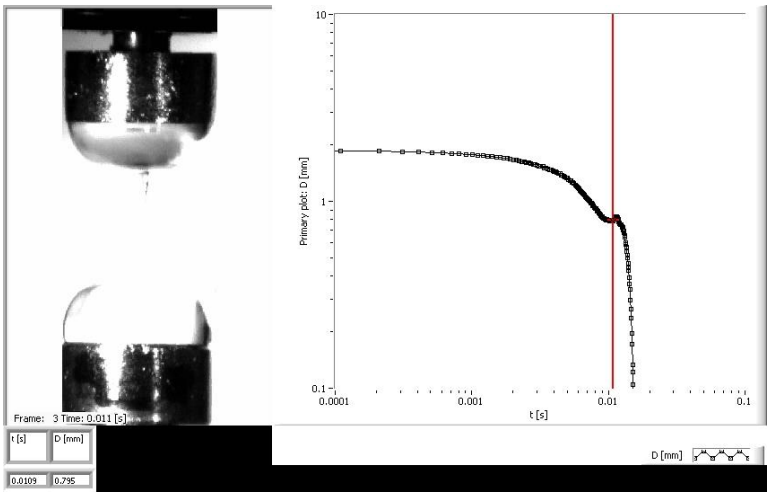

Figure 5. 6. Picture for 2% Laponite dispersions with 1.0% PEG2000 frame 3 at 0.011 seconds. The Filament Diameter as a function of time is displayed, as well. The red vertical line corresponds to the image.

Figure 5.7 shows the reduction of filament diameter as the fluids are stretched resulting in a breakup time for 2.0% Laponite dispersions with a Pluronic 17R4 (defoamer) dose response. Addition of Pluronic 17R4 (defoamer) show some similarities to the PEG2000 polymer response with a reduction in initial filament diameter and a small hump as the fluids approach the breakup times. However the

stretch times are substantially longer compared to PEG2000, extending beyond 0.01 seconds. This indicates that the functionality with a propyleneoxide block length enhances the interaction with Laponite by increasing the filament breakup times.

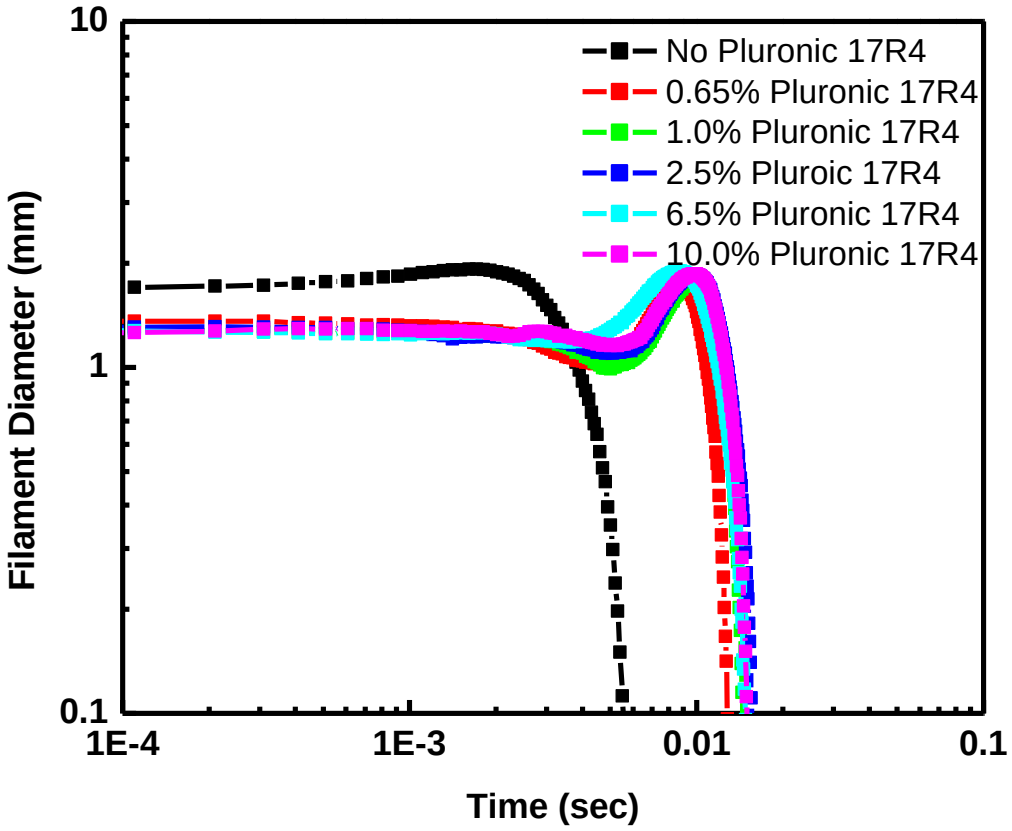

Figure 5. 7. Filament Breakup Time for 2% Laponite dispersions with no Pluronic 17R4 (black), 0.65% Pluronic 17R4 (red), 1.0% Pluronic 17R4 (green), 2.5% Pluronic 17R4 (blue), 6.5% Pluronic 17R4 (aqua) and 10.0% Pluronic 17R4 (magenta).

Figure 5.8 shows apparent extensional viscosities for the 2.0% Laponite dispersions with Pluronic 17R4 dose response. The viscosity and strain both increase for all fluids. Addition up to 6.5% Pluronic 17R4 increases the apparent extensional viscosity compared to Laponite alone. There is a reduction in apparent extensional viscosity for 10.0% Pluronic 17R4 with Laponite but this is still much higher than Laponite alone. This shows that the propyleneoxide block on Pluronic 17R4 enhances Laponite's extensional viscosity.

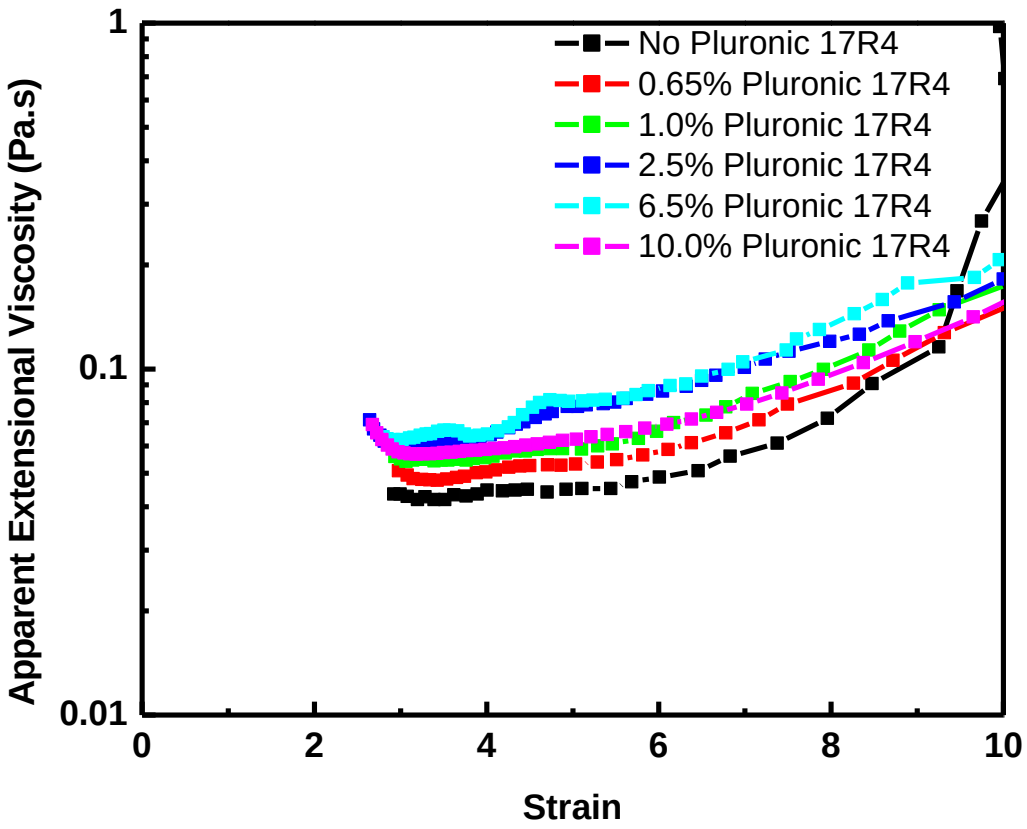

Figure 5. 8. Apparent Extensional Viscosities for 2% Laponite dispersions with no Pluronic 17R4 (black), 0.65% Pluronic 17R4 (red), 1.0% Pluronic 17R4 (green), 2.5% Pluronic 17R4 (blue), 6.5% Pluronic 17R4 (aqua) and 10.0% Pluronic 17R4 (magenta).

Figure 5.9 shows the 2.0% Laponite with 1.0% Pluronic 17R4 frame and filament graph. The frame on the left is linked to a filament experiment on the right in Figure 5.9. The red line is used to correlate the frame and filament diameter together in the experiment. Below the frame is a time and frame stamp along with the diameter of the fluid. This frame is very similar to the PEG2000 frame with a rounded liquid at the top

and bottom plates and no filament. In this particular experiment the drop has just passed through the laser as indicated from the red line in the filament diameter graph.

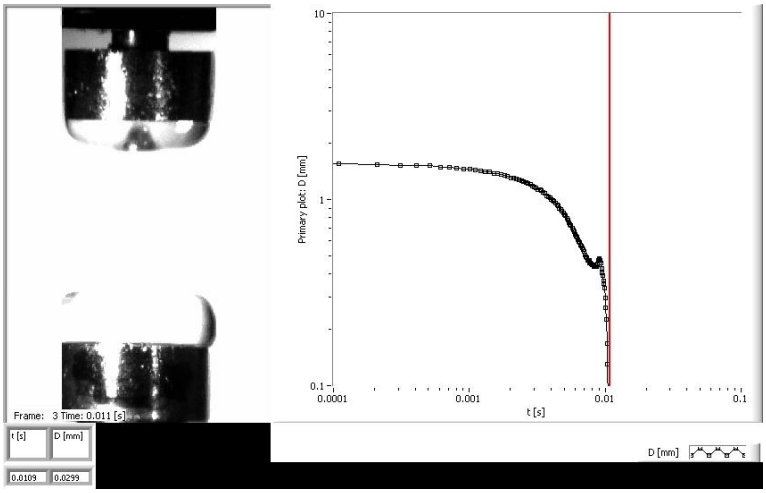

Figure 5. 9. Picture for 2% Laponite dispersions with 1.0% Pluronic 17R4 frame 3 at 0.011 seconds. The Filament Diameter as a function of time is displayed, as well. The red vertical line corresponds to the image.

Figure 5.10 shows the reduction of filament diameter as the fluids are stretched resulting in a breakup time for 2.0% Laponite dispersions with a Pluronic L62 (foamer) dose response. There are a few differences for the Pluronic L62 dose response compared to both PEG2000 and Pluronic 17R4. One item is that the initial filament diameter is larger than Laponite alone. Addition of Pluronic L62 (foamer) shows an increase with breakup times up to 1.0% Pluronic L62 and Laponite. However the stretch times are substantially longer for 2.5% and 6.5% Pluronic L62, neither break apart. This indicates that both are elastic fluids. Upon further addition of 10.0% Pluronic L62, the filament does begin drop approaching 0.1 seconds, indicative of a weakly elastic fluid. This indicates that the functionality and molecular architecture of the propyleneoxide

block length enhances the interaction with Laponite by modifying the filament breakup times.

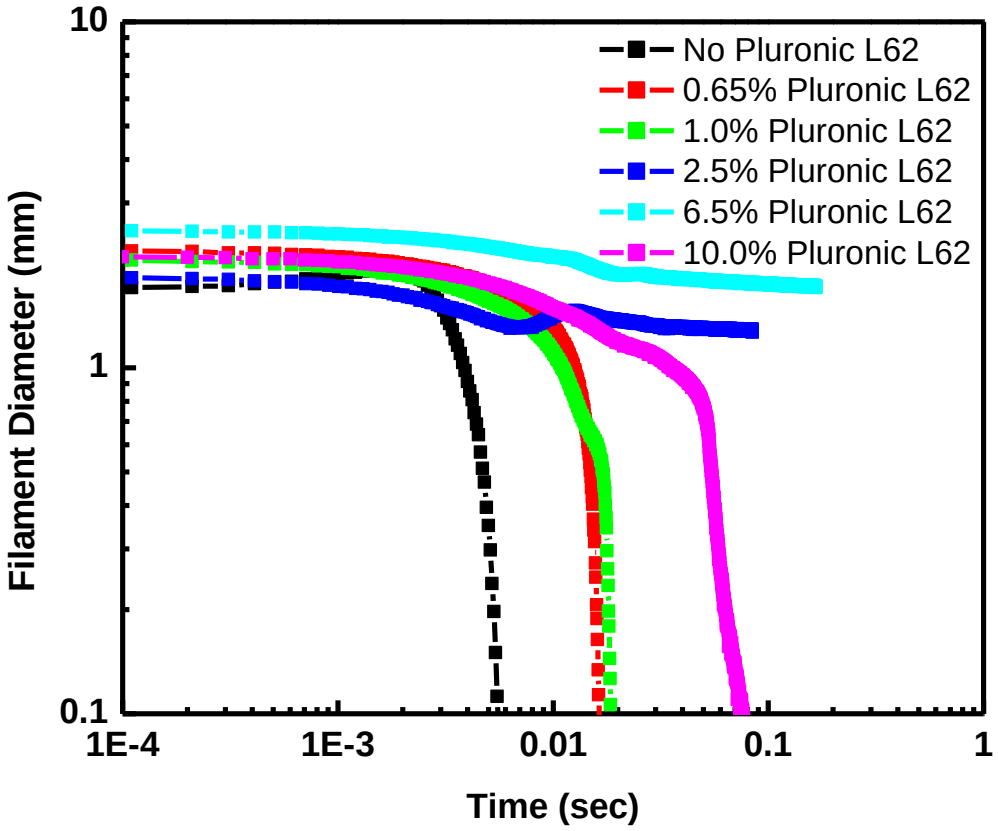

Figure 5. 10. Filament Breakup Time for 2% Laponite dispersions with no Pluronic L62 (black), 0.65% Pluronic L62 (red), 1.0% Pluronic L62 (green), 2.5% Pluronic L62 (blue), 6.5% Pluronic L62 (aqua) and 10.0% Pluronic L62 (magenta).

Figure 5.11 shows apparent extensional viscosities for the 2.0% Laponite dispersions with Pluronic L62 dose response. The viscosity and strain both increase for all fluids. Addition of 0.65%, 1.0% and 10.0% Pluronic L62 increases the apparent extensional viscosity compared to Laponite alone. Addition of 2.5% and 6.5% Pluronic

L62 show substantially higher apparent extensional viscosities compared to other polymer concentrations, due to both filaments not separating. There is a reduction in apparent extensional viscosity for 10.0% Pluronic L62 with Laponite but this is still much higher than Laponite alone. This shows that the architecture of Pluronic L62 enhances Laponite's extensional viscosity up to 6.5% Pluronic L62. Beyond 6.5% Pluronic L62, the hydrophobicity begins to destabilize the filament between Laponte and Pluronic L62.

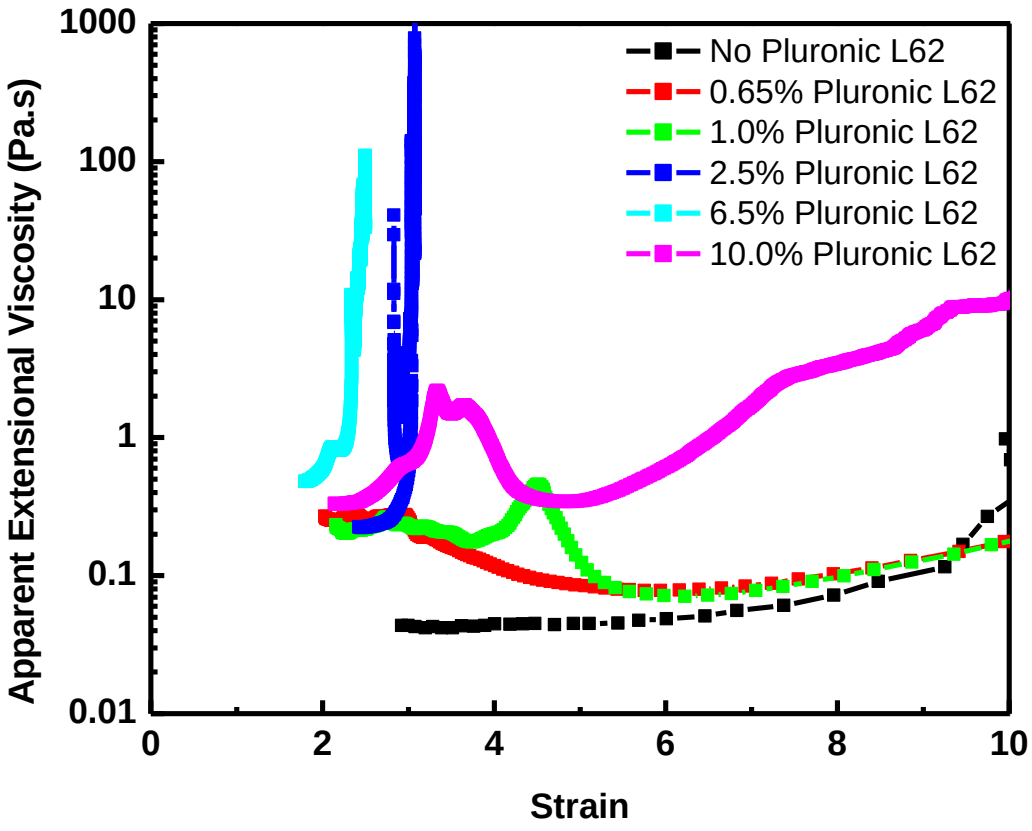

Figure 5. 11. Apparent Extensional Viscosities for 2% Laponite dispersions with no Pluronic L62 (black), 0.65% Pluronic L62 (red), 1.0% Pluronic L62 (green), 2.5% Pluronic L62 (blue), 6.5% Pluronic L62 (aqua) and 10.0% Pluronic L62 (magenta).

Figure 5.12 shows the frame and filament graphs for 2.0% Laponite with a series of Pluronic L62 concentrations. The frame on the left is linked to a filament experiment on the right in Figure 5.12. The red line is used to correlate the frame and filament diameter together in the experiment. Below the frame is a time and frame stamp along with the diameter of the fluid. Figure 5.12a shows Laponite with 1.0% Pluronic L62 with a filament, 1.02 mm, is formed between the top and bottom plates. Figure 5.12b shows that addition of 2.5%Pluronic L62 increases filament diameter to 1.44 mm. The filament does not separate between the top and bottom plates. The drop in diameter is an artifact in the filament diameter graph in Figure 5.12b. Figure 5.12c shows the addition of 6.5% Pluronic L62 with a filament diameter of 1.69 mm. This concentration of Pluronic L62 also shows no breakup between the top and bottom plates.

At 10.0% Pluronic L62 there is enough polymer concentration to separate the filament apart. The Figure 5.12d shows the addition of 10.0% Pluronic L62 with a filament diameter of 1.46 mm. The frames capture the importance of Pluronic L62 addition and interaction between 2.0% Laponite. There is a synergistic contribution of filament extensional properties and apparent extensional viscosities between the Pluronic L62 addition and Laponite. Molecular architecture and functionality of propylenexide enhances the extensional interactions between Pluronic L62 with 2.0% Laponite dispersions that may correlate to foam stability and mechanisms.

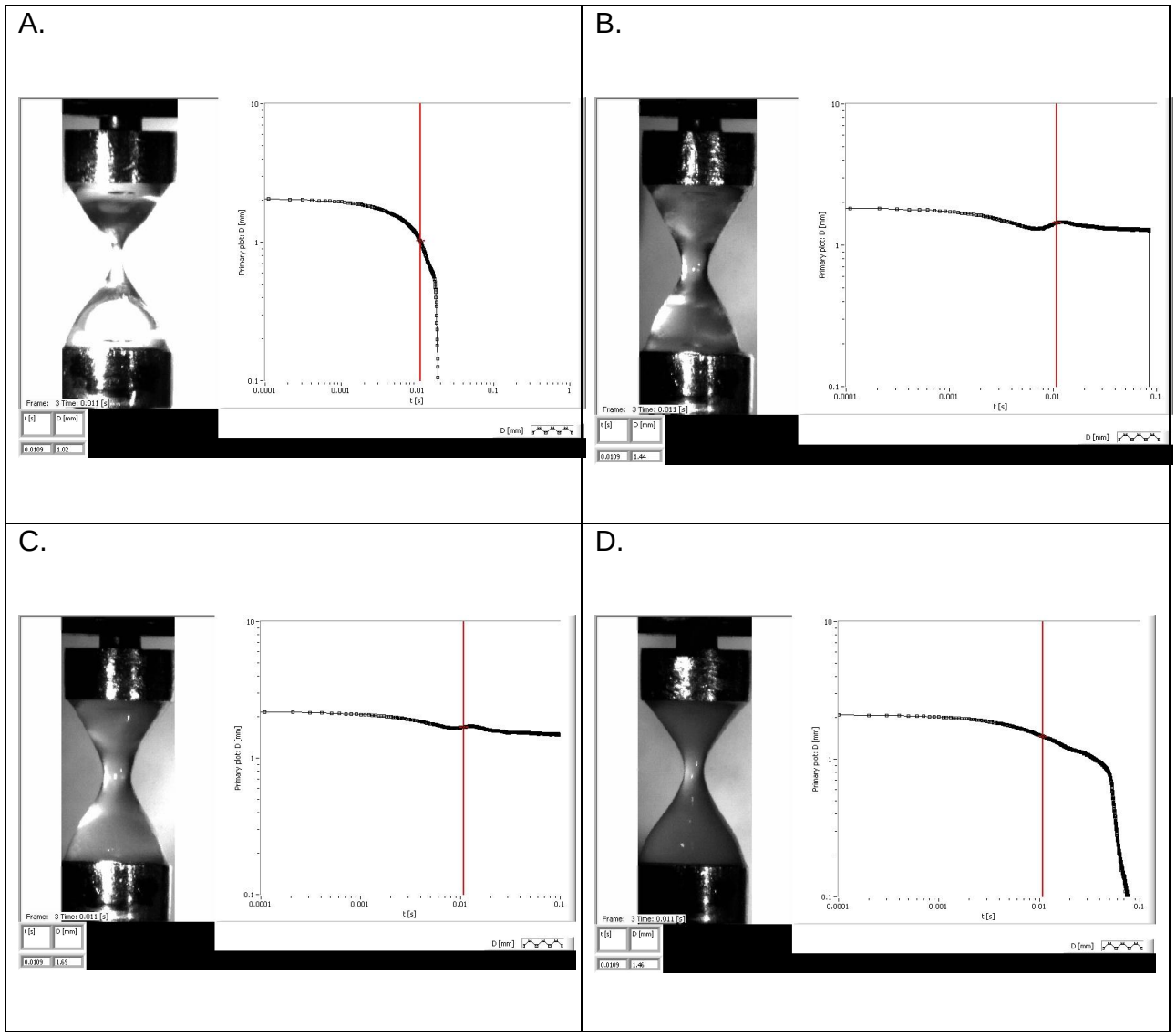

Figure 5. 12. Picture for 2% Laponite dispersions frame 3 at 0.011 seconds for A) 1.0% Pluronic L62, B) 2.5% Pluronic L62, C) 6.5% Pluronic L62 and D) 10.0% Pluronic L62. The Filament Diameter as a function of time is displayed as well. The red vertical line corresponds to the image.

5.3.3 Foam Stability

Figure 5.13 demonstrates the foam drainage for 2.0% Laponite with PEG2000 polymer dose response. Initial foam production approaches 75 mL and rapidly decays by 600 seconds. As the PEG2000 concentration increases the foam drainage time increases. Figure 5.14 shows the foam drainage for 2.0% Laponite with Pluronic 17R4 (defoamer) dose response. Initial foam production approaches 75 mL as in the PEG2000 dose and foam quickly drops by 120 seconds. Foam drainage time increases beyond 800 seconds for all Laponite and Pluronic 17R4 systems but at low foam volumes. Figure 5.15 shows the foam drainage for 2.0% Laponite with Pluronic L62 (foamer) dose response. Initial foam production increases with Pluronic L62 concentration up to foam volumes of 95 mL with addition of 10.0% Pluronic L62.

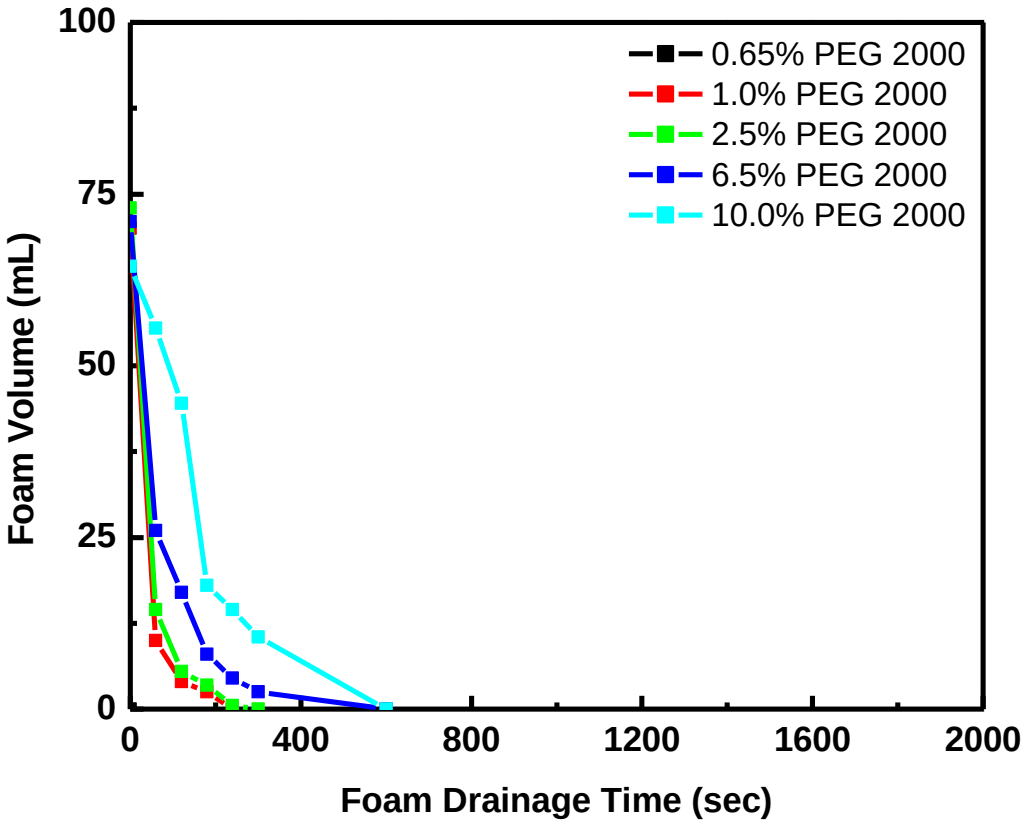

Figure 5. 13. Foam Volume as a function of Foam Drainage Time for 2.0% Laponite Dispersions with 0.65% PEG2000 (black), 1.0% PEG2000 (red), 2.5% PEG2000 (green), 6.5% PEG2000 (blue) and 10.0% PEG2000 (aqua).

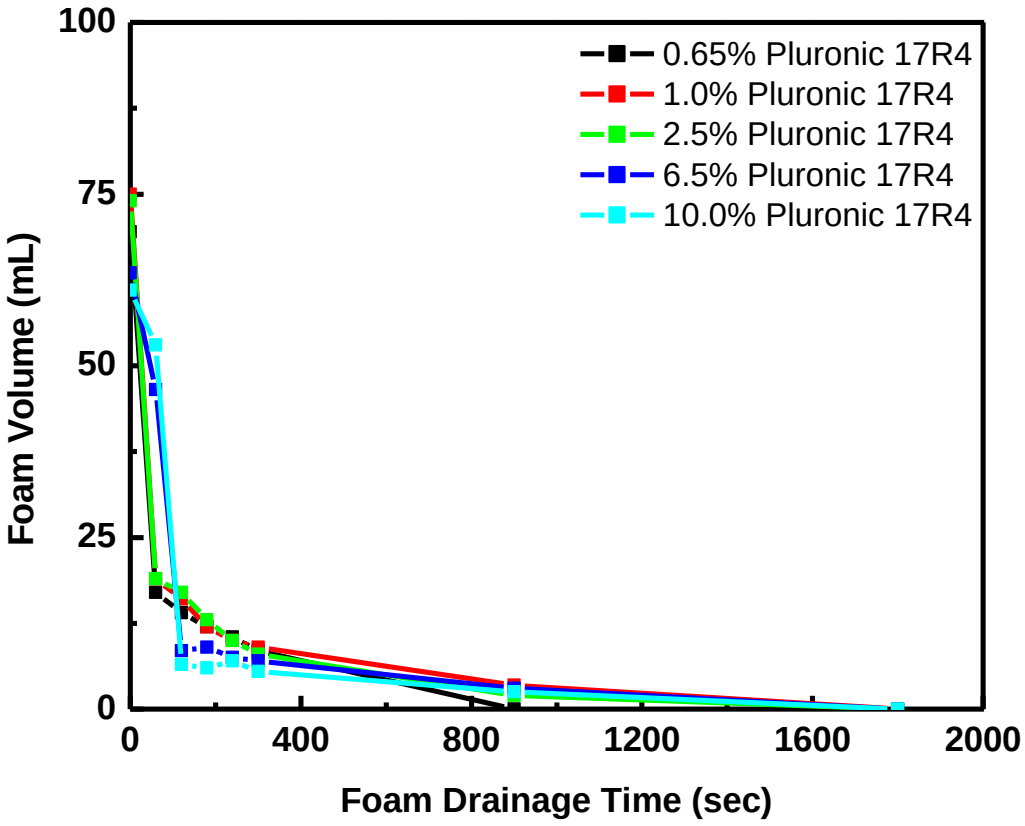

Figure 5. 14. Foam Volume as a function of Foam Drainage Time for 2.0% Laponite Dispersions with 0.65% Pluronic 17R4 (black), 1.0% Pluronic 17R4 (red), 2.5% Pluronic 17R4 (green), 6.5% Pluronic 17R4 (blue) and 10.0% Pluronic 17R4 (aqua).

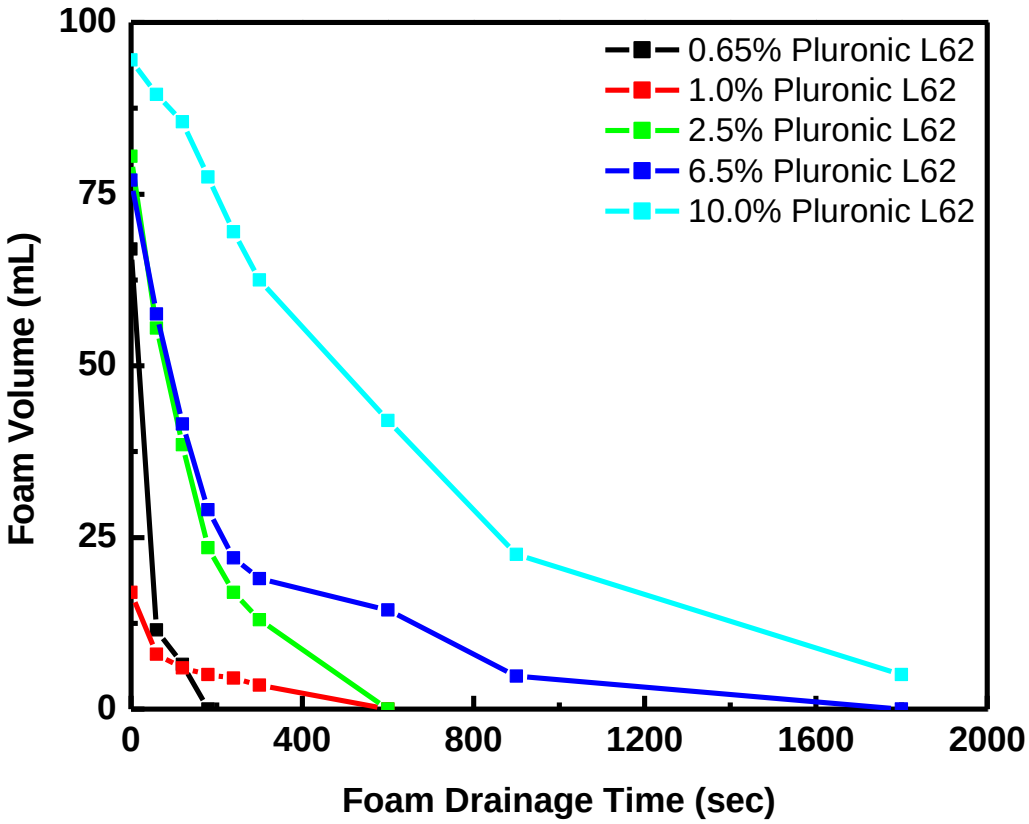

Figure 5. 15. Foam Volume as a function of Foam Drainage Time for 2.0% Laponite Dispersions with 0.65% Pluronic L62 (black), 1.0% Pluronic L62 (red), 2.5% Pluronic L62 (green), 6.5% Pluronic L62 (blue) and 10.0% Pluronic L62 (aqua).

Figure 5.16 summarizes the kinetic response for foam drainage by utilizing the area of foam volume relative to foam drainage time as a function of polymer concentration for PEG2000, Pluronic 17R4 and Pluronic L62. PEG2000 dose has a steady increase in foam area related to an increase to polymer addition. Pluronic 17R4

addition has a low foam area even with polymer addition. Addition is most significant for concentrations of 6.5% Pluronic L62 and higher.

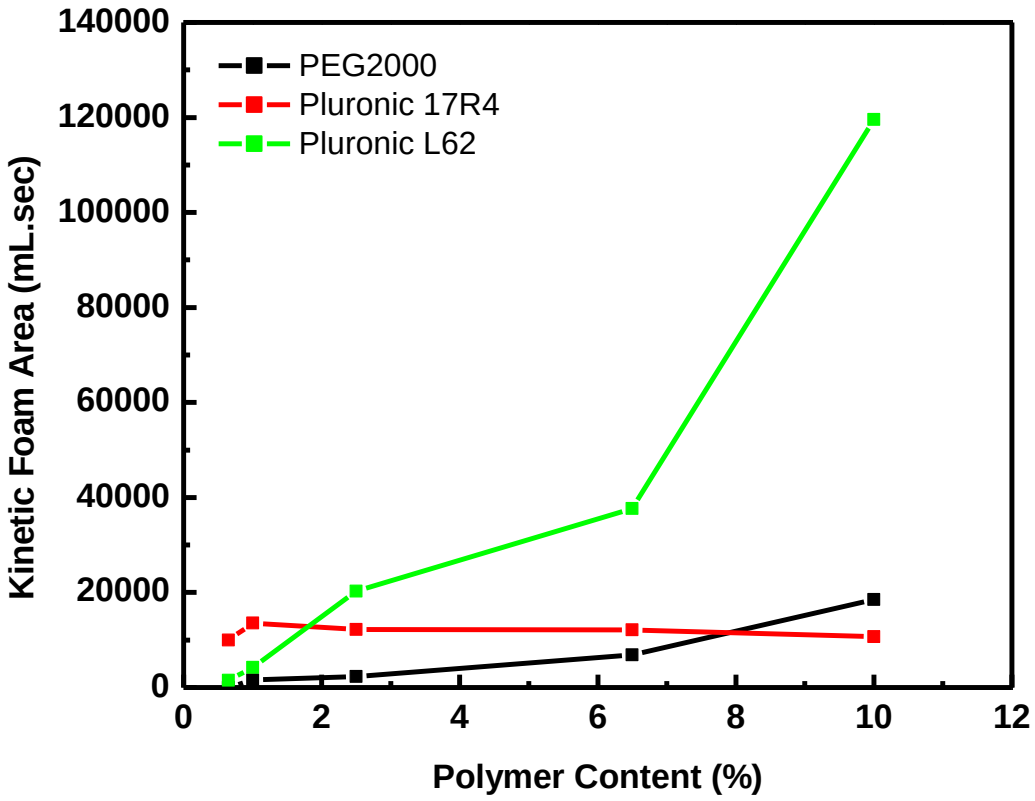

Figure 5. 16. Kinetic Foam Volume for PEG2000 (black), Pluronic 17R4 (red) and Pluronic L62 (green).

5.4 Conclusions

Aqueous dispersions were prepared using Laponite with three different polymers a hydrophilic PEG2000, the defoamer surfactant Pluronic 17R4 and the foamer Pluronic L62. These dispersions were characterized to determine how each polymer component contributes to lamella film drainage, filament stability and foam drainage in the presence

of Laponite. Two relatively simple but valuable techniques were used to differentiate the mechanism for good foaming properties. There was a direct relationship with functionality of the polymer for both Pluronic 17R4 and Pluronic L62 compared to PEG2000 for filament stability and foam drainage stability. A destabilized lamella film and rapid filament break up time was directly related to increased foam drainage and lower foam area for Laponite interactions with PEG2000 and Pluronic 17R4 relative to Laponite with Pluronic L62. Additon of PEG 2000 or Pluronic 17R4 showed a similar drop in lamella film breakup distance. Lamella film was maintained. A decrease in lamella film formation deviated at 2.5% Pluronic L62 and higher concentrations. A more complete understanding of particle stabilized foams has shown that molecular architecture and functionality of the nonionic surfactant of Pluronic L62 synergistically enhances the filament strength with Laponite. Finally, two simple techniques have been provided that can aid in differentiating the mechanisms of particle stabilized foam systems.

5.5 References

(1) a. Pugh, R.J., Foaming, Foam Films, Antifoaming and Defoaming, *Advances in Colloid & Interface Science*, **1996**, *64*, 67–142.

b. Stevenson, P., Foam Engineering: Principles and Applications, John Wiley & Sons Publishing, New York, **2012**, 121-138.

(2) a. Murray, B.S.; Ettelaie, R., Foam Stability: Proteins and Nanoparticles, *Current Opinion in Colloid Interface Science*, **2004**, *9*, 314–320.

b. Binks, B.P., Particles as Surfactants—Similarities and Differences, *Current Opinion in Colloid Interface Science*, **2002**, *7*, 21–41.

c. Hunter, T.N.; Pugh, R.J.; Franks, G.V.; Jameson, G.J., The Role of Particles in Stabilising Foams and Emulsions, *Advances in Colloid & Interface Sci*ence, **2008**, *137*, 57–81.

(3) Horozov, T.S., Foams and Foam Films Stabilized by Solid particles, *Current Opinion in Colloid Interface Science,* **2008**, *13*: 134–40.

(4) Wierenga, P.A.; Gruppen, H., New Views on Foams from Protein Solutions, *Current Opinion in Colloid Interface Science*, **2010**, *15*, 365–73.

(5) Perez, A.A.; Sanchez, C.C.; Patino, J.M.R.; Rubiolo, A.C.; Santiago, L.G., Foaming Characteristics of β-lactoglobulin as Affected by Enzymatic Hydrolysis and Polysaccharide Addition: Relationships with the Bulk and Interfacial Properties, *Journal of Food Engineering*, **2012**, *113 (1)*, 53-60.

(6) Murray, B.S.; Ettelaie, R., Foam Stability: Proteins and Nanoparticles, *Current Opinion in Colloid & Interface Science*, **2004**, *9 (5)*, 314-320.

(7) Rossen, W. R.; Venkatraman, A.; Johns, R. T.; Kibodeaux, K. R.; Lai, H.; Tehrani, N.M., Fractional Flow Theory Applicable to Non-Newtonian Behavior in EOR Processes, *Transport in Porous Media*, **2011**, *89 (2)*, 213-236.

(8) Graham, K.J.; Sewell, R.G.S., **1985** US Patent 4,543,872.

(9) a. Clark, K.P., Fire extinguishing or retarding material, **2006**, US patent 7,011,763.

b. Clark, K.P., Fluorochemical foam stabilizers and film formers, **1998**, US patent 5,750,043.

(10) Boos, J.; Drenckhan, W.; Stubenrauch, C., On How Surfactant Depletion oDuring Foam Generation Influences Foam Properties, *Langmuir*, **2012**, *28*, 9303-9310.

(11) Liu, Q; Zhang, S.; Sun, D.; Xu, J., Foams Stabilized by Laponite nanoparticles and alkylammonium bromides with different alkyl chain lengths, *Colloids and Surfaces A: Physicochemical Engineering Aspects*, **2010**, *355*, 151-157.

(12) Karakashev, S.I.; Ozdemir, O.; Hamptom, M.A.; Nguyen, A.V., Formation and Stability of Foams Stabilized by Fine Particleswith Similar Size, Contact Angle and Different Shape, *Colloids and Surfaces A: Physicochemical Engineering Aspects*, **2011**, *382*, 132-138.

(13) Monteux, C.; Fuller, G.G.; Bergeron, V., Shear and Dilatational Rheology of Oppositely Charged Polyelectrolyte/Surfactant Microgels Adsorbed at the Air-Water Interface. Influence on Foam Stability, *Journal of Physical Chemistry B*, **2004**, *108*, 16473-16482.

(14) a. Grandjean, J., Interaction of Poly(ethylene glycol) Monoalkyl Ethers with Synthetic Saponites in Aqueous Suspensions: A Multinuclear Magnetic Resonance Study, *Langmuir*, **1998**,*14*, 1037-1040.

b. Grandjean, J., Interaction of a Zwitterionic Surfactant with Synthetic Clays in Aqueous Suspensions: A Multinuclear Magnetic Resonance Study, *Journal of Colloid and Interface Science*, **2001**, *239*, 27-32.

c. Borsacchi, S.; Geppi, M.; Ricci, L.; Ruggeri, G.; Veracini, C.A., Interactions at the Surface of Organophilic Modified Laponites: A Multinuclear Solid-State NMR Study, *Langmuir*, **2007**, *23*, 3953-3960.

(15) Hunter, T.N.; Wanless, E.J.; Jameson, G.R.; Pugh, R.J., Non-ionic Surfactant Interactions with Hydrophobic Nanoparticles: Impact on Foam Stability, *Colloids and Surfaces A: Physicochemical Engineering Aspects*, **2009**, *347*, 81-89.

(16) Tran, D.N.H.; Whitby, C.P.; Fornasiero, D.; Ralston, J., Foamability of Aqueous Suspensions of Fine Graphite and Quartz Particles with a Triblock Copolymer, *Journal of Colloid and Interface Science*, **2010**, *348*, 460-468.

(17) Liu, Q.; Zhang, S.; Sun, D.; Xu, J., Aqueous Foams Stabilized by Hexylamine-Modified Laponite Particles, *Colloids and Surfaces A: Physicochemical Engineering Aspects*, **2009**, *338*, 40-46.

(18) Guillermic, R. M.; Salonen, A.; Emile, J.; Saint-Jalmes, A., Surfactant foams doped with laponite: unusual behaviors induced by aging and confinement, *Soft Matter*, **2009**, *5 (24)*, 4975-4982.

(19) Sani, A. M.; Mohanty, K. K., Incorporation of clay nano-particles in aqueous foams, *Colloids and Surfaces A: Physicochemical and Engineering Aspects*, **2009**, *340 (1-3)*, 174-181.

(20) Simulescu, V.; Manev, E.; Ilia, G., Drainage and Stability of Foam Films from Aqueous Solutions of a Single Nonionic Surfactant C12E6, *Optoelectronics and Advanced Materials Rapid Communications*, **2009**, *3 (2)*, 155-159.

(21) Kostoglou, M.; Georgiou, E.; Karapantsios, T. D., A New Device for Assessing Film Stability in Foams: Experiment and Theory, *Colloids and Surfaces, A: Physicochemical and Engineering Aspects*, **2011**, *382(1-3)*, 64-73.

(22) Adamson, A.W.; Gast, A.P., Physical Chemistry of Surfaces, 6th edition, 1997, New York, 500-536.

(23) Rodd, E. L.; Scott, T. P.; Cooper-White, J. J.; McKinley, G. H., Capillary Breakup Rheometry of Low-Viscosity Elastic Fluids, *Applied Rheology,* **2005**, *15*, 12–27.

(24) Duxenneuner, M.R.; Fischer, P.; Windhab, E.J.; Cooper-White, J.J., Extensional Properties of Hydroxypropyl Ether Guar Gum, *Biomacromolecules*, **2008**, *9*, 2989-2996.

(25) Hayward, J.; Ober, T.J.; Oliveira, M.S.N.; Alves, M.A.; McKinley, G.H., Extensional Rheology and Elastic Instabilities of a Worm-like Micellar Solution in a Microfluidic Cross-Slot Device, *Soft Matter*, **2012**, *8*, 536-555.

(26) Odell, J. A.; Haward, S. J., Viscosity enhancement in the flow of hydrolysed poly(acrylamide) saline solutions around spheres: implications for enhanced oil recovery, *Rheologica Acta*, **2008**, *47 (2),* 129-137.

CHAPTER 6

CONCLUSIONS

The following work illustrates the value of Laponite with Pluronic L62, a nonionic foaming surfactant polymer, to provide an optimized particle stabilized foam by understanding:

I. Laponite-Pluronic interactions and properties for improved performance in a particle stabilized foam.

II. Interfacial properties between air and the Laponite-Pluronic complex

Overall, a thorough and detailed approach by looking at molecular architecture and hydrophilicity of different polymer systems with similar molecular weights demonstrated how Pluronic L62 enhanced the bulk properties of Laponite. The opposite was observed at from interfacial experiments where Laponite enhanced the Pluronic L62 interfacial structure in storage modulus and shear. The surface energy demonstrated the importance of spreading using various liquids. The added benefit that this Laponite-PluronicL62 composite has is enhanced from the thermal resistance due to the incorporation of Laponite.

Chapter 3 discussed the bulk properties of Laponite with Pluronic L62 relative to PEG2000 and Pluronic 17R4. It was revealed that Pluronic L62 enhanced the rheological properties of Laponite through steric stabilization. The thermal properties revealed that Laponite and Pluronic L62 prevented water loss. Additionally, the thermal properties revealed that Laponite prevented Pluronic L62 loss. The electrostatic contributions showed that Pluronic L62 reduced the Laponite surface charge. Pluronic L62 adsorbs onto Laponite. It was determined that 2% Laponite and 2.5%-6.5%

Pluronic L62 were optimal ranges for enhanced bulk properties for in firefighting foam applications.

Chapter 4 discussed the interfacial properties further for Laponite and Pluronic L62 relative to PEG2000 and Pluronic 17R4. The Laponite Pluronic L62 film surface energy illustrated that the composite is compatible with various solvents that would be encountered in various fires. The XRD revealed that Pluronic L62 intercalated into the silicate matrix. This aided in the surface tension results confirming Pluronic L62 adsorbs as well at the interface with Laponite. The interfacial viscoelastic properties above 2.5% Pluronic L62 were enhanced in the presence of Laponite by increasing the interfacial storage modulus and shear stress.

What was most valuable in terms of new techniques to understand foaming properties came from the lamella breakpoint and CaBER experiments. First, the lamella breakpoint mimics the film drainage. The lamella of Laponite with 2.5% Pluronic L62 and higher had unusual break point curves much earlier than expected and mass much higher than expected. The CaBER showed no break in the filament with the Laponite and 2.5%/6.5% Pluronic L62 dispersions. The videos revealed the curvature and resistance to filament breakup. Both lamella break point and CaBER show promise as new simple tools for characterizing foam formulations by investigating the resistance from the lamella film and filaments formed during a dynamic process.

Chapter 5 demonstrated two new simple techniques to look at lamella film breakup and extensional filament strength and its relationship to foam stability of Laponite using Pluronic L62 compared to PEG2000 and Pluronic 17R4. Lamella break

points demonstrated how Laponite influenced Pluronic L62's film drainage profile. Extensional filament strength revealed the increased breakup time Laponite had on Pluronic L62. Foams produced with Laponite and Pluronic L62 was more stable than PEG2000 and Pluronic 17R4 due to hydrophobicity and molecular structure, respectively. Pluronic L62 increased foam stability for hydrophilic Laponite suspensions at concentrations above 2.5% Pluronic L62. To conclude, novel characterization techniques have been identified to characterize particle stabilized foams and a particle stabilized foam has been developed using Laponite and Pluronic L62 for firefighting applications. Therefore, from these characterization techniques we found that the best range for the Laponite is 1-2% and for the Pluronic L62 is 2.5-6.5%.